


2012-07-06

Therapeutic Silencing of Mutant *Huntingtin* by Targeting Single Nucleotide Polymorphisms: A Dissertation

Edith L. Pfister

University of Massachusetts Medical School

Follow this and additional works at: https://escholarship.umassmed.edu/gsbs_diss

 Part of the [Congenital, Hereditary, and Neonatal Diseases and Abnormalities Commons](#), [Genetic Phenomena Commons](#), [Genetics and Genomics Commons](#), [Mental Disorders Commons](#), [Nervous System Diseases Commons](#), [Neuroscience and Neurobiology Commons](#), [Nucleic Acids, Nucleotides, and Nucleosides Commons](#), and the [Therapeutics Commons](#)

Repository Citation

Pfister, EL. Therapeutic Silencing of Mutant *Huntingtin* by Targeting Single Nucleotide Polymorphisms: A Dissertation. (2012). University of Massachusetts Medical School. *GSBS Dissertations and Theses*. Paper 618. DOI: 10.13028/a5gf-1e13. https://escholarship.umassmed.edu/gsbs_diss/618

This material is brought to you by eScholarship@UMMS. It has been accepted for inclusion in GSBS Dissertations and Theses by an authorized administrator of eScholarship@UMMS. For more information, please contact Lisa.Palmer@umassmed.edu.

THERAPEUTIC SILENCING OF MUTANT *HUNTINGTIN* BY TARGETING
SINGLE NUCLEOTIDE POLYMORPHISMS

A Dissertation Presented

By

EDITH L. PFISTER

Submitted to the Faculty of the
University of Massachusetts Graduate School of Biomedical Sciences, Worcester
In partial fulfillment of the requirements for the degree of

DOCTOR OF PHILOSOPHY

JULY 6, 2012

PROGRAM IN NEUROSCIENCE

THERAPEUTIC SILENCING OF MUTANT *HUNTINGTIN* BY TARGETING
SINGLE NUCLEOTIDE POLYMORPHISMS

A Dissertation Presented
By
EDITH L. PFISTER

The signatures of the Dissertation Defense Committee signify completion and approval as to style and content of the Dissertation

Neil Aronin, MD, Thesis Advisor

Victor Ambros, Ph.D., Member of Committee

Eric Baehrecke, Ph.D., Member of Committee

Albert La Spada, MD, Ph.D., Member of Committee

Miguel Sena-Esteves, Ph.D., Member of Committee

The signature of the Chair of the Committee signifies that the written dissertation meets the requirements of the Dissertation Committee

Marc Freeman, Ph.D., Chair of Committee

The signature of the Dean of the Graduate School of Biomedical Sciences signifies that the student has met all graduation requirements of the school.

Anthony Carruthers, Ph.D.
Dean of the Graduate School of Biomedical Sciences

Program in Neuroscience
July 6, 2011

DEDICATION

To my husband Brian, for supporting me in everything I do.

To my son Alden, for inspiring me to be better.

And to the little one I don't know yet, for motivating me to finish.

ACKNOWLEDGEMENTS

I would like to thank my advisor, Neil Aronin, without whom this work would not have been possible. I appreciate the opportunities and challenges he has given me and the trust he has placed in me. I would also like to thank Phil Zamore, who has provided me with invaluable advice, guidance and support. With the help of you both, I have grown immensely.

Thank you to my committee members who have provided me with valuable advice, encouragement, and perspectives. I only wish that I had asked you for help more often.

Thank you to all the members of the Aronin and Zamore labs. Thanks especially to Lori Kennington, who was always willing to help out and to listen to me babble incessantly about my family, to Kathryn Chase for her patience and quiet efficiency and to Joanna Chaurette with whom I have shared this journey. Thank you for listening to all my crazy ideas and for commiserating over sleepless nights and teething toddlers. Thanks also to Meghan Sass and Wanzhao Liu, to Amanda, Erica, Sarah, and all the other people who have come through the lab.

Thank you to my family: to my husband and mother for their love and support, and to my sisters who have always been in front, showing me the way. Finally thank you to my father for showing me what it is to be a good scientist and for demonstrating that it is possible to love what you do.

COPYRIGHT INFORMATION

The contents of this dissertation have appeared in whole or in part in the following publications:

Five siRNAs targeting three SNPs in *Huntingtin* may provide therapy for three-quarters of Huntington's disease patients.

Pfister, EL, Kennington L, Straubhaar J, Wagh S, Liu W, DiFiglia M, Landwehrmeyer B, Vonsattel JP, Zamore PD, Aronin N. *Curr Biol*. 2009 May 12; 19(9): 774-778.

Huntington's disease: silencing a brutal killer.

Pfister EL, Zamore PD. *Exp Neurol*. 2009 Dec; 220(2): 226-9.

ABSTRACT

Huntington's disease (HD) is an autosomal dominant, progressive neurodegenerative disorder. Invariably fatal, HD is caused by expansion of the CAG repeat region in exon 1 of the *Huntingtin* gene which creates a toxic protein with an extended polyglutamine tract¹. Silencing mutant *Huntingtin* messenger RNA (mRNA) is a promising therapeutic approach²⁻⁶. The ideal silencing strategy would reduce mutant *Huntingtin* while leaving the wild-type mRNA intact. Unfortunately, targeting the disease causing CAG repeat expansion is difficult and risks targeting other CAG repeat containing genes.

We examined an alternative strategy, targeting single nucleotide polymorphisms (SNPs) in the *Huntingtin* mRNA. The feasibility of this approach hinges on the presence of a few common highly heterozygous SNPs which are amenable to SNP-specific targeting. In a population of HD patients from Europe and the United states, forty-eight percent were heterozygous at a single SNP site; one isoform of this SNP is associated with HD. Seventy-five percent of patients are heterozygous at least one of three frequently heterozygous SNPs. Consequently, only five allele-specific siRNAs are required to treat three-quarters of the patients in the European and U.S. patient populations. We have designed and validated siRNAs targeting these SNPs.

We also developed artificial microRNAs (miRNAs) targeting *Huntingtin* SNPs for delivery using recombinant adeno-associated viruses (rAAVs). Both U6

promoter driven and CMV promoter driven miRNAs can discriminate between matched and mismatched targets in cell culture but the U6 promoter driven miRNAs produce the mature miRNA at levels exceeding those of the vast majority of endogenous miRNAs. The U6 promoter driven miRNAs can produce a number of unwanted processing products, most likely due to a combination of overexpression and unintended export of the pri-miRNA from the nucleus. In contrast, CMV-promoter driven miRNAs produce predominantly a single species at levels comparable to endogenous miRNAs. Injection of recombinant self complementary AAV9 viruses carrying polymerase II driven *Huntingtin* SNP targeting miRNAs into the striatum results in expression of the mature miRNA sequence in the brain and has no significant effect on endogenous miRNAs. Matched, but not mismatched SNP-targeting miRNAs reduce inclusions in a knock-in mouse model of HD. These studies bring us closer to an allele-specific therapy for Huntington's disease.

TABLE OF CONTENTS

Title.....	ii
Signatures	iii
Dedication	iv
Acknowledgements	v
Copyright Information	vi
Abstract	vii
Table of Contents	ix
List of Tables	xiii
List of Figures	xiv
Chapter I: Introduction	1
Huntington’s disease.....	2
Genetics of HD.....	3
<i>Functions of wild-type Huntingtin</i>	4
<i>Toxicity of mutant Huntingtin</i>	6
<i>Therapeutic strategies for HD</i>	8
The RNAi pathway	9
<i>History of RNAi</i>	9
<i>Core Machinery of the RNAi pathway</i>	10
<i>The mammalian RNAi pathway</i>	11
RNAi Therapeutics.....	16
<i>Challenges and Strategies</i>	16

<i>Toxicity: Seed mediated off-target effects</i>	23
<i>Toxicity: Immune Stimulation</i>	24
<i>Toxicity: Saturation of the RNAi machinery</i>	25
RNAi Therapy for Huntington’s Disease	29
<i>CAG Targeting</i>	32
<i>Gene-specific silencing</i>	32
<i>Targeting single nucleotide polymorphisms</i>	35
Chapter II: Five siRNAs targeting three SNPs in Huntingtin may provide therapy for three-quarters of Huntington’s disease patients	38
Preface	39
Summary	40
Results.....	41
<i>Sequencing and analysis of Huntingtin SNP sites in HD and control patients</i>	41
<i>An additional two SNPs achieve patient coverage > 75%</i>	49
<i>Luciferase reporter assays using matched and mismatched targets are good predictors of efficacy and selectivity for endogenous mRNA targets</i>	52
<i>Development of allele-specific siRNAs</i>	57
Discussion	75
Materials and Methods.....	76
<i>Patient Samples, Sequencing, and Statistical Analysis</i>	76
<i>Reporter Constructs and Assays</i>	78
<i>Western Blotting</i>	79
<i>Quantitative PCR</i>	80

Acknowledgements.....	85
Chapter III: Processing and therapeutic applications of artificial miRNAs targeting Huntingtin SNPs	86
Preface	87
Summary	88
Introduction	89
Results.....	92
<i>Design of SNP targeting shRNA and miRNA</i>	<i>92</i>
<i>U6 promoter driven miRNA hairpins produce small RNA species with multiple seed sequences.....</i>	<i>103</i>
<i>CMV promoter driven artificial miRNAs produce primarily small RNAs with a single seed sequence.....</i>	<i>114</i>
<i>Discrimination between matched and mismatched targets can be improved by adding additional mismatches in the 3'-region of the siRNA.....</i>	<i>117</i>
<i>Self-complementary AAV9 delivery of artificial miRNAs into the mouse striatum.....</i>	<i>125</i>
<i>SNP targeting artificial miRNAs reduce inclusions in a mouse model of HD </i>	<i>136</i>
Discussion	141
Materials and Methods.....	142
<i>Construction of shRNA and miRNA plasmids and viral vectors.....</i>	<i>142</i>
<i>Reporter Constructs and Assays.....</i>	<i>143</i>
<i>Small RNA cloning.....</i>	<i>144</i>
<i>Sequence extraction, analysis and statistics</i>	<i>146</i>

<i>Animals and Injections</i>	147
<i>Immunohistochemistry and Inclusion Counting</i>	147
Supplemental Figures and Tables	149
Acknowledgements.....	155
Chapter IV: Summary and Conclusions.....	156
Oligonucleotide Therapeutics for Huntington’s disease	157
<i>Progress and Challenges</i>	157
<i>Targeting Strategies</i>	159
<i>Methods for designing SNP targeting siRNAs and miRNAs</i>	162
<i>Off-target effects</i>	164
The Future of Huntington’s Disease Therapeutics	165
<i>Restoring normal Huntingtin function</i>	165
<i>Systemic Delivery</i>	166
<i>Gene Therapy: Developing an exit strategy</i>	167
<i>Combination Therapies</i>	168
Bibliography.....	169
Appendix I: Therapeutic silencing of mutant <i>Huntingtin</i> with siRNA attenuates striatal and cortical neuropathology and behavioral deficits	192

LIST OF TABLES

Table 2.1. Frequency of Heterozygosity for 24 SNP sites in the Huntingtin mRNA	45
Table 2.2. The U Isoform of SNP rs362307 at Huntingtin mRNA Nucleotide 9,633 Is Associated with the Expanded CAG Disease Allele	47
Table 2.3. Validation of siRNAs Designed to Discriminate between Isoforms of the rs362307 SNP	60
Table 2.4. Validation of siRNAs designed to distinguish between matched and mismatched SNP isoforms	66
Table S2.1. Primers Used for SNP Analysis and Resequencing	82
Table 3.1. SNP sites and heterozygosity in cell lines and selected mouse models of HD	99
Table 3.2. RNA species from HeLa cell small RNA libraries	104
Table 3.3. RNA reads from HeLa cell small RNA libraries.....	106
Table 3.4. Screening of siRNAs to improve discrimination at rs362273	120
Table 3.5. RNA species from mouse striatal small RNA libraries	126
Table 3.6. RNA reads from mouse striatal small RNA libraries	128
Table 3.7. Small RNAs mapping to scAAV9-miRNA viruses in the mouse striatum	130
Table S3.1. shRNA and miRNA sequences	154

LIST OF FIGURES

Figure 1.1. The mammalian RNAi pathway	12
Figure 1.2. Types of therapeutic RNAi constructs	17
Figure 1.3. Therapeutic RNAi constructs and the RNAi pathway	21
Figure 1.4. RNAi approaches to Huntington's disease	30
Figure 2.1. Analysis of SNPs in the human Huntingtin mRNA.....	42
Figure 2.2. Heterozygosity of SNPs in HD patients	50
Figure 2.3. Repression of Luciferase Expression in Reporter Assays Corresponds to Depletion of Endogenous Huntingtin mRNA	53
Figure 2.4. A Fully Matched siRNA That Reduces Expression of Both a Luciferase Reporter and Endogenous Huntingtin mRNA Causes a Corresponding Depletion of Endogenous Huntingtin Protein.....	55
Figure 2.5. siRNAs with single mismatches at position 10 or 16 do not discriminate between the U and C isoforms of rs362307	58
Figure 2.6. Representative Data for the Development of an Allele-Specific siRNA Targeting SNP rs362307, Which Is Associated with HD	63
Figure 2.7. Representative Data for the siRNAs Targeting the rs363125 SNP Site	69
Figure 2.8 Representative data for the development of isoform-specific siRNAs targeting the rs362273 SNP Site	71
Figure 2.9. Adding a Position 5 Mismatch to a Position 10 Mismatched Increased the Ability of an siRNA to Discriminate between the Two Isoforms of the rs362273 SNP	73
Figure 3.1. Expected processing of shRNA and miRNA expression constructs .	93
Figure 3.2. shRNAs and miRNA-like hairpins discriminate between matched and mismatched luciferase reporters at an HD associated SNP site.....	96
Figure 3.3. Discrimination of an artificial miRNA at the rs362273 SNP site	101

Figure 3.4. U6-promoter driven miRNA-like hairpins produce multiple small RNA products.....	109
Figure 3.5 Endogenous miRNA profiles of HeLa cells transfected with U6-promoter driven artificial miRNAs	112
Figure 3.6. CMV promoter driven artificial miRNAs produce a single dominant small RNA species	115
Figure 3.7. Screening of siRNAs to improve discrimination at rs362273	118
Figure 3.8. A triple mismatched artificial miRNA discriminates between isoforms at rs362273.....	123
Figure 3.9. Self-complementary AAV9 delivery of artificial miRNAs to the mouse striatum.....	132
Figure 3.10. Length distributions of virally introduced artificial miRNAs	134
Figure 3.11. Matched but not mismatched miRNAs reduce inclusions in an HD mouse model.....	137
Figure 3.12. Reductions in inclusions in mice receiving scAAV9-2273G are not due to neuron loss	139
Figure S3.1. U6 promoter driven shRNA and miRNA can cause a non-specific increase in luciferase activity.....	150
Figure S3.2. miRNAs without a central bulge are not functional against matched or mismatched targets in a luciferase reporter assay	152

CHAPTER I: INTRODUCTION

Huntington's disease

Huntington's disease (HD) is an autosomal dominant, progressive and invariably fatal neurodegenerative disorder. Early symptoms include cognitive impairment and depression while later stages of the disease are characterized by involuntary movements (chorea), which can cause injury, and disabling impairments in voluntary movements, such as swallowing. As the disease progresses, patients become unable to care for themselves and often unable to speak. The movement disorder is accompanied by changes in cognition and personality and by additional psychiatric symptoms which can include depression, anxiety, obsessive compulsive behaviors, psychosis. Patients often take a variety of medications to try to control the psychological symptoms of the disease, but these medications often have side-effects and they do nothing to prevent or delay the progression of the disease. The most direct approach to treating HD is to silence expression of the mutant *Huntingtin* gene while leaving the normal *Huntingtin* intact (allele-specific silencing); for this we turned to RNA interference. RNA interference (RNAi) is a sequence-specific method for targeting messenger RNAs for degradation. Unfortunately, targeting the CAG repeat expansion which causes the HD has proven difficult⁷. Targeting frequently heterozygous single nucleotide polymorphisms in the *Huntingtin* mRNA provides an alternative approach.

Genetics of HD

HD is caused by expansion of the CAG repeat region in exon 1 of the *Huntingtin* gene¹. Expansion results in the production of a toxic polyglutamine (poly(Q)) expanded protein, which is particularly damaging to cortical and striatal neurons. *Huntingtin* alleles can be classified by the number of CAG repeats they contain. The normal allele contains fewer than 35 repeats. Alleles containing 27-35 repeats do not cause disease, but are unstable and prone to expansion into the disease range in the next generation.

In general, patients with longer CAG repeat expansions develop disease symptoms earlier^{8,9}. Patients with repeat lengths between 36 and 39 have very late onset and may even appear to be disease free throughout their lives, whereas patients with more than 60 repeats often develop symptoms before age 20. The majority of patients have 39-50 repeats and become symptomatic between the ages 30 and 50. Age of onset has traditionally been defined as the age at which motor symptoms appear, but subtle psychiatric or cognitive changes likely precede motor symptoms. Defining and predicting the early course of the disease may be important, as it may influence the outcome of therapeutic intervention. CAG repeat length variation accounts for approximately 70% of the variation in age of onset. Up to 60% of the remaining variability may be explained by other genetic factors¹⁰ including CAG repeat length of the normal *Huntingtin* allele and polymorphisms in the GluR6 gene^{11,12}. The remaining 12% of variability in age of onset is likely attributable to environmental factors. HD

homozygotes are phenotypically similar to heterozygotes and have a similar age of onset^{13,14} but homozygosity may accelerate disease progression¹⁵. For affected families, the financial and emotional costs of the disease are high. Average survival after symptom onset may be as long as 20 years, and as the disease progresses many patients require long-term institutional care.

Expanded *Huntingtin* alleles are unstable and particularly prone to expansion in the male germ line, giving rise to the phenomenon known as anticipation where the age of onset falls in subsequent generations, particularly when the mutant allele is inherited from the father⁸. The majority of juvenile HD cases are paternally inherited^{16,17}. Somatic instability has also been reported and may account for differences in disease progression or cell type vulnerability^{18,19}.

Functions of wild-type Huntingtin

Huntingtin is a large (~350kD), widely expressed, cytoplasmic protein composed of a series of HEAT (*Huntingtin*, Elongation factor 3, protein phosphatase 2A, TOR1) repeats²⁰⁻²². HEAT repeats are degenerate sequences approximately 50 amino acids long that form an α -helical hairpin. HEAT repeat proteins contain multiple tandem repeats, which are thought to provide a flexible scaffold for multiple protein-protein interactions. In agreement with this, yeast two-hybrid assays have been used to identify a large number of potential *Huntingtin* interaction partners²³.

Huntingtin is ubiquitously expressed, but it is present at high concentrations in the brain and testis^{24,25}. Mice lacking wild-type *Huntingtin* exhibit increased apoptosis and embryonic lethality which precedes nervous system development²⁶⁻²⁸. Heterozygotes exhibit neuronal loss and behavioral abnormalities²⁸. Conditional inactivation of *Huntingtin* in the adult brain results in neuronal degeneration, behavioral abnormalities, and reduced lifespan²⁹.

In neurons, *Huntingtin* is associated with microtubules and vesicles³⁰⁻³², functions in vesicle trafficking,³³ and regulates receptor recycling by affecting the guanine nucleotide exchange factor Rab11³⁴. Impaired vesicle recycling leads to increased reactive oxygen species and may contribute to HD pathology^{35,36}. In *Drosophila*, loss of wild-type *Huntingtin* causes axon transport defects³⁷ and in mouse striatal neurons, reducing the level of wild-type *Huntingtin* below 50% results in reduced mitochondrial speed³⁸. Loss of wild-type *Huntingtin* may reduce trophic support for striatal neurons. BDNF transport from the cortex to the striatum protects striatal neurons, while loss of cortical BDNF results in neuronal degeneration³⁹. Wild-type *Huntingtin* enhances BDNF transport along microtubules, upregulates transcription of BDNF by binding to the transcription factor Repressor Element-1 Transcription Factor/Neuron Restrictive Silencer Factor (REST/NRSF)^{40,41}, and is neuroprotective in cell culture⁴². The interaction between *Huntingtin* and REST/NRSF may also promote the maintenance of neuronal specification. REST/NRSF is a repressor of neuron specific gene which binds a DNA sequence called the neuron-restrictive silencer element (NRSE)

and represses transcription of neuronal genes in nonneuronal cells^{43,44}. Interaction of REST/NRSF with wild-type *Huntingtin* sequesters it in the cytoplasm and prevents its binding to NRSEs⁴¹; therefore loss of wild-type *Huntingtin* may shift the transcriptional profile of neurons towards that of nonneuronal cells.

Wild-type *Huntingtin* is anti-apoptotic and protective against a variety of toxic stimuli⁴⁵⁻⁴⁷. In mice, depletion of wild-type *Huntingtin* causes activation of caspase-3 and increased susceptibility to cell death, while overexpression inhibits both caspase-3 activation and excitotoxic cell death⁴⁸. Loss of wild-type *Huntingtin* exacerbates behavioral defects in mice expressing full length human *Huntingtin*⁴⁹. Although the primary cause of HD is toxicity of mutant *Huntingtin*, any therapeutic approach should take into consideration the neuroprotective properties of the wild-type protein.

Toxicity of mutant Huntingtin

Huntington's disease, like many neurodegenerative diseases, is characterized by the abnormal formation of cytoplasmic and nuclear aggregates or inclusions⁵⁰. These inclusions contain ubiquitin and N-terminal cleavage products of mutant *Huntingtin*⁵⁰. Changes in protein folding^{51,52}, cleavage⁵³⁻⁶⁰, clearance⁶¹⁻⁶³ or aberrant protein-protein interactions^{23,64} may contribute to the toxicity and accumulation of mutant *Huntingtin*. Additional sources of toxicity include: disruption of axonal transport^{38,65,66}, impaired mitochondrial function^{67,68},

overproduction of reactive oxygen species⁶⁹⁻⁷¹, disturbed calcium homeostasis^{72,73}, neuroinflammation⁷⁴, and deregulation of transcription⁷⁵.

Microglial activation and neuroinflammation may contribute to the pathology of HD. Microglia are macrophages resident in the mammalian CNS. In the healthy brain, they are quiescent, but in response to injury they rapidly become activated. Activated or reactive microglia display a variety of cell surface antigens and secrete both cytotoxic molecules, including reactive oxygen species and pro-inflammatory cytokines, and cytoprotective molecules such as growth factors⁷⁶. These secreted molecules in turn affect neighboring cells. Reactive microglia have been found in the striatum and cortex of brains from HD patients⁷⁷ and in mouse models of polyglutamine toxicity⁷⁸. Activation of microglia in HD may represent an attempt at repair, but it could also contribute to the cytotoxic cascade which leads ultimately to cell death.

The effect of mutant *Huntingtin* on transcription is partially mediated by binding of the polyglutamine region to glutamine rich transcription factors⁷⁹. Among the transcription factors known to be affected are CREB binding protein (CBP, a transcriptional co-activator and histone acetyltransferase)⁸⁰⁻⁸², specificity protein 1 (Sp1, a sequence specific transcription activator)^{83,84} and REST/NRSF^{41,85}. BDNF, REST/NRSE, Sp1, and *Huntingtin* are linked together in a complex feedback loop that is disrupted by mutant *Huntingtin*. Binding of mutant *Huntingtin* to CBP sequesters CBP in the cytoplasm and prevents activation of its target genes in the nucleus^{81,82} while binding of mutant *Huntingtin*

to Sp1 may prevent its activity by interfering with its ability to form a complex with components of the transcriptional machinery^{83,84}. Sp1 levels are increased in models of HD and reduction of Sp1 appears to be neuroprotective⁸⁶. Sp1 binds to and activates the REST/NRSF promoter⁸⁷ and *Huntingtin* itself may be upregulated by Sp1⁸⁸. Mitochondrial dysfunction is linked to transcriptional deregulation: mutant *Huntingtin* binds to the peroxisome proliferator-activated receptor γ coactivator-1 α (PGC-1 α) promoter, reducing the expression of PGC-1 α , a regulator of mitochondrial respiration⁸⁹.

Mutant *Huntingtin* mRNA may be toxic. RNA transcripts with expanded CAG repeats are neurotoxic in *Drosophila* models of Machado-Joseph disease⁹⁰ and myotonic dystrophy⁹¹ and there are some indications that RNA toxicity is present in HD^{92,93}. Therapeutics which target *Huntingtin* at the mRNA level may therefore be preferable to those targeting the protein.

Therapeutic strategies for HD

The complexity of *Huntingtin* interactions makes developing treatment strategies based on downstream pathogenic processes difficult. Potential therapeutic strategies include: NMDA receptor antagonists to reduce excitotoxicity, histone deacetylase (HDAC) inhibitors to restore transcriptional regulation⁹⁴⁻⁹⁶, caspase inhibitors to prevent *Huntingtin* cleavage⁹⁷⁻⁹⁹, compounds to enhance mitochondrial function^{70,97,100,101}, induction of heat shock proteins to reduce protein aggregation^{102,103} and *Huntingtin* misfolding¹⁰⁴, and induction of

autophagy to improve protein degradation¹⁰⁵. Many of these strategies have shown promise in animal models of HD and in some early clinical studies^{100,106} but results from longer term studies have shown little benefit^{101,107}.

Mutant *Huntingtin* disrupts a large number of cellular pathways and treatment strategies targeting single aberrant pathways may be ineffective. The most direct treatment approach would be to destroy the mutant mRNA and prevent the production of mutant *Huntingtin* protein. Studies in mice suggest that mutant *Huntingtin* toxicity is reversible¹⁰⁸⁻¹¹⁰. RNA interference, which provides a mechanism for sequence specific gene silencing, is a promising therapeutic approach.

The RNAi pathway

History of RNAi

RNA silencing was accidentally discovered in plants when attempts to overexpress the chalcone synthase (CHS) gene --an enzyme responsible for flower pigmentation-- in petunias resulted in plants with white or partially white rather than deep purple flowers^{111,112}. Additional evidence came from studies of viral resistance in tobacco plants: transgenic tobacco plants expressing a non-translatable version of the tobacco etch virus coat protein (TEV CP) could become immune to, or recover from, TEV. These studies suggested that it was not the coat protein that was responsible for viral resistance^{113,114}. Further studies in plants using non-viral transgene sequences confirmed that the silencing signal

was most likely nucleic acid¹¹⁵. In the meantime, a similar silencing of endogenous genes by homologous transgenes, known as quelling, was discovered in fungi¹¹⁶.

The first clue that silencing could occur in animals came from an attempt to inhibit the *par-1* gene in *Caenorhabditis elegans* using antisense RNA¹¹⁷. The researchers found that contrary to their expectations, both sense and antisense RNA could inhibit the gene. In 1998, Fire and Mello established that 21-22 nucleotide double stranded RNA could trigger sequence specific silencing¹¹⁸. These small RNA triggers were termed siRNAs. Only a small amount of siRNA was required to initiate silencing, indicating that silencing was an active process and that the signal was amplified¹¹⁸. Following this discovery, RNAi was uncovered in a number of other species including in *Drosophila*¹¹⁹ and in mammals^{120,121}. Initially, RNAi in mammals appeared to be limited to cells lacking the interferon response, an anti-viral defense that causes non-specific inhibition of protein translation and apoptosis in response to double-stranded RNA. Fortunately, short double stranded RNA including 21-22 nucleotide siRNAs, effectively silence endogenous mRNAs in mammals and do not trigger the interferon response¹²².

Core Machinery of the RNAi pathway

The RNAi pathway is evolutionarily conserved from plants to mammals. At the heart of the RNAi machinery is a core set of proteins, called Argonautes.

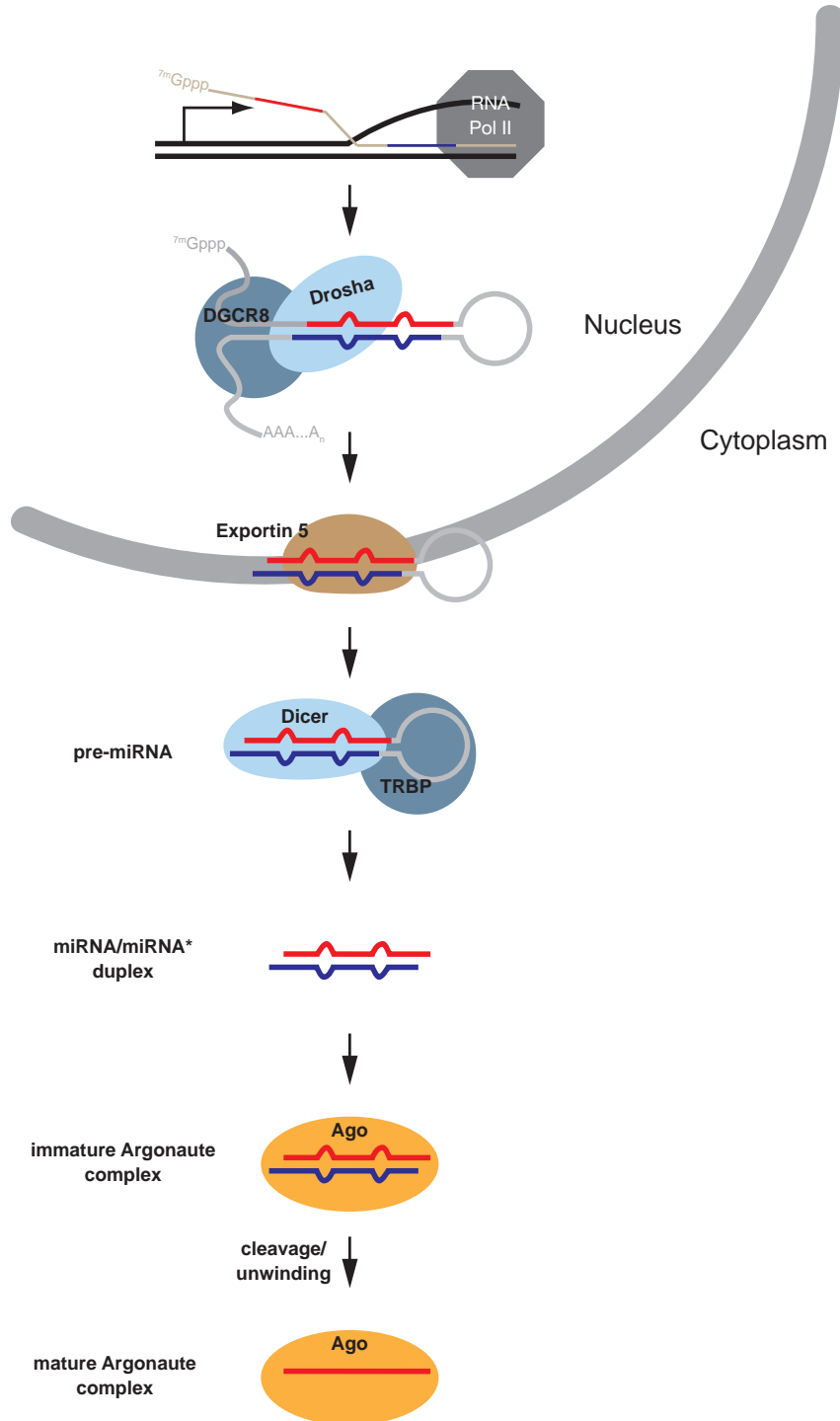
Argonaute proteins use small (18-30 nucleotide) RNAs to guide sequence-specific silencing of mRNA transcripts. Argonaute proteins are composed of four domains: N-terminal, PAZ, Mid and PIWI domains. The Mid and PAZ domains position the small RNA guide strand¹²³⁻¹²⁵ while the PIWI domain is an RNase H domain. Three conserved amino acids (DDH) in the PIWI domain form the catalytic triad required for the endonucleolytic cleavage activity of the enzyme^{123,126-129}. The N-domain of the protein is thought to participate in unwinding of the RNA duplex during Argonaute complex maturation¹³⁰.

The mammalian RNAi pathway

In the mammalian RNAi pathway (Figure 1.1), small RNAs called microRNAs (miRNAs) are transcribed as long hairpins (pri-miRNAs), primarily by polymerase II promoters. Pri-miRNAs are processed in the nucleus by Drosha/DGCR8 to pre-miRNA hairpins approximately 70 nucleotides in length^{95,128,131,132} and exported from the nucleus via Exportin-5^{133,134}. In the cytoplasm, pre-miRNAs are further processed by Dicer/TRBP¹³⁵⁻¹³⁷ to miRNA/miRNA* duplexes, which form complexes with Argonaute proteins. Thermodynamic stability at the 5' end of the duplex determines which strand will be incorporated into the mature Argonaute complex^{138,139}: the strand that is less thermodynamically stable becomes the miRNA while the other strand, called the miRNA* strand, is discarded during complex maturation. Maturation can occur by cleavage of the miRNA* strand¹⁴⁰⁻¹⁴⁴ or by duplex unwinding^{145,146}.

Figure 1.1. The mammalian RNAi pathway

Figure 1.1



Much of the work on RNAi in vertebrates has been done in fruit flies where there are several distinct small RNA pathways. In flies, cleavage of long double-stranded RNA by members of the Dicer family¹³⁶ produces fully complementary siRNAs duplexes. miRNA duplexes, which contain mismatches, are produced from long transcripts (pri-miRNAs) by sequential Drosha and Dicer processing¹⁴⁷. *Drosophila* siRNAs and miRNAs are sorted into distinct complexes: siRNAs into Ago2 complexes¹³⁶, and miRNAs into Ago1 complexes, based on the internal structure of the RNA duplex¹⁴⁸. Ago2-siRNA complexes and Ago1-miRNA complexes silence their targets by different mechanisms. Complexes containing Ago2, which is an efficient endonuclease, can cleave fully complementary mRNAs. Ago1 complexes can silence mRNAs with multiple, partially complementary binding sites¹⁴⁹. Humans have four Argonaute proteins (Ago1-Ago4) but only Ago2, which is homologous to *Drosophila* Ago1, is capable of target cleavage^{128,150}. Ago3 contains a catalytic triad, but is catalytically inactive. Ago1 and Ago4 lack the catalytic triad^{129,150,151}. Despite the existence of distinct Argonaute proteins and the similarity in structure between miRNAs from flies and miRNAs from mammals, most mammalian miRNAs associate with multiple Argonaute proteins^{151,152}.

Argonaute complexes recognize their targets primarily via pairing of the seed sequence, nucleotides 2-8 of the guide strand. Nucleotides outside of this region influence target affinity and mode of silencing of Argonaute complexes. When there is extensive pairing between an mRNA target and an

Argonaute:miRNA complex, competent Argonautes can catalyze endonucleolytic cleavage of the mRNA^{128,150,153-155}. Argonautes cut between positions 10 and 11 of the RNA guide strand¹⁵⁶. Mismatches between the siRNA and target around the cleavage site prevent this activity¹⁵⁶⁻¹⁵⁸. In the absence of cleavage, Argonaute complexes may inhibit translation^{159,160} or cause mRNA destabilization¹⁶¹. Many mammalian miRNAs exhibit only partial complementarity to their mRNA targets^{162,163}. Multiple, adjacent, partially complementary sites can participate in cooperative silencing^{160,164,165}, where binding of a single Argonaute complex promotes binding of complexes to adjacent sites. This mode of silencing requires a higher concentration of the siRNA than does silencing by siRNAs with extensive complementarity¹⁶⁵.

Therapeutic small RNAs are typically designed to be fully complementary to their targets at a single site and to act via cleavage. While extensive pairing between a miRNA and its target mRNA can result in target cleavage, in both flies and humans it can also trigger the degradation of the miRNA. In flies, Ago1 loaded siRNAs are protected from degradation by 2'-O-methylation¹⁶⁶. Whether this finding has any significance for therapeutic applications of RNAi has yet to be determined.

RNAi Therapeutics

Challenges and Strategies

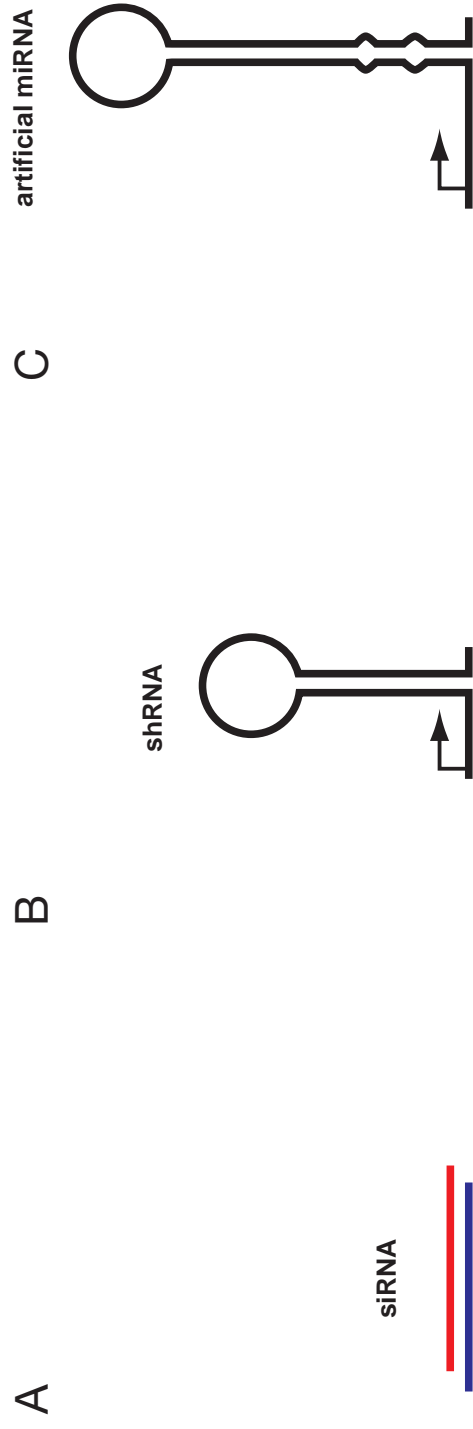
Our mechanistic understanding of RNAi is rapidly improving but therapeutic applications present their own challenges, among them delivery and safety are perhaps the most critical. Effective delivery strategies should address tissue and cell-type specific targeting, effective intracellular delivery, and distribution of the small RNA effector. Safety concerns include off-target silencing of genes with partial complementarity to the therapeutic small RNA, induction of innate immune responses, and saturation of the cellular RNAi machinery.

Therapeutic small RNAs (Figure 1.2A) generally fall into two classes: siRNAs and virally expressed hairpins (shRNAs and artificial miRNAs). siRNAs are small, 19-23 nucleotide, synthetic double-stranded RNAs designed to mimic the products of Drosha and Dicer cleavage. They are delivered to the cytoplasm and incorporate into Argonaute complexes to produce transient silencing. Long term silencing of genes requires chronic infusion or repeated siRNA administration and dosage can be monitored and adjusted during the course of treatment. Although there have been several reports of successful in vivo silencing of endogenous genes by local administration of naked siRNAs¹⁶⁷⁻¹⁷⁰, siRNAs do not readily enter the cell by diffusion. Conjugation^{5,171,172} or encapsulation of siRNAs into liposomes or nanoparticles may improve stability

Figure 1.2. Types of therapeutic RNAi constructs.

(A) siRNAs are designed to mimic the products of sequential cleavage by Drosha and Dicer while shRNAs (B) resemble the products of Drosha cleavage. (C) Artificial miRNAs incorporate the structure of endogenous miRNAs and can be co-transcribed with protein coding genes from polymerase II promoters.

Figure 1.2



and promote entry into the cell by endocytosis. Transfection reagents^{3,173,174} have been used to improve intracellular delivery of siRNAs, but they carry the risk of cytotoxicity. Once inside the cell, siRNAs must dissociate from delivery vehicles, escape the endosomal compartment and incorporate into Argonaute complexes in the cytoplasm. For delivery to the brain, the blood brain barrier presents a significant hurdle therefore most studies have used local rather than systemic delivery. However, delivery of siRNA following intravenous injection of siRNAs complexed to a short peptide from the rabies virus glycoprotein (RVG) has been reported¹⁷⁵. The same RVG peptide has been used to facilitate systemic delivery of liposome-siRNA complexes targeting the prion protein, PrP^C¹⁷⁶ and exosomes loaded with siRNA targeting GAPDH¹⁷⁷.

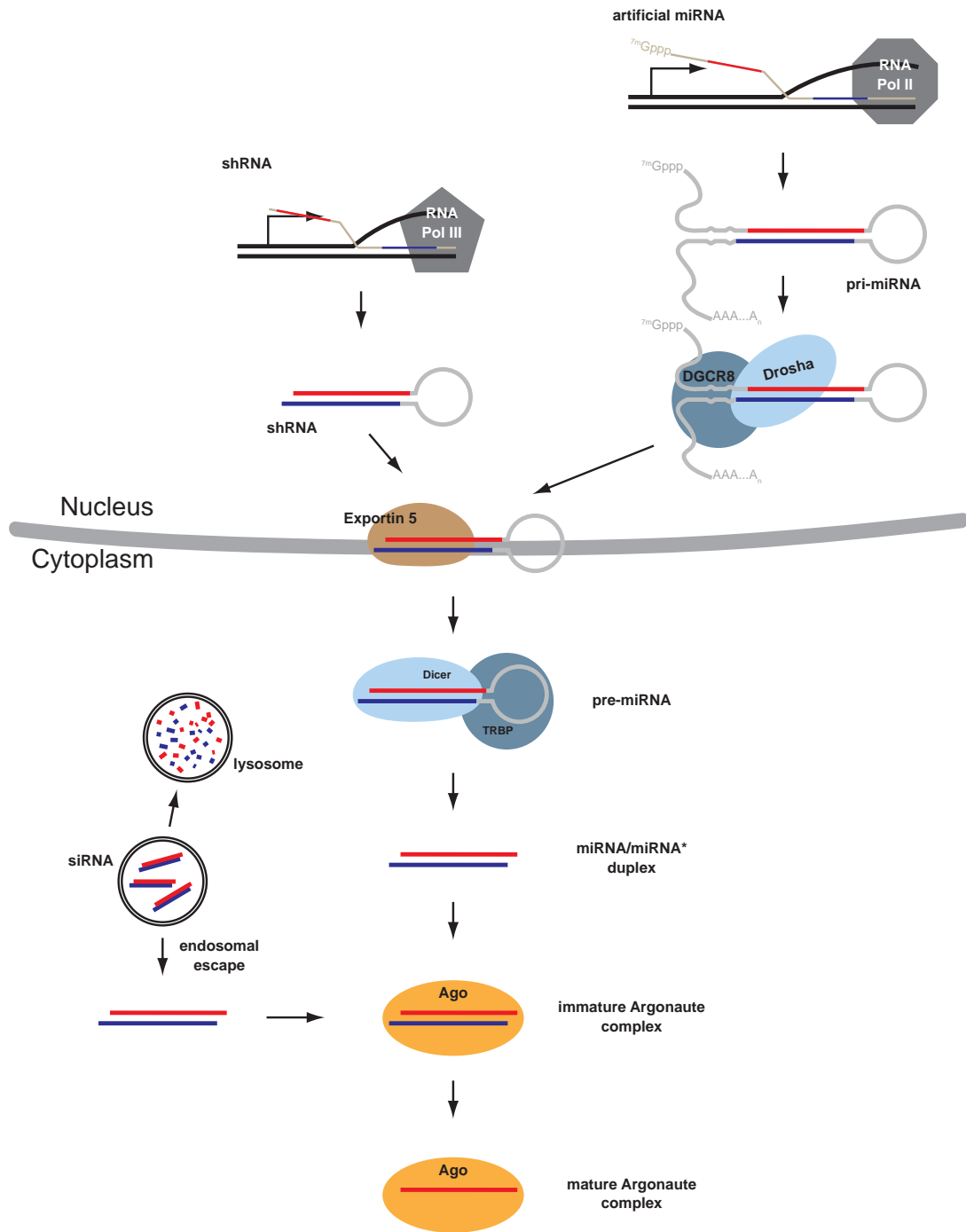
Short hairpin RNAs (shRNAs, Figure 1.2B) and artificial miRNAs (Figure 1.2C) are both hairpin-type constructs expressed from plasmids or viruses. Short hairpin RNAs are generally expressed from RNA polymerase III (Pol III) promoters, which are specialized for transcribing small non-coding RNAs (ribosomal RNAs, small nuclear RNAs, tRNAs). After transcription in the nucleus and export into the cytoplasm by Exportin 5, shRNAs are designed to enter the RNAi pathway at the Dicer processing step (Figure 1.3). Artificial miRNAs are usually transcribed from RNA polymerase II (Pol II) and can be incorporated into longer mRNA transcription units, this makes them ideal for situations in which co-delivery of a protein coding gene and a miRNA is desirable. They are designed to be substrates for processing by Drosha in the nucleus (Figure 1.3). For

therapeutic applications, shRNAs and artificial miRNAs are almost universally packaged into viruses and delivered locally, although some AAV vectors have been shown to cross the blood brain barrier¹⁷⁸. Cell type and tissue specificity is accomplished by selecting a virus with appropriate tropism and can be refined by incorporating binding sites for endogenous miRNA to restrict expression to the tissue of interest¹⁷⁹. Because they mediate long-term target silencing, virally delivered shRNA and miRNA expression constructs are most suitable for conditions that require long term silencing of endogenous genes and where there is little expectation of toxicity.

Figure 1.3. Therapeutic RNAi constructs and the RNAi pathway

siRNAs are delivered to the cytoplasm. Complexed or encapsulated siRNAs must escape the endosomal compartment prior to loading into Argonaute complexes. shRNAs are designed to be transcribed in the nucleus by polymerase III promoters and exported to the cytoplasm by exportin-5. In the cytoplasm they are processed by Dicer and loaded into Argonaute complexes. Artificial miRNAs are primarily transcribed by polymerase II promoters and enter the RNAi pathway at the Drosha processing step.

Figure 1.3



Toxicity: Seed mediated off-target effects

Sequence specific off-target effects can occur when an exogenous small RNA has partial complementarity to endogenous mRNAs^{180,181}. These off-target effects are due largely to complementarity between mRNAs and the 6-7 nucleotide small RNA seed sequence^{68,182,183}. Messenger RNAs with only a seed matching miRNA target site are generally only modestly downregulated in response to the miRNA^{144,184}, therefore the importance of seed-mediated off-target effects is unclear. However, in one study 51 out of 176 randomly selected siRNAs targeting two different mRNAs reduced cell viability in culture. The toxic phenotype was independent of on-target silencing and dependant on components of the RNAi machinery¹⁸⁵. Owing to divergences in the 3'-UTRs of mRNAs and to differences in mRNA expression patterns, off-target effects are species specific¹⁸⁶ and likely cell type specific. Chemical modifications^{187,188} and nucleotide substitutions that destabilize seed:mRNA pairing^{189,190} can reduce guide strand mediated off-target effects.

Seed mediated off-targeting effects can also be occur if the passenger, rather than the guide strand of an siRNA duplex incorporates into the Argonaute complex. Increasing the asymmetry of the siRNA to favor loading of the intended strand can reduce these effects. Strategies to increase asymmetry include: introducing a deliberate mismatch between the 5'-end of the guide strand and the 3'-end of the passenger strand¹³⁹, introducing chemical modifications into the guide or passenger strand^{191,192} or modifying the siRNA structure¹⁹³.

Some nucleotide hexamers are more commonly found in 3'-UTRs than others. The frequency of seed mediated off-target effects can be reduced by avoiding seed sequences that target hexamers that are abundant in the 3'-UTRs of transcribed genes^{194,195}. This may be especially important when designing shRNA or artificial miRNAs. Minimizing sequence specific off targeting of shRNAs and artificial miRNAs can only be accomplished by selecting appropriate sequences, as promoter driven hairpins cannot be chemically modified to reduce off-targeting effects or to favor loading Argonaute loading of the appropriate strand. Unfortunately, selection for low frequency seed sequences limits the pool of potential therapeutic sequences and could preclude targeting of specific disease-associated sites.

Toxicity: Immune Stimulation

In mammalian cells, long double stranded RNA can induce non-specific degradation of RNA and translational repression by a mechanism involving activation of PKR, phosphorylation of elongation factor 2 α ¹⁹⁶, and activation of RNase L¹⁹⁷. Initially, double stranded RNAs shorter than 30bp were thought to escape this response^{122,198} but later studies showed that 21 nucleotide siRNAs can activate PKR and upregulate interferon response genes¹⁹⁹. Short double and single stranded RNAs can also activate an immune response by signaling through Toll-like receptors (TLRs). TLR3, an extracellular receptor which recognizes dsRNA, can be activated non-specifically by siRNAs^{200,201} and signals

through NF- κ B to stimulate production of type I interferons (IFNs)²⁰². TLR7 and TLR8 recognize GU rich single- and potentially double-stranded RNAs²⁰³⁻²⁰⁵ and are thought to be responsible for the sequence-specific immune response to siRNAs²⁰⁶⁻²⁰⁸. Like seed-mediated off-target effects, activation of innate immunity by short RNAs can be prevented by 2'-O-methyl modification²⁰⁹.

Immune responses can be affected by mode of delivery^{206,210}. siRNAs entering the cell via endocytosis (as occurs with liposomal formulations) can be exposed to endosomal TLR3, TLR7 and TLR8 resulting in activation of the immune response. Delivery methods that bypass endocytosis may avoid the same immune response. Two types of RNAi triggers are commonly used to induce RNAi: plasmid- or virally-expressed hairpins and siRNA duplexes. The preceding discussion focused primarily on immune responses to siRNAs, but virally delivered hairpins can also elicit immune responses^{211,212} these responses may depend on expression levels, on structural characteristics of the hairpin or on the animal's previous viral exposure. Very little information is available regarding stimulation of immunity by small RNAs specifically in the brain therefore any RNAi therapeutic for Huntington's disease will need to be evaluated for potential immune stimulation.

Toxicity: Saturation of the RNAi machinery

Overexpression of shRNAs is thought to be responsible for another safety issue: saturation of the small RNA silencing pathway. In mice, intravenous injection of

high doses of virally expressed shRNAs can induce liver toxicity and death. Toxicity is not sequence specific, but is correlated with high shRNA expression and decreased levels of the endogenous liver miRNA, miR-122 suggesting that the shRNAs interfere with endogenous miRNA processing. Overexpression of exportin-5 increases silencing by the shRNA²¹³ but overexpression also increases toxicity²¹⁴ suggesting that toxicity can be caused both by saturation of exportin-5 and by saturation of downstream components²¹⁴. The sequence of an shRNA can affect its expression levels and processing: highly similar shRNA can show dramatically different expression levels and some are inefficiently processed²¹³. Toxicity can be eliminated by lowering the expression of the shRNA using a weaker, tissue-specific promoter²¹⁵. Loss of shRNA-induced silencing in the liver is caused by loss of shRNA expressing cells and is therefore an indication of hepatotoxicity. Overexpression of either Ago-2 or Exportin-5 increases the duration of shRNA induced silencing in the liver, indicating decreased toxicity. Prolonged maximal silencing is only produced by combining a low toxicity shRNA with reduced shRNA dose²¹⁴.

Saturation or overexpression toxicity can occur in the brain as well.

Davidson and colleagues found that injection of two specific AAV-shRNAs targeting exon 2 and 30 of *Huntingtin* (AAVsh2.4-GFP, AAVsh30.1-GFP) into the striatum caused microglia activation and loss of staining for dopamine and cAMP-regulated protein (DARPP-32), a marker of medium spiny neurons. A third shRNA targeting exon 8 of *Huntingtin* (AAVsh8.2-GFP) was not toxic²¹⁶. The

passenger strand and the unprocessed shRNA transcript were undetectable in the brain, indicating that the shRNA was exported to the cytoplasm, processed by Dicer and loaded into Argonaute complexes. Toxicity was correlated with higher expression of the mature guide strand suggesting that a later component of the RNAi pathway, possibly Argonaute, was limiting. Lowering the viral titer reduced both toxicity and silencing efficacy, whereas incorporating the sequences into a miRNA backbone lowered the levels of the precursor and mature guide strand in cell culture and reduced toxicity in vivo without affecting *Huntingtin* silencing²¹⁶. In an attempt to compare the silencing efficiency of shRNAs and artificial miRNAs, Davidson's group developed optimized shRNAs and miRNAs expressed from the same U6 promoter and producing the same mature guide strand sequence. They found that the shRNAs were more potent, but that the precursor transcript accumulates both in the nucleus and in the cytoplasm indicating that overexpression of shRNAs may saturate the RNAi machinery at multiple steps²¹⁶. In contrast, precursors from artificial miRNAs do not accumulate. Toxicity caused by overexpression of shRNAs is not limited to mice. Similar findings have been reported in the rat substantia nigra^{217,218} and in dog heart²¹⁹.

Saturation of the endogenous miRNA machinery can cause competition between exogenous small RNAs and endogenous miRNAs. In competition assays, shRNAs reduce the efficiency and processing of co-expressed GFP miRNAs, whereas artificial miRNAs do not⁶. There is evidence of competition

between siRNAs: co-administration of inactive with active siRNAs reduces silencing²²⁰. Argonaute-2 in particular may be limiting. Reduced expression of Ago2, but not of exportin-5 or of other components of the RNAi pathway decreases siRNA potency and increases competition between siRNAs²²¹. Overexpression of exportin-5 increases both shRNA potency and toxicity in the liver²¹⁴, again suggesting that the miRNA pathway can be saturated downstream of exportin-5²¹⁴.

It has been suggested that artificial miRNAs do not compete for saturable components of the RNAi machinery²²² but the components of the RNAi pathway are expressed at different levels in different cell types and in different tissues. Toxicity may depend both on the type of construct and on the target tissue. In addition to the striatal loss of neurons described by the Davidson group²¹⁶, it has recently been shown that striatal delivery of U6 promoter driven shRNAs targeting torsinA, which causes the dominantly inherited disease DYT1 dystonia, can cause lethal toxicity²²³. The cause of this toxicity is unclear, but 129/SvEv mice were more susceptible than C57BL/6²²³.

Disruption of endogenous miRNAs in the brain may be of particular concern. A large number of miRNAs are expressed in the brain²²⁴, some of these appear to be involved in maintaining neuronal differentiation²²⁵. Disruption of miRNA biogenesis in the brain can cause behavioral and neuropathological defects: deletion of Dicer in cerebellar Purkinje cells²²⁶ or in astroglia²²⁷ causes progressive neurodegeneration. Changes in miRNA expression and alteration of

miRNA networks, including one involving a feedback loop between REST/CoREST and mir9/mir9^{*228-230} may play a role in HD pathogenesis. In mouse models of HD, global changes in miRNA expression coincide with changes in the levels of key components of the miRNA processing machinery²³¹. Disruption of the endogenous miRNA pathway in HD may increase the likelihood of pathway saturation and complicate the development of HD therapeutics.

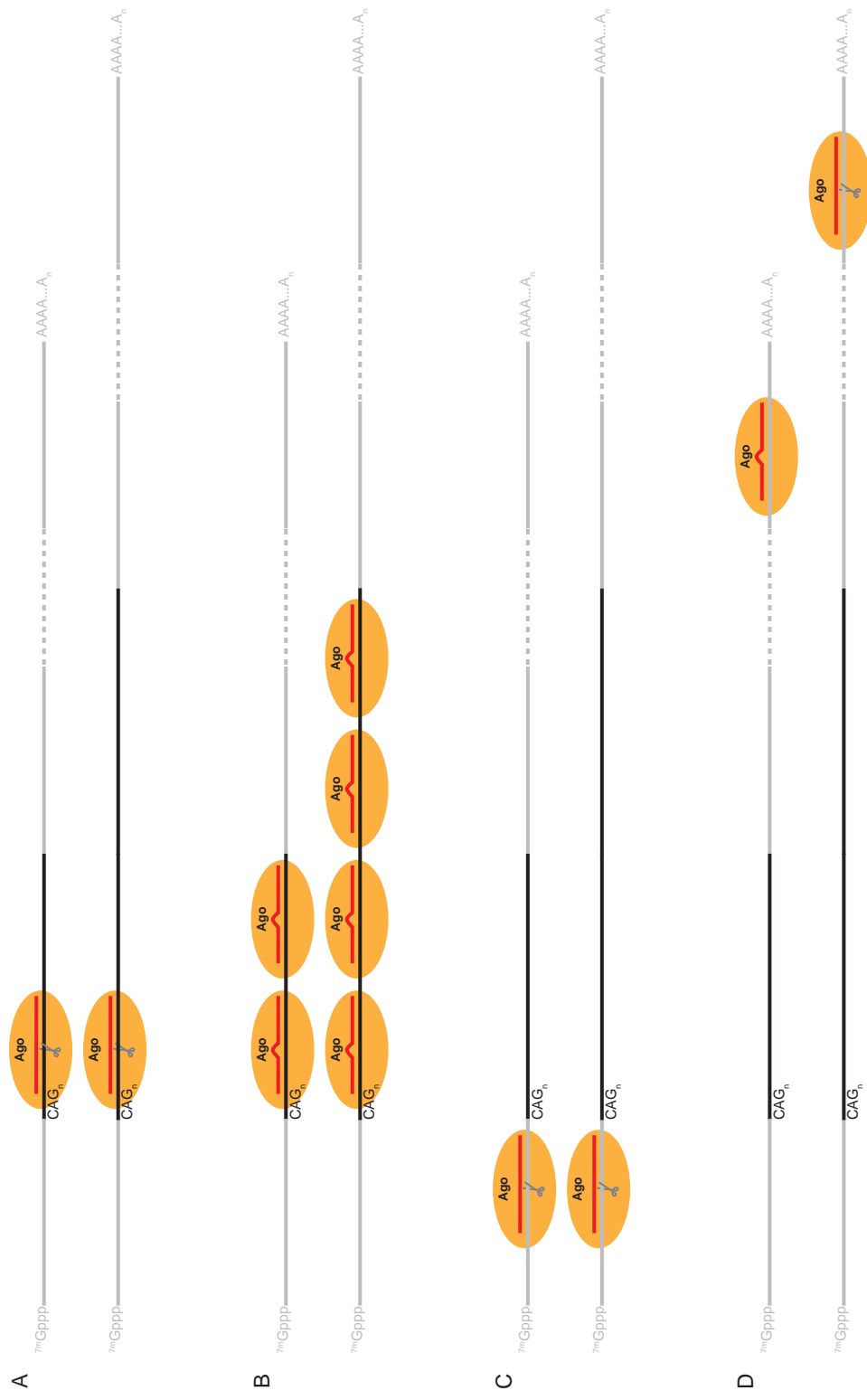
RNAi Therapy for Huntington's Disease

Three main approaches to RNAi therapeutics for HD have emerged (Figure 1.4), simultaneous silencing of mutant and normal *Huntingtin* (nonallele-specific silencing), direct targeting of the CAG repeat region, and targeting of polymorphisms in the *Huntingtin* gene. For any disease therapy there are two goals: treat the disease and minimize the side effects. For an autosomal dominant disease, like HD, the most direct approach would be to specifically eliminate the toxic gene product.

Figure 1.4. RNAi approaches to Huntington's disease

(A) An siRNA with perfect complementarity to the CAG repeat region of the Huntingtin mRNA cleaves both the normal and the expanded isoforms. (B) Translational repression by an imperfectly matched CAG targeting siRNA requires multiple binding sites. The mutant Huntingtin mRNA, with more binding sites, is preferentially targeted. (C) Gene-specific (nonallele-specific) targeting of Huntingtin by perfectly complementary siRNAs outside of the CAG repeat region. (D) Targeting of single nucleotide polymorphisms to distinguish between mutant and normal isoforms.

Figure 1.4



CAG Targeting

The most obvious target in HD is the CAG repeat expansion itself. Normal *Huntingtin* contains 18-35 CAGs or 2-5 binding sites for a typical 21 nucleotide siRNA. A perfectly matched siRNA, which requires only a single binding site, should bind and cleave both the normal and the mutant *Huntingtin* mRNA (Figure 1.4A). Preventing cleavage by introducing mismatches between the siRNA guide and its miRNA target so that multiple binding sites are required to achieve silencing (Figure 1.4B) may allow discrimination between long and short isoforms²³². However, there are over 400 CAG repeats in the human genome. Over 60 protein coding genes containing CAG repeats are translated into proteins having 5 or more consecutive glutamines²³³. Oligonucleotides targeting the CAG repeat region alone may not be gene specific.

Gene-specific silencing

Because of the difficulties involved in CAG repeat targeting, many studies have used gene specific (nonallele-specific) small RNAs. Polymerase III driven short hairpin RNAs (shRNAs) perfectly matched to human *Huntingtin* but containing mismatches to the mouse mRNA reduce neuronal inclusions and improve or delay behavioral deficits in transgenic mice expressing truncated versions of human *Huntingtin*^{2-4,234}. Transgene mRNA levels in the striatum were reduced by 50%⁴ to 75%²³⁴ and protein by 40%²³⁴. The shRNAs used in these studies contain mismatches to the mouse *Huntingtin*. One study used an shRNA with

mismatches to mouse *Huntingtin* at positions 4, 9-11 and 17. The authors report no reduction of mouse *Huntingtin* by qRT-PCR⁴. Notably, although the intended guide strand is easily detected in Northern blots, the shRNA used in this study likely exhibits inappropriate strand biasing⁴. Rodriguez-Lebron²³⁴ and colleagues tested two shRNAs: a 19-mer targeting the 5'-UTR of human *Huntingtin* (siHUNT-1) and a 21-mer targeting sequences in exon1 upstream of the CAG repeat region (siHUNT-2). The 5'-UTR targeting shRNA is likely human specific, but siHUNT-2 contains only 3 mismatches to the mouse *Huntingtin* at positions 1, 10 and 19. It is unclear if these mismatches are sufficient to prevent partial silencing of mouse *Huntingtin*. siHUNT-2 but not siHUNT-1 caused a reduction in the levels of several other striatal mRNA transcripts in both R6/1 and wild-type mice²³⁴. This effect was sequence specific, as ribozymes targeting the same region produced similar disruptions in striatal mRNA transcripts²³⁵.

siRNAs can also reduce clinical and neuropathological symptoms in mice. Injection of siRNAs targeting the same region of exon1 of the human *Huntingtin* into newborn mice prolongs lifespan and reduces behavioral defects in a rapid onset transgenic model of HD (R6/2)³. Co-injection of cholesterol conjugated siRNA targeting *Huntingtin* exon 1 can reduce neuropathology induced by an AAV virus encoding an N-terminal (1,395 nucleotides), CAG expanded human *Huntingtin* fragment⁵. Although the siRNA in this experiment also matches mouse *Huntingtin*, the time course of this experiment was too short to draw any conclusions about the effects of mouse *Huntingtin* knockdown.

Studies targeting human *Huntingtin* transgenes in the presence of mouse *Huntingtin*^{2-5,234} have shown promise, but the presence of the wild-type mouse *Huntingtin* complicates the interpretation of results. Silencing the mutant transgene generally improves behavior and reduces neuropathology, but when mouse *Huntingtin* is left intact, these studies more closely resemble allele-specific rather than gene-specific silencing. Unfortunately, the sequences used cannot be expected to achieve allele-specific silencing in humans.

In order to examine the effects of simultaneous silencing of wild-type and mutant *Huntingtin* (gene-specific silencing, Figure 1.4D), Boudreau and colleagues used an artificial miRNA targeting both human and mouse *Huntingtin*. HD-N171-82Q. Mice treated with this miRNA showed improved performance in behavioral assays (rotarod) and improved survival when compared to control treated mice⁶. In microarray experiments, silencing of mouse *Huntingtin* in wild-type mice caused two fold or greater expression changes in 473 transcripts and subtle changes in transcripts containing RE1/NRSE binding sites⁶. Simultaneously, a second group showed, using a lentiviral shRNA, that 65-75% reduction in endogenous rat *Huntingtin* caused gene expression changes in pathways associated with wild-type *Huntingtin* function, but did not produce any signs of toxicity¹¹⁰. Overall, these results indicate that partial nonallele-specific silencing of *Huntingtin* may be tolerated. However, the long term effects of subtle changes caused by reduction of wild-type *Huntingtin*, in particular on the ability of neurons to respond and recover from toxic insults, are difficult to predict. The

clear advantage of both CAG repeat targeting and nonallele-specific silencing is that both approaches support a single treatment, which could be optimized for potency and specificity and would be suitable for all HD patients.

Targeting single nucleotide polymorphisms

One alternative to direct CAG targeting or nonallele-specific silencing is to use heterozygous single nucleotide polymorphisms to distinguish between the mutant and wild-type *Huntingtin* mRNA. siRNAs can distinguish between mRNAs differing at a single nucleotide^{158,236,237}. Discrimination depends on the position and composition of the mismatch between the siRNA guide strand and the mRNA target: purine:purine mismatches at positions 10 or 16 are good candidates for single-nucleotide discrimination^{237,238}. For siRNA:mRNA pairs where single nucleotide mismatches do not provide sufficient discrimination between two SNP isoforms, additional mismatches in the seed region or at the 3'-end of the siRNA guide strand can improve discrimination^{239,240}.

Allele-specific siRNAs have been developed for SNPs in several disease causing genes including the SOD1, *Huntingtin* and ataxin-3 genes^{236,237,240}.

Allele-specific shRNAs targeting SNP sites have been developed for other CAG repeat expansion diseases²⁴⁰⁻²⁴². Expansion of the CAG repeat region in the coding region of the ataxin-3 gene causes Machado-Joseph disease/spinocerebellar ataxia type 3 (MJD/SCA3)²⁴³. In rats, co-delivery of an shRNA targeting a SNP at the 3'-end of the CAG repeat region of ataxin-3

decreases neuropathology in a lentiviral model of MJD²⁴¹. Both shRNAs and artificial miRNAs targeting a SNP site in ataxin-7, the gene responsible for spinocerebellar ataxia type 7 (SCA7) discriminate between the mutant and wild-type isoforms in cell culture but the miRNA may be safer²⁴². The shRNA, but not the miRNA, competes with a co-delivered GFP shRNA causing a reduction in GFP silencing²⁴².

In the previous examples, selecting a SNP to target is straightforward. A single nucleotide polymorphism in the SOD1 mRNA causes an inherited form of Amyotrophic Lateral Sclerosis (ALS) and specific haplotypes are associated with both SCA7 and SCA3. In contrast, the HD CAG repeat expansion was not previously thought to be associated with any specific SNPs. For SNP targeting to be practical for HD, there must be sufficient heterozygosity in the *Huntingtin* gene for a majority of patients to be covered by a small number of SNP sites. Hayden and colleagues provided evidence that the SNP distribution of HD and normal chromosomes differ²⁴⁴. Ninety-five percent of HD chromosomes belong to a single haplotype defined by 10 SNPs; only fifty-three percent of control chromosomes belong to this same haplogroup. Consequently, approximately forty-five percent of patients can be expected to be heterozygous and could, in theory, be treated with a single siRNA targeting one of the SNPs that defines this haplogroup. However, this study did not distinguish between SNPs occurring in introns, which are not useful for RNAi, and those in exons, which are candidate therapeutic targets. Our strategy was to develop a panel of SNP targeted RNAi

therapeutics. In individual patients, the appropriate SNP-selective therapeutic would be chosen from among the panel using SNP linkage by circularization (SLic)²⁴⁵. In this method, circularization of a PCR amplified fragment of the *Huntingtin* cDNA brings the CAG repeat and a heterozygous SNP site into close proximity, and linkage between the CAG repeat and the SNP can be established by sequencing (Fig. 1.6). Once the SNP-CAG linkage is established, the appropriate RNAi therapeutic could be selected from the panel. However, if each SNP covers only a few patients, the cost of developing such a panel would not only be prohibitive, but a meaningful phase III drug trial might be impossible. This dissertation describes our approach to developing SNP targeting RNAi therapy for HD.

**CHAPTER II: FIVE SIRNAS TARGETING THREE SNPS IN HUNTINGTIN MAY
PROVIDE THERAPY FOR THREE-QUARTERS OF HUNTINGTON'S DISEASE
PATIENTS**

Preface

The work presented in this chapter was a collaborative effort. Lori Kennington and Sujata Wagh performed the genotyping of human DNA samples. Lori Kennington and I analyzed the sequencing results. Juerg Straubhaar performed the statistical analyses and generated Figure 2.1B. Wanzhou Liu determined the SNP-CAG linkage presented in Table 2.2. Lori Kennington and I cloned the SNP sites into the luciferase reporters. I designed the siRNAs and generated and analyzed the data for the luciferase assays. I did the Western blotting and qRT-PCR.

This work has appeared as:

Five siRNAs targeting three SNPs in *Huntingtin* may provide therapy for three-quarters of Huntington's disease patients.

Pfister, EL, Kennington L, Straubhaar J, Wagh S, Liu W, DiFiglia M, Landwehrmeyer B, Vonsattel JP, Zamore PD, Aronin N. *Curr Biol*. 2009 May 12; 19(9): 774-778.

Summary

Among dominant neurodegenerative disorders, Huntington's disease (HD) is perhaps the best candidate for treatment with small interfering RNAs (siRNAs)^{2-5,246-250}. Invariably fatal, HD is caused by expansion of a CAG repeat in the *Huntingtin* gene, creating an extended polyglutamine tract that makes the *Huntingtin* protein toxic¹. Silencing mutant *Huntingtin* mRNA should provide therapeutic benefit, but no siRNA strategy can yet distinguish among the normal and disease *Huntingtin* alleles and other mRNAs containing CAG repeats⁷. siRNAs targeting the disease isoform of a heterozygous single-nucleotide polymorphism (SNP) in *Huntingtin* provide an alternative^{158,236,237,251,252}, because such siRNAs should preserve expression of normal *Huntingtin*, which likely contributes to neuronal function^{29,253,254}. We sequenced 22 predicted SNP sites in 225 human samples corresponding to HD and control subjects. We find that 48% of our patient population is heterozygous at a single SNP site; one isoform of this SNP is associated with HD. Several other SNP sites are frequently heterozygous. Consequently, five allele-specific siRNAs, corresponding to just three SNP sites, could be used to treat three-quarters of the United States and European HD patient populations. We have designed and validated selective siRNAs for the three SNP sites, laying the foundation for allele-specific RNAi therapy for HD.

Results

Current strategies for designing single nucleotide-selective siRNAs rely on SNPs that produce a purine:purine mismatch between the siRNA guide strand and the counter-selected mRNA target^{237,238}. Only 4 of the 12 nucleotide mismatches satisfy this criterion. Even when purine:purine mismatches are available, single-mismatch siRNAs vary in their selectivity, ranging in one study, for example, from 4.3- to 133-fold discrimination between the fully complementary targeted RNA and the mismatched, counter-selected RNA²³⁷.

Sequencing and analysis of Huntingtin SNP sites in HD and control patients

We sequenced twelve PCR amplicons spanning 22 known SNP sites in *Huntingtin* using genomic DNA from 109 Huntington's disease patients and 116 non-HD controls (Figure 2.1). The sequenced DNA encompassed six complete coding exons and the portion of exon 67 that contains the stop codon and part of the 3' untranslated region (UTR). Twenty-two of the SNP sites were reported in the SNPper database^{255,256}. Four of these reported SNP sites were present only as a single isoform in our population. We identified an additional two sites by resequencing exons 2–67 in the *Huntingtin* locus from six HD patient samples.

Figure 2.1. Analysis of SNPs in the human *Huntingtin* mRNA

We sequenced PCR amplicons from genomic DNA from 109 HD patients and 116 controls spanning 22 SNP sites within the *Huntingtin* mRNA. The SNP at nucleotide 9,633 (rs362307, shown in red) is associated with HD and sites for which we have designed siRNAs are in bold..

Figure 2.1

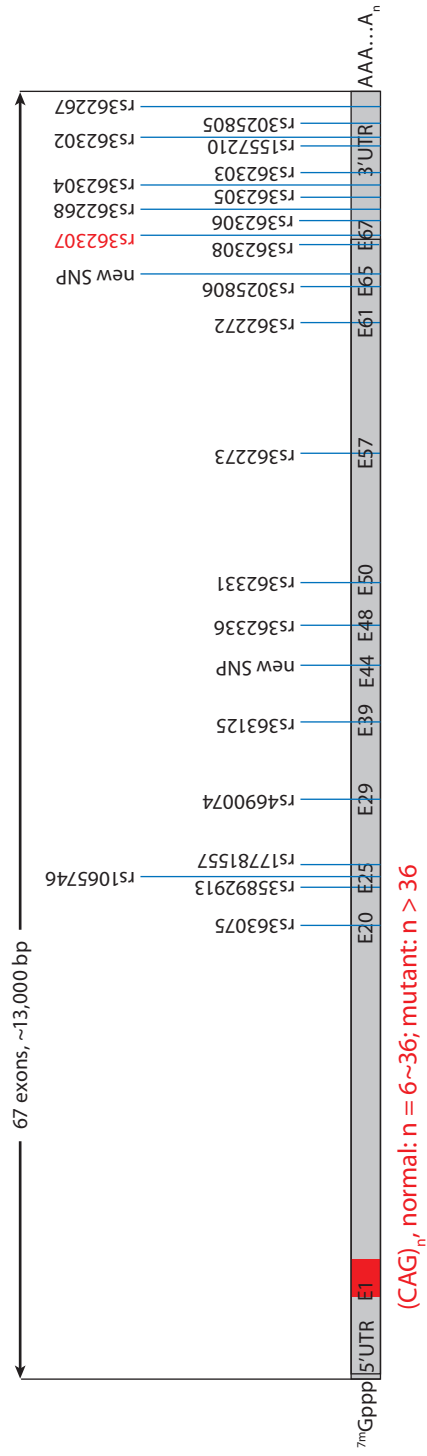


Table 2.1 reports the frequency of heterozygosity for each SNP site for patient and control DNA.

Of the 24 SNPs, rs362307 at nt 9,633 (exon 67) of the mRNA was significantly associated with HD ($p = 0.0000523$). After Bonferroni correction for multiple testing, the association remained significant ($p = 0.000890$). More than 48% of the HD patients we examined—which are believed to be representative of the US and European patient pool—were heterozygous at this site (Table 2.1). The U isoform of the rs362307 SNP comprised 26% of *Huntingtin* alleles among the patients we tested, but in only 6% of alleles among the controls. This finding suggests that a single, allele-specific siRNA selectively targeting the U mRNA isoform of this SNP could be used to treat nearly half of this patient population. To confirm our statistical analysis, we used a previously reported method to determine the rs362307 SNP isoform linked to the CAG repeat expansion allele²⁴⁵ for 16 patient blood samples. Eight out of the 16 patients were heterozygous at this site; of the eight, the U isoform was linked to the expanded CAG repeat for seven patients (Table 2.2). We conclude that the U isoform of this SNP is associated with the disease allele of *Huntingtin* mRNA.

Table 2.1. Frequency of Heterozygosity for 24 SNP sites in the *Huntingtin* mRNA

The SNP sites for which we tested siRNAs are in bold; the SNP associated with HD is shaded.

Table 2.1

Location in mRNA (position, nt)	Reference Number	Percent heterozygosity	
		Controls	HD patients
ORF, exon 20 (2822)	rs363075	G/A, 10.3% (G/G, 89.7%)	G/A, 12.8% (G/G, 86.2%; A/A 0.9%)
ORF, exon 25 (3335)	rs35892913	G/A, 10.3% (G/G, 89.7%)	G/A, 13.0% (G/G, 86.1%; A/A, 0.9%)
ORF, exon 25 (3389)	rs1065746	G/C, 0% (G/G 100%)	G/C, 0.9% (G/G 99.1%)
ORF, exon 25 (3418)	rs17781557	T/G, 12.9% (T/T, 87.1%)	T/G, 1.9% (T/T, 98.1%)
ORF, exon 29 (3946)	rs4690074	C/T, 37.9% (C/C, 50.9%; T/T, 11.2)	C/T, 35.8% (C/C, 59.6%; T/T, 4.6%)
ORF, exon 39 (5304)	rs363125	C/A, 17.5% (C/C, 79.0%; A/A, 3.5%)	C/A, 11.0% (C/C, 87.2%; A/A, 1.8%)
ORF, exon 44 (6150)	exon 44 (new)	G/A, 0% (G/G, 100%)	G/A, 2.8% (G/G, 97.2%)
ORF, exon 48 (6736)	rs362336	G/A, 38.7% (G/G, 49.6%; A/A, 11.7%)	G/A, 37.4% (G/G, 57.9%; A/A, 4.7%)
ORF, exon 50 (7070)	rs362331	T/C, 45.7% (T/T, 31.0%; C/C, 23.3%)	T/C, 39.4% (T/T, 49.5%; C/C, 11.0%)
ORF, exon 57 (7942)	rs362273	A/G, 40.3% (A/A, 48.2%; G/G, 11.4%)	A/G, 35.2% (A/A, 60.2%; G/G, 4.6%)
ORF, exon 61 (8501)	rs362272	G/A, 37.1% (G/G, 51.7%; A/A, 11.2%)	G/A, 36.1% (G/G, 59.3%; A/A, 4.6%)
ORF, exon 65 (9053)	rs3025806	A/T 0% (C/C, 100%)	A/T 0% (C/C, 100%)
ORF, exon 65 (9175)	exon 65 (new)	G/A, 2.3% (G/G, 97.7%)	G/A, 0% (G/G, 100%)
ORF, exon 67 (9523)	rs362308	T/C, 0% (T/T, 100%)	T/C, 0% (T/T, 100%)
3' UTR, exon 67 (9633)	rs362307	C/T, 13.0% (C/C, 87.0%)	C/T, 48.6% (C/C, 49.5%; T/T 1.9%)
3' UTR, exon 67 (9888)	rs362306	G/A, 36.0% (G/G, 52.6%; A/A, 11.4%)	G/A, 35.8% (G/G, 59.6%; A/A, 4.6%)
3' UTR, exon 67 (9936)	rs362268	C/G, 36.8% (C/C, 50.0%; G/G 13.2%)	C/G, 35.8% (C/C, 59.6%; G/G, 4.6%)
3' UTR, exon 67 (9948)	rs362305	C/G, 20.2% (C/C, 78.1%; G/G 1.8%)	C/G, 11.9% (C/C, 85.3%; G/G, 2.8%)
3' UTR, exon 67 (10060)	rs362304	C/A, 22.8% (C/C, 73.7%; A/A, 3.5%)	C/A, 11.9% (C/C, 85.3%; AA, 2.8%)
3' UTR, exon 67 (10095)	rs362303	C/T, 18.4% (C/C, 79.8%; T/T, 1.8%)	C/A, 11.9% (C/C, 85.3%; T/T, 2.8%)
3'-UTR, exon 67 (10704)	rs1557210	C/T, 0% (C/C 100%)	C/T, 0% (C/C 100%)
3' UTR, exon 67 (10708)	rs362302	C/T, 4.3% (C/C, 95.7%)	C/T, 0% (C/C, 100%)
3'-UTR, exon 67 (10796)	rs3025805	G/T, 0% (G/G 100%)	G/T, 0% (G/G 100%)
3' UTR, exon 67 (11006)	rs362267	C/T, 36.2% (C/C, 52.6%; T/T, 11.2%)	C/T, 35.5% (C/C, 59.8%; T/T, 4.7%)

Table 2.2. The U Isoform of SNP rs362307 at Huntingtin mRNA Nucleotide 9,633 Is Associated with the Expanded CAG Disease Allele

Table 2.2

Patient number	Linkage		
	Nucleotide	Mutant allele	Normal allele
4	C/U	U	C
5	C/U	U	C
7	C/U	U	C
8	C/U	U	C
9	C/U	C	U
11	C/U	U	C
14	C/U	U	C
15	C/U	U	C

An additional two SNPs achieve patient coverage > 75%

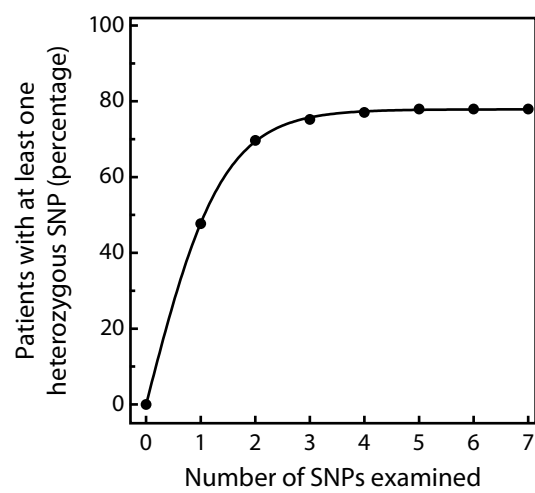
Eight other SNP sites were each heterozygous in > 33% of our patient population, but did not show a statistically significant association with HD. Because no particular isoform of these SNPs is associated with HD in our patient population, each SNP site requires two distinct, isoform-selective siRNAs. We calculated the maximum coverage (i.e., the number of patients with at least one heterozygous SNP site) for all possible combinations of 1 to 7 SNPs. Adding two additional SNP sites covered ~75% of our patient population. Using four or more SNP sites as potential targets for siRNA therapy is not predicted to provide much additional benefit: using even seven SNP sites achieves < 80% coverage, but would require 13 isoform-selective siRNAs (Figure 2.2).

Figure 2.2. Heterozygosity of SNPs in HD patients

The maximum percentage of patients to have at least one heterozygous SNP using any combination of 1 to 7 SNPs was calculated using the experimentally determined frequency of heterozygosity for the SNP sites in our study. Three SNPs cover ~75% of the patient population analyzed here

Figure 2.2. Repression of Luciferase Expression in Reporter Assays Corresponds to Depletion of Endogenous Huntingtin mRNA

Figure 2.2



Luciferase reporter assays using matched and mismatched targets are good predictors of efficacy and selectivity for endogenous mRNA targets

To verify that luciferase reporter assays are good predictors of the efficacy and selectivity of siRNAs for endogenous mRNA targets, we compared the ability of a pair of siRNAs (Figure 2.3A) targeting a SNP site (rs363125) to discriminate between matched and mismatched isoforms of endogenous HeLa cell *Huntingtin* mRNA to the ability of the same set of siRNAs to reduced luciferase activity of the matched and mismatched reporters. HeLa cells have a C at this position in the mRNA. In luciferase assays, the siRNA matched to the C isoform of the SNP has an IC₅₀ of 0.06nM and reduces luciferase activity by 88%, whereas the siRNA targeting the U isoform has an IC₅₀ of 0.11nM and reduces activity from the C target by 55% (Figure 2.3B). We measured the levels of endogenous HeLa cell *Huntingtin* mRNA by quantitative RT-PCR and found that the IC₅₀ of the matched siRNA targeting the endogenous HeLa cell mRNA is 0.5nM. *Huntingtin* mRNA levels are reduced by an average of 87%. We are unable to calculate an IC₅₀ using the mismatched siRNA, but *Huntingtin* mRNA levels are reduced by 66% (Figure 2.3C). We observed a corresponding difference in the levels of endogenous *Huntingtin* protein (Figure 2.4).

Figure 2.3. Repression of Luciferase Expression in Reporter Assays Corresponds to Depletion of Endogenous Huntingtin mRNA

(A) Matched and mismatched siRNAs targeting the SNP rs363125 at nt 5,304 of Huntingtin mRNA. siRNAs are shown in capital letters with the passenger strand at top and the guide strand paired to the mRNA, in lower case letters. The mismatch is at siRNA position 10. Dose-response analysis for these siRNAs using (B) transfected plasmids expressing luciferase reporters and (C) quantitative RT-PCR assays measuring endogenous Huntingtin mRNA. HeLa cells are homozygous for the C isoform of this SNP (data not shown).

Figure 2.3

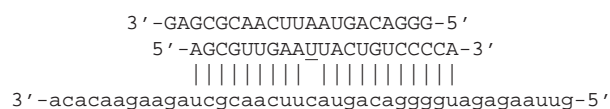
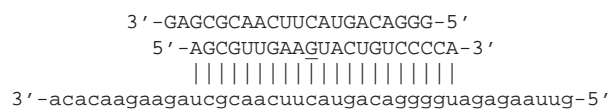
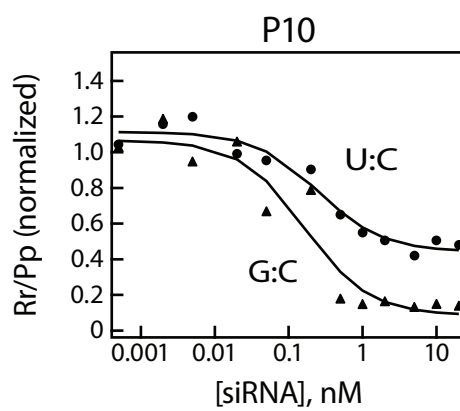
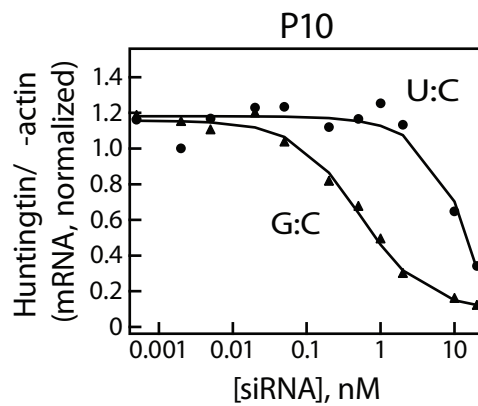
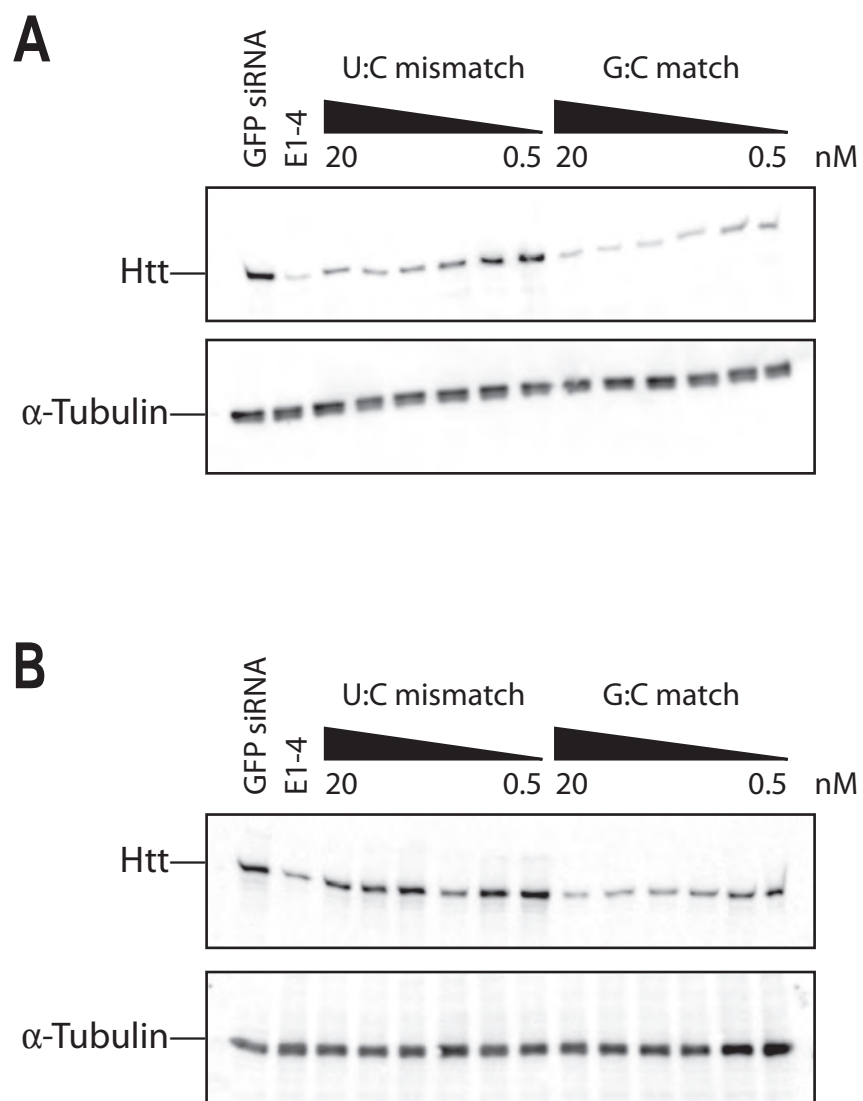
A**B****C**

Figure 2.4. A Fully Matched siRNA That Reduces Expression of Both a Luciferase Reporter and Endogenous *Huntingtin* mRNA Causes a Corresponding Depletion of Endogenous Huntingtin Protein

An identical siRNA, but for a position 10 (P10) mismatch to the luciferase reporter and to the endogenous Huntingtin mRNA, was far less effective at suppressing Huntingtin protein production. HeLa cells were transfected with either the P10 match or P10 mismatch siRNA targeting SNP rs363125 at nt 5,304 of the Huntingtin mRNA, GFP siRNA alone, or a positive control siRNA targeting a non-polymorphic site in Exon 1 (E1-4) of the Huntingtin mRNA⁵. Cells were lysed 48 h after transfection and analyzed by Western blotting using antibodies to Huntingtin and α -Tubulin, which served as a loading control. (A) and (B) show independent replicates of the experiment.

Figure 2.4



Development of allele-specific siRNAs

The HD-associated SNP site at position 9,633 of the *Huntingtin* mRNA does not fall into the category of SNPs predicted to be readily amenable to selective targeting, because it does not create a purine:purine mismatch between siRNA and mRNA^{237,238}. However, our analysis of *Huntingtin* SNPs in HD patients and controls (Figure 2.2 and Table 2.1) suggests that a practicable RNA silencing therapy for HD requires an siRNA that targets the disease isoform at this site, but spares the normal *Huntingtin* mRNA. To this end, we designed siRNAs targeting the U isoform of the position 9,633 SNP. We tested both the efficacy and selectivity of the siRNAs in cultured human HeLa cells co-transfected with the siRNA and luciferase reporters containing in their 3' UTRs either the U or C isoform of the sequence containing the SNP. Previous work has shown that such SNP selective siRNAs can reduce mutant *Huntingtin* levels while leaving normal *Huntingtin* intact²⁵⁷.

siRNAs whose guide strand was fully matched to the U isoform, which is associated with HD, but mismatched at position 10 or position 16 to the C isoform, were functional, but failed to discriminate between U and C reporter mRNAs (Figure 2.5). (siRNAs that bear purine:pyrimidine mismatches to their counter-selected targets generally show poor discrimination²³⁷.) We also tested single mismatches at positions 2 through 9 (Table 2.3), but found that all of these were less specific than the most selective position 10 + seed mismatch.

Figure 2.5. siRNAs with single mismatches at position 10 or 16 do not discriminate between the U and C isoforms of rs362307

siRNAs targeting the U isoform of rs362307 and mismatched to the C isoform at either position 10 or position 16 did not discriminate between matched and mismatched luciferase reporter mRNAs. Representative data are shown.

Figure 2.5

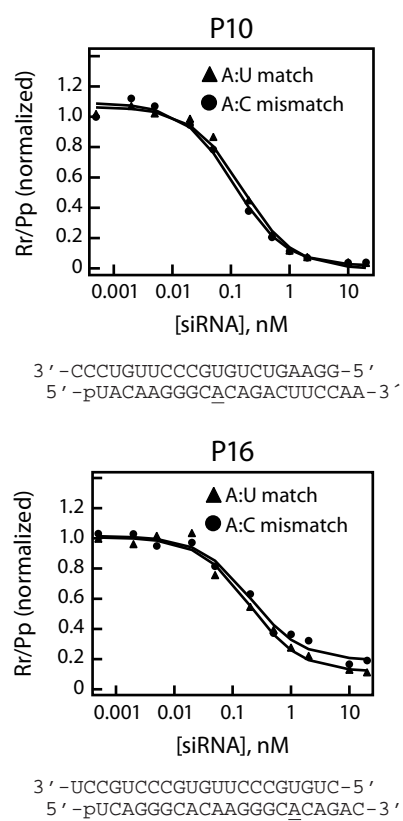


Table 2.3. Validation of siRNAs Designed to Discriminate between Isoforms of the rs362307 SNP

The IC50 is reported as > 20 nM for siRNAs that failed to achieve half maximal inhibition at the highest concentration tested.

Table 2.3

siRNA guide strand	SNP position	primary mismatch	secondary mismatch position	secondary mismatch	IC50 (nM)		Discrimination ratio
					Match	Mismatch	
5' -ua cagacuu ccaaaaggcuccg-3'	2	A:C	none	none	0.30 ± 0.07	0.23 ± 0.04	0.77
5' -uc a cagacuu ccaaaaggcucc-3'	3	A:C	none	none	0.52 ± 0.10	0.94 ± 0.62	1.8
5' -ugc a cagacuu ccaaaaggcuc-3'	4	A:C	none	none	0.88 ± 0.32	6.0 ± 3.7	6.8
5' -uggc a cagacuu ccaaaaggcu-3'	5	A:C	none	none	0.66 ± 0.32	1.8 ± 0.33	2.7
5' -ugggc a cagacuu ccaaaaggc-3'	6	A:C	none	none	0.93 ± 0.29	2.6 ± 0.89	2.8
5' -uaagggc a cagacuu ccaaaagg-3'	7	A:C	none	none	0.45 ± 0.09	0.88 ± 0.49	1.9
5' -uaagggc a cagacuu ccaaaag-3'	8	A:C	none	none	0.36 ± 0.11	0.53 ± 0.12	1.5
5' -ucaagggc a cagacuu ccaaaa-3'	9	A:C	none	none	1.07 ± 0.06	0.93 ± 0.27	0.87
5' -uggcacaagggc a cagacuu c-3'	13	A:C	none	none	0.25 ± 0.10	0.42 ± 0.11	1.7
5' -guagggcacaagggc a cagac-3'	16	A:C	2	U:G	3.5 ± 2.9	>20	> 5.7
5' -gcggggcacaagggc a cagac-3'	16	A:C	3	C:U	>20	>20	~1
5' -gcauggcacaagggc a cagac-3'	16	A:C	4	U:C	>20	>20	~1
5' -gcauggcacaagggc a cagac-3'	16	A:C	5	U:C	18 ± 8	>20	> 1.1
5' -gcauggcacaagggc a cagac-3'	16	A:C	6	U:C	7.8 ± 5.5	>20	> 2.6
5' -gcauggcacaagggc a cagac-3'	16	A:C	7	U:G	0.74 ± 0.08	9.4 ± 3.9	12.7
5' -gcagggcacaagggc a cagac-3'	16	A:C	15	A:G	>20	>20	~1
5' -gcagggcacaagggc a cagac-3'	16	A:C	15	U:G	>20	>20	~1
5' -gcagggcacaagggc a cagac-3'	16	A:C	17	U:G	1.0 ± 0.12	5.1 ± 0.67	5.1
5' -gcaagggcacaagggc a cagac-3'	16	A:C	17	A:G	> 20	> 20	~1
5' -caagggcacaagggc a cagac-3'	15	A:C	16	U:G	0.38 ± 0.02	0.64 ± 0.06	1.7

Previous work has shown that adding a second mismatch can improve the ability of siRNA to discriminate between alleles²³⁹. We reasoned that adding a mismatch in the seed sequence of the siRNA might sufficiently destabilize our siRNA so that the doubly mismatched siRNA would lose its ability to silence the wild-type *Huntingtin* mRNA, while pairing at the SNP site would allow the singly mismatched siRNA to retain silencing activity for the disease allele. Double-mismatch strategies based on a position 16 mismatch with the counter-selected isoform had very low activity (Table 2.3). Therefore, we tested doubly mismatched siRNAs combining a seed mismatch with a position 10 mismatch. We prepared siRNAs predicted to mismatch at position 10 with the normal *Huntingtin* mRNA and also bearing an additional mismatch to both normal and disease alleles at one of the six seed positions (2–7). Mismatches at positions 5 or 6, combined with a position 10 mismatch with the counter-selected isoform, resulted in a reduction or loss of silencing of the SNP-mismatched target, while retaining good activity against the SNP-matched target (Figure 2.6A).

Figure 2.6. Representative Data for the Development of an Allele-Specific siRNA Targeting SNP rs362307, Which Is Associated with HD.

(A) Placing an additional mismatch in the seed sequence of the siRNA bearing a position 10 mismatch to the C isoform improved its selective targeting of the U isoform. (B) A doubly mismatched siRNA targeting the C isoform also distinguished between reporter mRNAs corresponding to the position 10 matched, C isoform and the position 10 mismatched, U isoform.

Figure 2.6

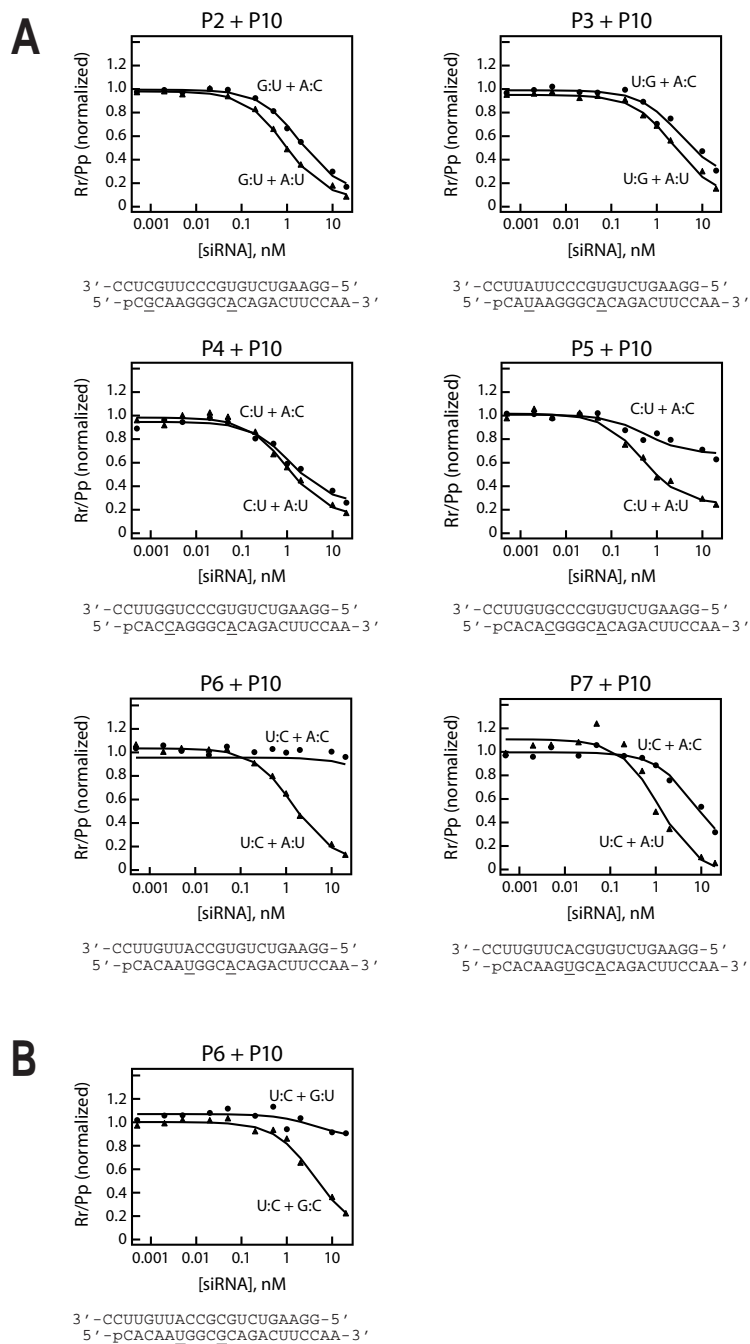


Table 2.4 reports “discrimination ratios”—the ratio of the IC₅₀ of the siRNA for the counter-selected target to the IC₅₀ of the targeted mRNA. The P10 (SNP) + P5 siRNA ($IC_{50_{P10 \text{ mismatch}}} > 20$; $IC_{50_{P10 \text{ match}}} = 0.62 \pm 0.43 \text{ nM}$) had a discrimination ratio > 32 and at 20 nM—the highest concentration tested—reduced expression of the counter-selected reporter by only 33%. The P10 + P6 siRNA achieved no appreciable reduction in expression of the mismatched reporter, even at 20 nM ($IC_{50_{P10 \text{ mismatch}}} > 20 \text{ nM}$), but was less effective against the matched reporter ($IC_{50_{P10 \text{ match}}} = 1.5 \pm 0.31 \text{ nM}$), yielding a lower discrimination ratio. We often observed such a trade-off between the efficacy and the selectivity of SNP-specific siRNAs. We also designed and tested an siRNA targeting the C isoform; while it was less active than the siRNA targeting the U isoform, it selectively targeted the P10-matched allele ($IC_{50_{P10 \text{ mismatch}}} > 20$; $IC_{50_{P10 \text{ match}}} = 3.2 \pm 2.2 \text{ nM}$; Figure 2.4C and Table 2.4)

Table 2.4. Validation of siRNAs designed to distinguish between matched and mismatched SNP isoforms.

IC50 values are given as the average \pm standard deviation for at least three independent experiments. The IC50 is reported as > 20 nM for siRNAs that failed to achieve half-maximal inhibition at the highest concentration tested.

Table 2.4

Reference Number	siRNA guide strand	SNP position	primary mismatch	secondary mismatch position	secondary mismatch	IC50 (nM)		Discrimination ratio
						Match	Mismatch	
rs363125	5'-agcguugaa <u>g</u> uacugucccca-3'	10	G:A	none	none	0.17 ± 0.11	0.27 ± 0.25	1.6
rs363125	5'-agcguugaa <u>u</u> uacugucccca-3'	10	U:C	none	none	0.18 ± 0.09	0.22 ± 0.07	1.2
rs363125	5'-ucuuuagcguugaa <u>g</u> uacug-3'	16	G:A	none	none	0.36 ± 0.24	>20	>55
rs363125	5'-ucuuuagcguugaa <u>u</u> uacug-3'	16	U:C	none	none	0.74 ± 0.40	>20	>27
rs362307	5'-cacaaggcc <u>g</u> cagacuuccaa-3'	10	G:U	none	none	0.36 ± 0.04	0.77 ± 0.16	2.1
rs362307	5'-uacaaaggcc <u>a</u> cagacuuccaa-3'	10	A:C	none	none	0.16 ± 0.09	0.14 ± 0.10	0.87
rs362307	5'-gcaggccacaaggcc <u>g</u> cagac-3'	16	G:U	none	none	0.73 ± 0.12	0.72 ± 0.12	0.99
rs362307	5'-ucaggccacaaggcc <u>a</u> cagac-3'	16	A:C	none	none	0.19 ± 0.02	0.20 ± 0.06	1.1
rs362307	5'-cgaaggcc <u>a</u> cagacuuccaa-3'	10	A:C	2	G:U	1.0 ± 0.35	1.9 ± 0.27	1.9
rs362307	5'-cauaaggcc <u>a</u> cagacuuccaa-3'	10	A:C	3	U:G	3.0 ± 1.8	3.5 ± 1.6	1.2
rs362307	5'-cacaggcc <u>a</u> cagacuuccaa-3'	10	A:C	4	C:U	1.0 ± 0.22	1.6 ± 1.2	1.6
rs362307	5'-cacaaggcc <u>a</u> cagacuuccaa-3'	10	A:C	5	C:U	0.62 ± 0.43	>20	>32
rs362307	5'-caca <u>u</u> ggccagacuuccaa-3'	10	A:C	6	U:C	1.5 ± 0.31	>20	>13
rs362307	5'-cacaag <u>u</u> cagacuuccaa-3'	10	A:C	7	U:C	1.3 ± 0.51	5.9 ± 1.9	4.5
rs362307	5'-caca <u>u</u> ggccagacuuccaa-3'	10	G:U	6	U:C	3.2 ± 2.2	>20	>6
rs362273	5'-guugaucu <u>g</u> uagcagcagcuu-3'	10	U:G	none	none	0.09 ± 0.14	0.01 ± 0.006	0.11
rs362273	5'-guugaucu <u>c</u> agcagcagcuu-3'	10	C:A	none	none	0.12 ± 0.06	0.44 ± 0.11	3.7
rs362273	5'-cucggguugaucu <u>g</u> uagcag-3'	16	U:G	none	none	0.01 ± 0.002	0.007 ± 0.002	0.7
rs362273	5'-cucggguugaucu <u>c</u> agcag-3'	16	C:A	none	none	0.01 ± 0.003	0.004 ± 0.001	0.41
rs362273	5'-ucugaucu <u>g</u> uagcagcagcuu-3'	10	U:G	2	C:A	0.01 ± 0.002	0.06 ± 0.008	5.9
rs362273	5'-uucgaucu <u>g</u> uagcagcagcuu-3'	10	U:G	3	C:A	0.02 ± 0.003	0.29 ± 0.04	15
rs362273	5'-uuuauaucu <u>g</u> uagcagcagcuu-3'	10	U:G	4	U:C	0.03 ± 0.006	0.37 ± 0.11	11
rs362273	5'-uuug <u>c</u> ucug <u>u</u> agcagcagcuu-3'	10	U:G	5	C:U	0.02 ± 0.003	0.59 ± 0.08	31
rs362273	5'-uuuga <u>c</u> cug <u>u</u> agcagcagcuu-3'	10	U:G	6	C:A	0.02 ± 0.002	0.06 ± 0.015	2.7
rs362273	5'-uuuga <u>u</u> uug <u>u</u> agcagcagcuu-3'	10	U:G	7	U:G	0.006 ± 0.001	0.10 ± 0.02	17
rs362273	5'-uuug <u>c</u> ucug <u>c</u> agcagcagcuu-3'	10	C:A	5	C:U	0.15 ± 0.04	0.74 ± 0.11	4.9

To cover 75% of HD patients requires siRNAs targeting additional SNPs. Because no specific nucleotide isoform of these SNP sites is associated with HD, selective siRNAs are needed for both isoforms. Our long-term strategy would be to screen patients to determine the SNP isoform associated with the expanded CAG repeat *Huntingtin* allele²⁴⁵ and select the corresponding for therapy. As a first step toward this goal, we tested its ability to target one isoform of the SNP while minimizing silencing of the other isoform. For the SNP site rs363125, which lies at nt 5,304 (exon 39) and occurs as either an A or a C, placing the mismatch at position provided some discrimination (Figure 2.7A), but a mismatch at position 16 was sufficient to provide a high degree of selectivity for the fully matched target for both the A (>27-fold discrimination; $IC_{50_{\text{mismatch}}} > 20 \text{ nM}$; $IC_{50_{\text{match}}} = 0.74 \pm 0.40 \text{ nM}$) and C ($IC_{50_{\text{mismatch}}} > 20\text{nM}$; >55-fold discrimination; $IC_{50_{\text{match}}} = 0.36 \pm 0.24 \text{ nM}$) isoforms (Figure 2.7B and Table 2.4). For a second SNP, rs362273, which lies at nt 7,942 (exon 57) in the *Huntingtin* mRNA and occurs as either an A or a G, the P10 (SNP) + P5 siRNA design targeting the A isoform of the SNP provided ~30-fold selectivity ($IC_{50_{\text{P10 mismatch}}} = 0.59 \pm 0.08 \text{ nM}$; $IC_{50_{\text{P10 match}}} = 0.02 \pm 0.003 \text{ nM}$, Figure 2.8A), whereas the siRNA targeting the G isoform ($IC_{50_{\text{P10 mismatch}}} = 0.74 \pm 0.11 \text{ nM}$; $IC_{50_{\text{P10 match}}} = 0.15 \pm 0.04 \text{ nM}$, Figure 2.8B) gave ~4.9-fold selectivity (Figure 2.8, Figure 2.9 and Table 2.4).

Figure 2.7. Representative Data for the siRNAs Targeting the rs363125 SNP Site

- (A) siRNAs bearing a mismatch at position 10 to the C or the A isoform of rs363125 did not discriminate well between matched and mismatched targets.
- (B) siRNAs mismatched at position 16 discriminated between luciferase reporter mRNAs bearing either the C or the A isoform of the rs363125 SNP site.

Figure 2.7

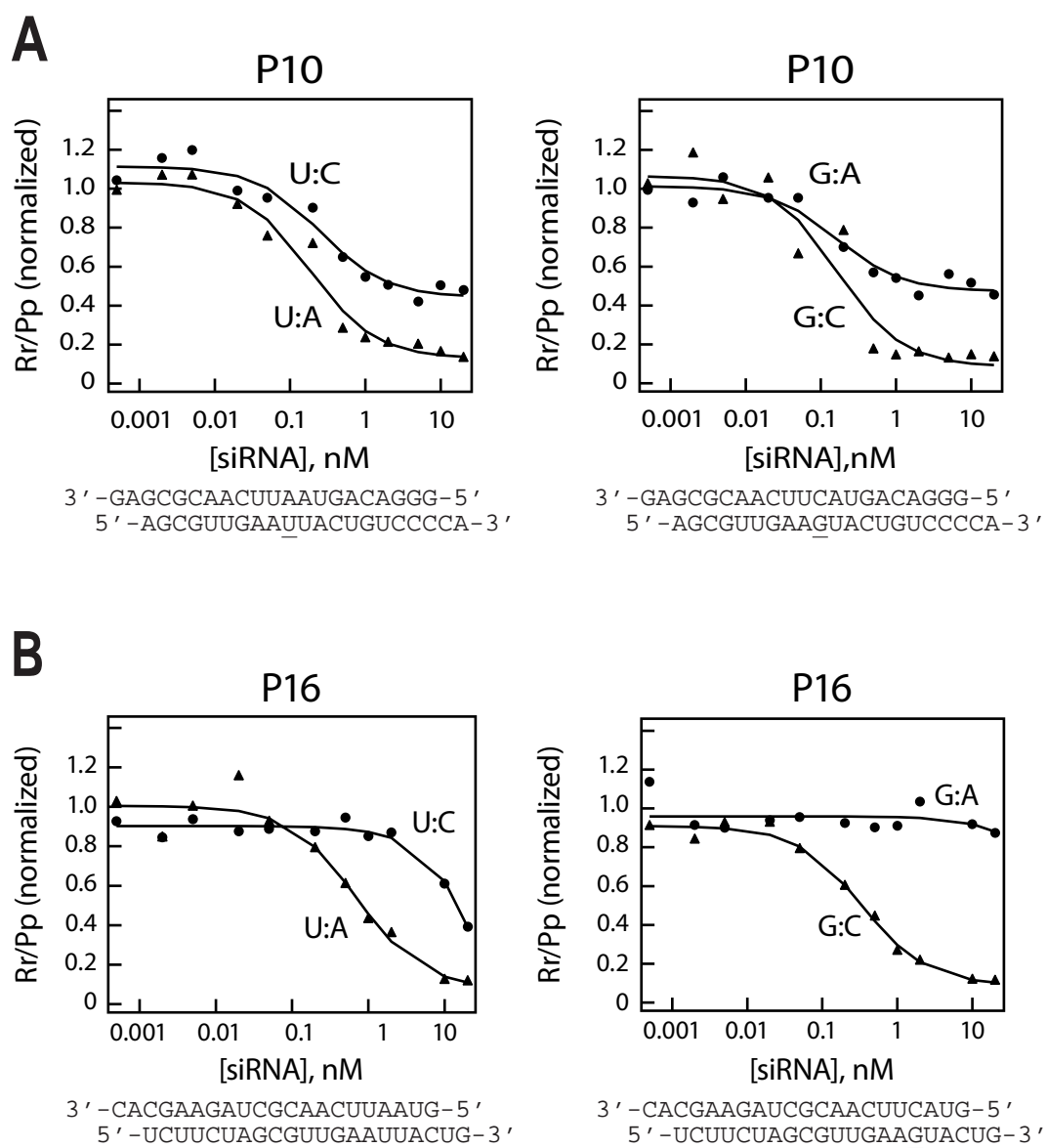


Figure 2.8. Representative data for the development of isoform-specific siRNAs targeting the rs362273 SNP Site

siRNAs bearing a mismatch to the SNP site at position 10 and an additional position 5 mismatch discriminated between the A (A) or G (B) isoforms of the rs362273 SNP site.

Figure 2.8

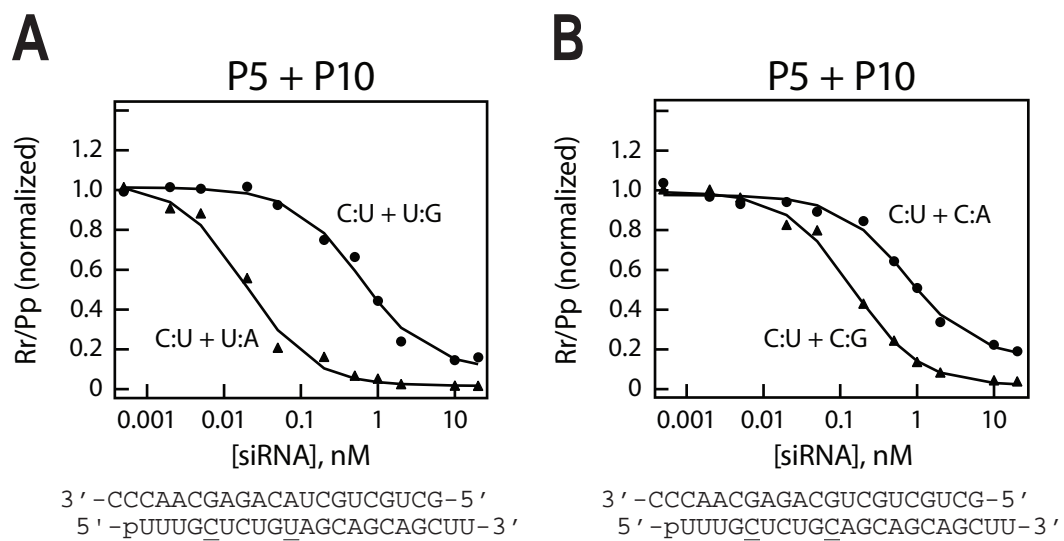
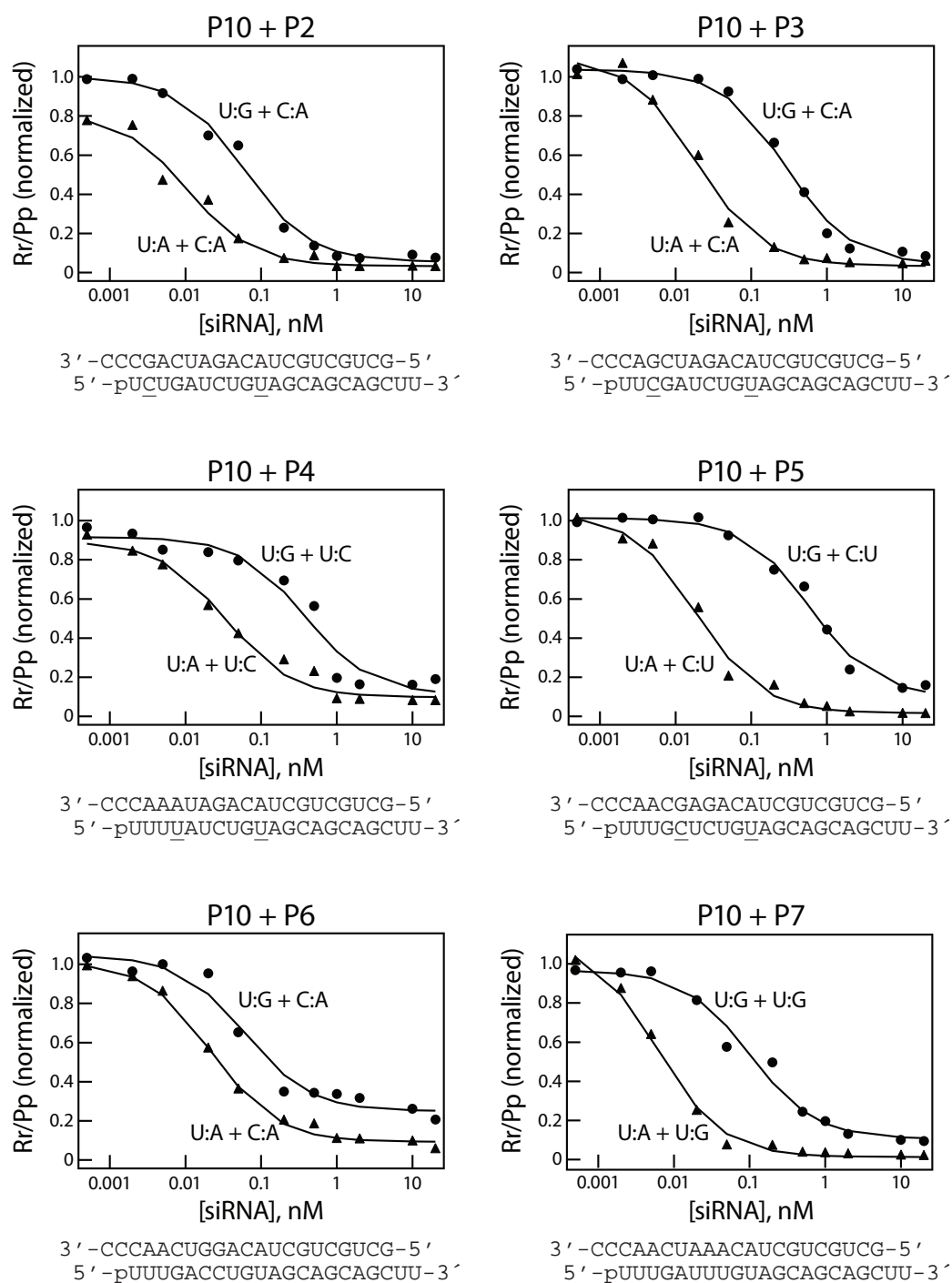


Figure 2.9. Adding a Position 5 Mismatch to a Position 10 Mismatched Increased the Ability of an siRNA to Discriminate between the Two Isoforms of the rs362273 SNP

We evaluated the efficacy and selectivity of siRNAs combining mismatches at positions 2,3,4,5,6 or 7 with a mismatch at position 10. The position 10 + position 5 siRNA was best able to distinguish between the matched and mismatched reporters. Representative data are shown.

Figure 2.9



Discussion

Targeted reduction of mutant *Huntingtin* mRNA is considered an ideal strategy for treating HD. The primary obstacles to the development of such a therapy have been concerns about the number of siRNAs that would require testing in clinical trials. It is not clear if drug regulatory agencies will permit patient-specific siRNAs to be used in humans without large-scale clinical trials. Such trials are, of course, not possible if only small numbers of patients share a common SNP isoform. Our results suggest that there is sufficient heterozygosity at a small number of SNP sites among American and European HD patients to support SNP-specific siRNA therapy. Targeting just three SNPs with five siRNAs should cover the majority of HD patients in the population studied here. This is possible because of the presence of several highly heterozygous SNPs and because a single SNP isoform for SNP rs362307 is associated with HD. One siRNA targeting this HD-associated isoform should target the mutant *Huntingtin* allele in nearly 50% of our patient population. We have developed an siRNA that selectively targets the disease-associated isoform of this SNP in cultured human cells. In the near future, pre-clinical testing of this siRNA for efficacy, selectivity, and safety is clearly of the highest importance.

What of the ~25% of patients predicted to be beyond the reach of the five siRNAs developed here? Unfortunately, our analysis predicts that a very large number of siRNAs will be required to provide siRNA therapy for this sub-population. Adding an additional four siRNAs (for a total of nine siRNAs

corresponding to 5 SNP sites) only increases the treatable patient population by 3%. A further increase in the number of siRNAs provides no real additional benefit.

Finally, we find that by using potentiating mismatches in the seed sequence, isoform-selective siRNAs can be designed for SNP sites predicted to be poor candidates for the development of allele-selective siRNAs. Our data suggest that a single siRNA directed against a SNP isoform associated with HD could be used to treat nearly half the US and European HD population. Clearly, an siRNA directed against this SNP isoform, such as the siRNA presented here, merits thorough pre-clinical validation to test its promise as a candidate therapy for HD.

Materials and Methods

Patient Samples, Sequencing, and Statistical Analysis

Patient brain samples were obtained from brain repositories in Charlestown, MA and New York, NY, and DNA from the DNA repository in Ulm, Germany.

Genomic DNA was either extracted from brain tissue (USA patients) using a genomic DNA extraction kit (Lamda Biotech, St. Louis, MO) or obtained as purified (German patients). Candidate SNP sequences were amplified by PCR (Table S2.1) and sequenced (GENEWIZ, South Plainfield, NJ, USA, and Macrogen, Rockville, MD, USA). To identify new SNP sites, we selected six

subjects for sequencing of all 67 *Huntingtin* exons. All electrophoretograms were manually inspected for the forward and reverse directions.

One hundred-nine case and 116 control genomes from German and US populations were typed at 24 SNP positions in the HD gene on human chromosome 4. Of these, 9 were discarded because they were rarely heterozygous. All assayed SNPs had a call rate greater than 95%. Four SNPs with a minimal allele frequency (MAF) of less than 0.01 were removed from the set. Deviations from Hardy-Weinberg equilibrium (HWE) were determined with Pearson goodness-of-fit and Fisher's exact tests. All markers resulted in HWE p -values of greater than 0.01. Single SNP associations were calculated for associations of markers with the HD phenotype. Test statistics of the Pearson goodness-of-fit test was determined and significance evaluated against the chi squared distribution and against an empirical distribution of the statistic after 1000 permutations. Association was also tested with the Fisher's exact test and the Cochran-Armitage test. A single marker, rs362307, was found to be associated with a significance of 0.0000523. This marker remained significant after Bonferroni multiple testing adjustment for 17 tests at the level of 0.000890. SNP rs362307 is located in a ~80 kb block of 10 markers whose average local linkage disequilibrium value is $D' = 0.995666$. The power of the study to detect association at $p < 0.01$ was $> 90\%$. All statistical calculations were performed using the Haploview software, version 3.32²⁵⁸ and R (R: Development core team (2004). R: A language and environment for statistical computing. Vienna, Austria.

<http://www.r-project.org>). SNP data were imported into R and formatted for input into Haploview software.

Reporter Constructs and Assays

For rs363125, a 55-mer containing the SNP site (for 5'-cta gag GTT AAG AGA TGG GGA CAG TA[C/A] TTC AAC GCT AGA AGA ACA CAc tcg agc t-3', rev 5'-cta gag ctc gag TGT GTT CTT CTA GCG TTG AA[G/T] TAC TGT CCC CAT CTC TTA ACc t-3') was cloned into the pRL-TK vector (Promega Corporation, Madison, WI) using the XbaI site in the 3' UTR of the Renilla luciferase gene. Proper insertion was confirmed by PCR and sequencing. Luciferase assays were performed by co-transfection in 24 well plates of the siRNA with 0.025 µg/well of the SNP reporter (pRL3125) and 0.05 µg/well pGL3-control vector (Promega). For dose-response measurements, GFP siRNA (guide: 5'-GCA AGC UGA CCC UGA AGU UAA U-3'; passenger: 5'-GAA CUU CAG GGU CAG CUU GCC G-3') was added to each transfection mixture so that all transfections contained 20 nM total siRNA. Transfections were performed using Lipofectamine 2000 (Invitrogen Corporation, Carlsbad, CA), according to the manufacturer's protocol. Twenty-four hours after transfection the cells were lysed for 20 min in 1x passive lysis buffer (Promega). Luciferase activity was read in 96-well plates with the Dual-luciferase assay kit (Promega) using the GloMax multi-detection system (Promega).

For rs362307 and rs362273, a 45-mer (rs362273 forward: 5'-tcg aAG CCA CGA G AA GCT GCT GCT [A/G]CA GAT CAA CCC CGA GCG GGA-3', reverse: 5'- ggc cTC CCG CTC GGG GTT GAT CTG [T/C]AG CAG CAG CTT CTC GTG GCT-3', rs362307 forward: 5'-tcg aCC GGA GCC TTT GGA AGT CTG [C/T]GC CCT TGT GCC CTG CCT CCA-3', reverse: 5'-ggc cTG GAG GCA GGG CAC AAG GGC [G/A]CA GAC TTC CAA AGG CTC CGG-3') containing the SNP site was cloned into pSiCHECK-2 (Promega) between the XhoI and NotI restriction sites in the 3' UTR of a codon-optimized form of the *Renilla reniformis* luciferase gene. We used 0.025 µg/well of the psiCHECK vector in our luciferase assays, which were performed as above. Data were graphed and analyzed using Igor Pro software (WaveMetrics, Portland, OR).

Western Blotting

Cells were grown and transfected in 6-well plates. The final concentration of total siRNA transfected in each well was 20 nM (GFP siRNA plus *Huntingtin* siRNA). An siRNA targeting a non-polymorphic site in the *Huntingtin* mRNA ("E1-4"; guide: 5'-UUC AUC AGC UUU UCC AGG GUC-3'; passenger: 5'-CCC UGG AAA AGC UGA UGA CGG-3') served as a positive control. Cells were lysed 48 h after transfection using Passive Lysis Buffer (Promega) supplemented with protease inhibitors (Roche Applied Science, Indianapolis, IN, USA). Samples were diluted in Laemmli Sample buffer (Bio-Rad Laboratories, Hercules, CA, USA) and resolved by electrophoresis through a 4–15% polyacrylamide denaturing Tris-HCl

gel (Bio-Rad). After transfer to PVDF, blots were probed with anti-*Huntingtin* antibody (Ab1, 0.5 µg/ml)³² followed by an HRPconjugated anti-rabbit secondary antibody (NA934V, GE Healthcare, Buckinghamshire, UK) diluted 1:10,000. Chemiluminescent detection was performed with SuperSignal West Dura Extended Duration Substrate (Thermo Scientific, Pierce, Rockford, IL, USA) and images acquired with an LAS-3000 imaging system (Fujifilm, Tokyo, Japan). After probing with the anti-*Huntingtin* antibody, blots were stripped and re-probed with anti-α-Tubulin antibody (DM1A, Sigma Aldrich, St. Louis, MO, 1:1000) detected with anti-mouse secondary antibody (NA931V, GE Healthcare) diluted 1:10,000.

Quantitative PCR

Cells were grown and transfected in 6-well plates. The final concentration of total siRNA transfected in each well was 20 nM (GFP siRNA plus *Huntingtin* siRNA). RNA was extracted 24 h after transfection using TRI reagent solution (Ambion, Austin, TX), and then DNase treated with Turbo DNA-free DNase (Ambion). cDNA was synthesized using oligo(dT) primers, Superscript III reverse transcriptase (Invitrogen Corporation, Carlsbad, CA) and 0.5 µg total RNA. Quantitative PCR reactions were performed with primers to amplify *Huntingtin* (forward, 5'-cgc aga gtc aga tgt cag ga-3'; reverse, 5'-ggg tct ctt gct tgt tcg ag-3') or β-actin mRNA (forward, 5'-gga ctt cga gca aga gat gg-3', reverse 5'-agc act gtg ttg gcg tac ag-3') using the Quantitect SYBR Green PCR kit (Qiagen, Valencia,

CA). Data were analyzed using the $2^{-\Delta\Delta CT}$ method²⁵⁹ and β -actin mRNA for normalization.

Table S2.1. Primers Used for SNP Analysis and Resequencing

Exon	SNP i.d.	Forward primer	Reverse primer
2		5'-TGGAGTGGTAATCAACACA-3'	5'-GCCAGAAATATGGAAAAGG-3'
3		5'-AGAATTCATGCAGGACACC-3'	5'-GCAGACATCCTCAGGGACTC-3'
4		5'-TGATGGGATGTGCTTCCAT-3'	5'-GGTCAGGAGTTCGAGACCAG-3'
5		5'-ATGCAACCCTCTGGTGACT-3'	5'-CGACAAAAAACCAACATCCAG-3'
6		5'-TCAGCTGAGTTTCCCCATC-3'	5'-GAAGCACTCCACAGGACTC-3'
7		5'-CTGCTCTTGAGTGTCCTCCAAA-3'	5'-CCACTCATATGCCTCCACCT-3'
8		5'-CTCTGGAAGGACCTTGCTG-3'	5'-ATTACACATGCAGGGCCCTAGA-3'
9		5'-TTGGTGAAGTGATAGGAAA-3'	5'-GTTTTGGCAAGGAAGATGGA-3'
10		5'-TGCGATGTTAAGTGTTCCTG-3'	5'-CCTGGTTATCAGATTCAGCA-3'
11		5'-GCATTTACTTAATTTGAAGTCCITAT-3'	5'-CGAATATGCCCCATTTAAGC-3'
12		5'-CGTATTTTGAAGCCTGTG-3'	5'-CTCCCAAAGTGTGGATTA-3'
13, 14		5'-GTTGGAGGGCTTGCTCTTG-3'	5'-CAGGGATGGAAAAGCAATAA-3'
15, 16		5'-ACCTGGCTAAGTGCTGCTC-3'	5'-CTCGGCTAGTGA AACCAAAA-3'
17, 18		5'-GTTCCATGGCTGAGCAATTT-3'	5'-GCTGAGAGATGGATACATGGTG-3'
19		5'-CTTGCCTTGACCTTGTGTT-3'	5'-TGCATCAAGTGATCCCAGAA-3'
20, 21	rs363075	5'-CAAGCTGGCGGTAAGTGTGTT-3'	5'-TCCCCTCTCTTTCCATTCTCG-3'
22		5'-AAGTGGTGTCGGCTGGTAAC-3'	5'-GCC TAAAGAAAAGGCATCAGG-3'
23		5'-CGTTTCACTTAAAAGTTGAGACTGC-3'	5'-TTTCTTAGCAAGCCTCATGGA-3'
24		5'-CTTTGTGGTGTTGGGTG-3'	5'-TCCCACAGCTCCTGTCACTA-3'
25	rs35892913, rs1605746, rs17781557	5'-TGTGACATGCCCTTCCCTTTG-3'	5'-AAAGGGACAAGCCATCACTG-3'
26		5'-CAGTCCCCAAGCAATTTGT-3'	5'-CCATCCACATGGTCACATTT-3'
27		5'-TCAGGGTCCAGAACAATAATG-3'	5'-GCTTCAGACCAAAAAGGTGGT-3'
28		5'-TTTCCAGTAATCTTTAAAACCTGG-3'	5'-TAAAAAGATGCAGAGGCCCAT-3'
29	rs4690074	5'-GGCCAGTAACCGTGTGTTCT-3'	5'-TCATGGCTAAGGCAGAGTCA-3'
30		5'-GGATTCCGTACAATAACGGGTCA-3'	5'-GGAGCTTCTGGTGTCTCTG-3'

31		5'-TTCACGGCTGTGAGTCTTTGC-3'	5'-CTCTTTTGGTGTCTCCACCA-3'
32		5'-TGCTTCCCTTTATCCCAAT-3'	5'-CCTGAAAGTCTCAGCTCCA-3'
33		5'-TGCTTGAAGCTTTTAGTTGAAGG-3'	5'-ATGAGGGAAACATGCAGACC-3'
34		5'-TGTGAAATTTTATTTCCCTTCTG-3'	5'-TTCCATTTAAGAAAAACAGCAAAA-3'
35		5'-TGATGTGTGCTTGCTGTCAA-3'	5'-ACACACATGCAGAGCCTGAG-3'
36		5'-GATGTTGAGAGCAGTTTCCAA-3'	5'-GCCCAAACCTGGTTCAAAGT-3'
37		5'-CGTCTCTTGGCAGCAGACTT-3'	5'-TATGCAACAACAAGCCAAAGG-3'
38		5'-GGGTACAGGAAGCTGCTGTT-3'	5'-GCCCTACCCAAACTGACTGA-3'
39	rs363125	5'-GCAATTGGGGAAATTTAATC-3'	5'-CATCACGTGACTTCCCAAAA-3'
40		5'-TGATACTTGGCGTAAGTGCTTT-3'	5'-ACTGGGCAAGGCAGAGTTT-3'
41		5'-GGACCGAGATGAAAGCAAAG-3'	5'-GCCAAAGCTCAGGTTACTGG-3'
42		5'-CTCACTGCCATCCAGAAACA-3'	5'-TTTAGTTTCGATGGAGCTTGG-3'
43		5'-GGCATTAACTCGTGGTCTCTTCT-3'	5'-TTTAAGCAGGGAAAACTGC-3'
44		5'-ATTGCCAGTTGCAGTTTCC-3'	5'-AAAAGCCAGCCACCTGTTTT-3'
45		5'-TGAACGTACACATCAGTTTCATCC-3'	5'-TAAACCCACCTATAAGGCACATC-3'
46		5'-TGATTTTCCCTTAAAGAGCCACT-3'	5'-ACAGGTGACAGAGGCACACTCA-3'
47		5'-AGCTCCAGGGATGGAAGTC-3'	5'-CAGACTGGAGTCCCCAACAT-3'
48	rs362336	5'-TGTTTGTAAACCTTAAATGCTCTGA-3'	5'-TATACTGGCCCTGGAATGCT-3'
49		5'-GCTTGACTGCCCTTTCGAAAGT-3'	5'-TGGAAAAGTGACTGGACTGG-3'
50	rs362331	5'-GGCATTCTGTGACTCGGTA -3'	5'-GATAGGAACCCACCCGTTTCAT-3'
51		5'-GGCTAGTCTGTCTATCCCCTTCA-3'	5'-TCCAGGAGTCCACACTCACC-3'
52		5'-CAGCTGGTTGAGGTCATGC-3'	5'-GGTCTTCTGCAAGGAAACGAG-3'
53		5'-GCTTCCCTGCTTCCCTCACAGT-3'	5'-TTGCCAACACTGCAAAAATGT-3'
54		5'-ACAGGCTTGAAAGGTTGA-3'	5'-AGACCTCAGCAGGCTTGTGC-3'
55		5'-GAGGTGGTTGTGGGTGCTT-3'	5'-CACCTTTGGGTCTGCATCTC-3'
56		5'-CACGGACAGGTGCTCACTTA-3'	5'-GGTGAGCATGCCAGTCTTCT-3'
57	rs362273	5'-AGTGACAAATCCCCAAGACC-3'	5'-GAGCTTTTCTCCTGGGTGTG-3'
58, 59		5'-TAGACGGTAGGCATGTGCTG-3'	5'-GTGTGGCCTGTGTGTGTGTT-3'
60		5'-GGATTCTAACAGCGCGATTCT-3'	5'-GTTCCGGGTCAACTCTTGGAA-3'
61	rs362272	5'-CGGCCCTGCTGTGTAGTCTCT-3'	5'-TCTTGGCTCTCACTGACCCTC-3'

62, 63		5'-ACATGCTGTGAAGCCCTCTC-3'	5'-GTCGAGGTCCCTTGAGTGAG-3'
64		5'-CCCCTGTGTACAAAGCACTG-3'	5'-GCTGTGGTGGGAATCACT-3'
65	rs3025806	5'-ATTTACACATCGGCATTTTCC-3'	5'-AACTCCACCTCCAGGCTTTC-3'
66		5'-GAAAGCCTGGAGGTGGAGTT-3'	5'-ACATGAGCCTCGGTGTTGAC-3'
67 (primer set 1)	rs362308, rs362307	5'-GCTCTGCTCGCTCTCCAG-3'	5'-GCAGAGACACGCACGTTG-3'
	rs362306, rs362268, rs362305, rs362304, rs362303		
67 (primer set 2)	rs1557210, rs362302, rs3025805, rs362267	5'-TGACCAGGTCCTTCTCCTG-3'	5'-GGCCTTGGGATTCACATACT-3'
67 (primer set 3)		5'-ATGGATGCATGCCCTAAGAG-3'	5'-TCTAGGGCTGAGGAAAGCAGA-3'

Acknowledgements

This work was supported, in part, by grants from the NIH to NA, MD, and PDZ (NS38194), to the Diabetes and Endocrinology Research Center (P30DK032520-25), and from the CHDI (High Q Foundation) to NA and PDZ.

**CHAPTER III: PROCESSING AND THERAPEUTIC APPLICATIONS OF
ARTIFICIAL MIRNAS TARGETING HUNTINGTIN SNPS**

Preface

The work presented in this chapter was a collaborative effort. I cloned the miRNAs and shRNAs for the cell culture experiments. Lori Kennington and I performed the transfections and ran the luciferase assays. I analyzed the data. I cloned the small RNAs and analyzed the sequencing results. Christian Mueller and members of the Flotte lab cloned the miRNAs into the AAV9 backbone and the viruses were produced at the University of Massachusetts Gene Therapy Vector Core. Kathryn Chase and I injected the mice. Joanna Chaurette and I did the immunohistochemistry and Joanna Chaurette counted the inclusions and DARPP-32 labeled neurons.

Summary

Huntington's disease (HD) is a neurodegenerative disorder caused by expansion of a CAG repeat region in exon 1 of the *Huntingtin* gene. The polyglutamine protein causes premature neuronal death in the cortex and striatum. Lowering mutant *Huntingtin* levels using RNA interference (RNAi) shows therapeutic promise and siRNAs targeting single nucleotide polymorphisms (SNPs) can specifically target the mutant *Huntingtin*. To facilitate delivery and promote long-term silencing, we developed artificial microRNAs targeting *Huntingtin* SNPs for delivery using recombinant adeno-associated viruses (rAAVs). In cell culture, both U6 promoter driven and CMV promoter driven miRNAs can discriminate between matched and mismatched targets. Canonical 21 nucleotide siRNAs are not perfect models for SNP discriminating miRNAs as our miRNAs show generally poorer discrimination than siRNAs. Additional mismatches can improve discrimination. U6 promoter driven microRNAs (miRNAs) are overexpressed and can produce many more unwanted processing products than polymerase II driven miRNAs. Polymerase II driven artificial miRNAs produce asymmetric small RNAs from the guide strand (miRNA) and the passenger strand (miRNA*) at a ratio of approximately 15:1. No other products are produced at significant levels. In vivo, polymerase II driven miRNAs are expressed at moderate levels following direct injection of self-complementary AAV9-miRNA vectors and *Huntingtin* miRNAs have no significant effect on the endogenous miRNA profile. Finally, artificial miRNAs targeting a human SNP site reduce inclusions in a knock-in

mouse model of HD. These studies bring us closer to a safe and effective therapeutic strategy for Huntington's disease.

Introduction

Huntington's disease (HD) is a dominantly inherited monogenetic neurodegenerative disease. It is a prime candidate and test case for RNAi gene therapy. HD is caused by expansion of a CAG repeat region in exon 1 of the *Huntingtin* gene that produces a toxic protein containing an extended polyglutamine stretch. Three main silencing strategies have emerged for HD therapy: simultaneous silencing of mutant and normal *Huntingtin* (gene specific or nonallele specific silencing), silencing mutant *Huntingtin* by direct targeting of the CAG repeat region, and silencing of mutant *Huntingtin* by targeting single nucleotide polymorphisms. While there have been indications that gene specific (nonallele-specific) silencing may be tolerated^{6 110,260}, there is concern about the long term consequences of reducing normal *Huntingtin*, which contributes to neuronal function. Targeting the CAG repeat is the most direct approach to allele-specific silencing, and there is some evidence that siRNAs can discriminate between *Huntingtin* within the normal CAG repeat range and expanded *Huntingtin*²³². However, there are more than 60 human proteins that contain CAG repeat regions²³³ any of which could also potentially be targeted by CAG repeat targeting RNAi therapies. An alternative to CAG targeting is targeting single nucleotide polymorphisms (SNPs) in the *Huntingtin* gene. There

are over 1,000 SNP sites in the *Huntingtin* gene, many of which are highly heterozygous among HD patients from Europe and the United States^{261,262}. A small number of heterozygous SNP sites could be used to cover the majority of patients and siRNAs targeting these SNP sites can discriminate between isoforms in cell based luciferase assays and in patient derived fibroblasts^{257,261,262}. However, delivering siRNA to the brain presents a challenge. Cholesterol conjugated siRNA can reduce the levels of a co-injected AAV *Huntingtin* fragment, but we have been unable to show consistent and widespread knockdown of endogenous *Huntingtin* using siRNAs delivered to the striatum. Delivery of siRNAs using polycationic polyethylenimine (PEI) nanoparticles and liposomes requires endocytosis and therefore their effectiveness depends on endosomal escape. Endocytotic delivery can also lead to toxicity caused by innate immune activation or lysosomal rupture. On the other hand, viruses expressing small hairpin RNAs injected directly into the brain have been successfully used to knockdown endogenous genes, including *Huntingtin*^{4,6,216,263} and have shown little toxicity when the hairpin is placed in the correct context²¹⁶.

There are several different types of small RNA hairpins that can be used for viral delivery. First generation short hairpin RNAs are driven by polymerase III promoters and consist of a 19 nucleotide stem and a short terminal loop. One arm of the stem corresponds to the siRNA guide strand and the other to the passenger strand. The two arms are connected by a short loop sequence. These

shRNAs are intended to enter the RNAi pathway at the Dicer processing step. While these shRNAs can produce good knockdown, they can also be toxic, most likely because of their high expression levels^{213,216,223}. More recently, constructs incorporating more components of endogenous microRNA structure have been developed^{216,264}. These shRNAmirs or artificial miRNAs are designed to enter the RNAi pathway at the Drosha processing step. They can be expressed from polymerase II promoters which can be regulated by drugs such as doxycycline, or rapamycin. For gene therapy, co-expression of a protein coding gene and a miRNA may be desirable. One strategy for gene replacement is to express a miRNA and a non-targetable wild-type copy of the gene. This can be achieved by placing the miRNA in the 3'-UTR or in an intron of the protein coding gene²⁶⁵. To increase the concentration of a single miRNA or to include miRNAs targeting multiple sites, miRNA can be placed in tandem ("miRNA chaining"). Perhaps because they are expressed at lower levels, miRNA-adapted hairpins have fewer toxic effects than the first generation shRNAs^{216,222}. Although there are advantages to the miRNA adapted hairpin design, using it to target single nucleotide polymorphisms may be more complicated. While shRNAs are processed only by Dicer, miRNAs must be processed by both Drosha and Dicer. If either enzyme is imprecise, a single artificial miRNA might produce multiple mature miRNA sequences. These mature miRNA could differ in their ability to differentiate between matched and mismatched targets; therefore, we set out to design and optimize a SNP specific hairpin targeting mutant *Huntingtin*.

Results

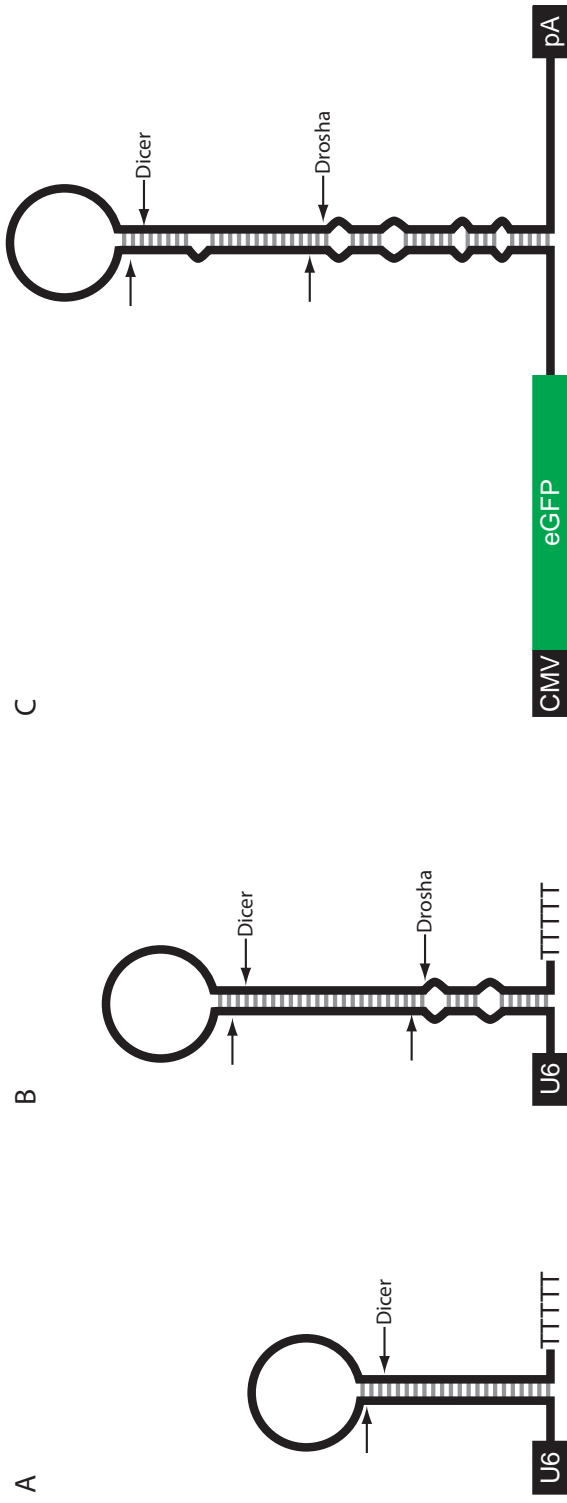
Design of SNP targeting shRNA and miRNA

We began with three initial hairpin designs: an shRNA driven by the human U6 promoter (Figure 3.1A), a hybrid U6 promoter driven miRNA (Figure 3.1B) consisting of the hairpin sequence of the shRNA plus a minimal amount of miRNA context based on the endogenous mir30 sequence, and an artificial miRNA based on mir155 where the miRNA is expressed from the 3'-UTR of a CMV promoter driven GFP reporter (Figure 3.1C).

In 50% of US and European patients, a U at SNP site rs362307 (position 9,633) in the 3'-UTR of the *Huntingtin* mRNA is associated with the expanded CAG repeat. An siRNA targeting the U isoform of the rs362307 SNP has a discrimination ratio greater than 12.5²⁶¹. We incorporated the sequence targeting the U isoform into plasmids following our initial hairpin designs (U6-shRNA, U6-miRNA and CMV-miRNA). To test for selectivity and potency, we measured luciferase activity following co-transfected these plasmids with matched or mismatched luciferase reporters. For each of the shRNAs, miRNAs and siRNAs, we report “discrimination ratios” for shRNAs, miRNA and siRNAs. The discrimination ratio, which is the IC50 of the siRNA for the mismatched target to the IC50 of the

Figure 3.1. Expected processing of shRNA and miRNA expression constructs
(A) shRNA expressed from a U6 promoter. (B) miRNA expressed from a U6 promoter. (C) Artificial miRNA expressed from a CMV promoter. Expected Drosha and Dicer cleavage sites are indicated by arrows.

Figure 3.1

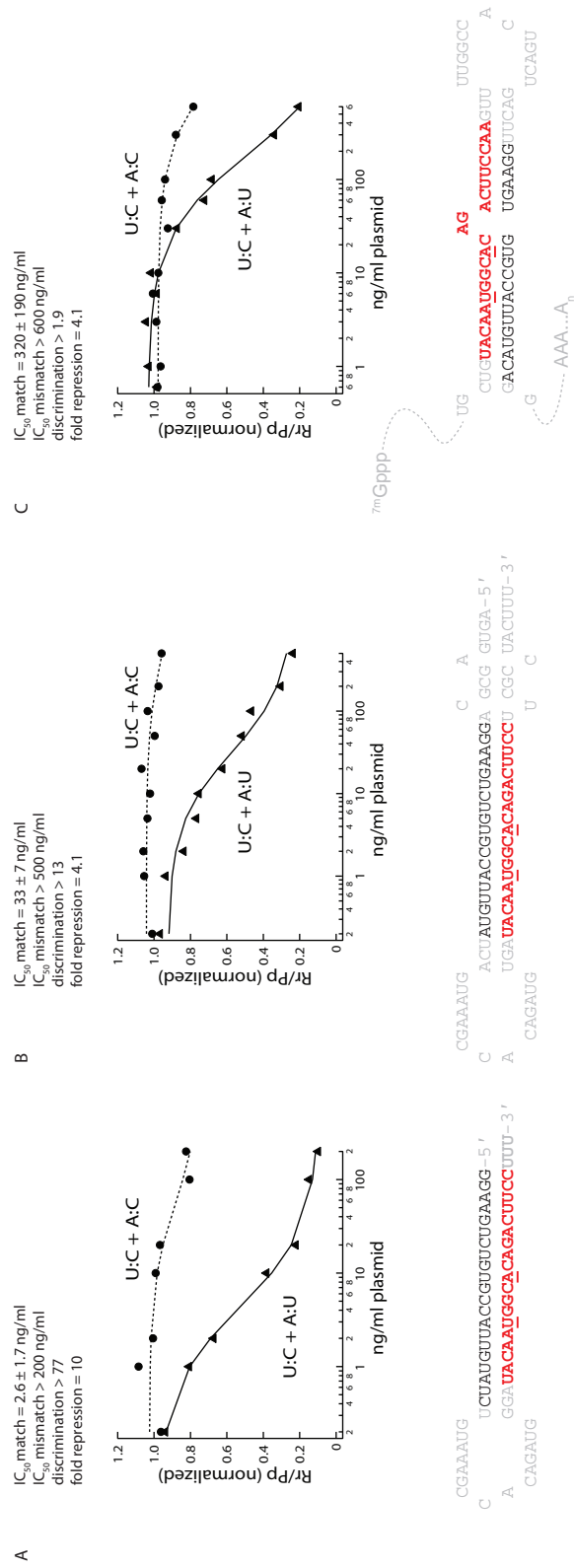


matched target ($IC_{50_{\text{mismatch}}}/IC_{50_{\text{match}}}$), is a measure of the ability of an siRNA (or miRNA) to selectively silence a matched target over a range of concentrations. A second measure of selectivity, the fold repression ratio measures selectivity at a single concentration. This is useful in cases where maximum repression of an siRNA or miRNA differs but the IC_{50} does not, or in cases where there is greater than 50% silencing of the target at high concentrations but where we cannot generate a reliable IC_{50} curve. All three plasmids reduce luciferase activity from the matched, but not the mismatched target (Figure 3.2). None of the plasmids achieved 50% silencing of the mismatched reporter, so we report their IC_{50} s as greater than the maximum amount of plasmid transfected; therefore, the differences in discrimination ratio primarily reflect the difference in silencing of the matched reporter. The discrimination ratios range from greater than 77 for the U6-shRNA (Figure 3.2A) to only greater than 1.9 for the CMV-miRNA (Figure 3.2C). The U6-shRNA was the most potent in silencing the matched reporter and had the highest discrimination ratio. The CMV-miRNA was far less potent than either of the U6 promoter driven hairpins, but achieved a fold repression ratio of 4.1, indicating that it was selectively silencing the matched target at high concentrations. We sometimes observed a non-specific increase in luciferase activity with high doses of both of the U6 promoter driven hairpins (Figure S3.1), therefore the maximum dose of those plasmids is lower than that of the CMV-promoter driven hairpin. We do not know what causes this non-specific increase,

Figure 3.2. shRNAs and miRNA-like hairpins discriminate between matched and mismatched luciferase reporters at an HD associated SNP site

Representative luciferase reporter assays for the U6-shRNA (A), U6-miRNA (B) and CMV-miRNA (C) targeting SNP site rs362307. The intended guide strand is shown in red and mismatches are underlined. The primary mismatch (to the SNP site) is at position 10 with a secondary mismatch at position 6. The IC₅₀ is reported for at least three independent replicates.

Figure 3.2



but we observed a similar phenomenon earlier when we were testing siRNAs using a two reporter system for this site.

Although the rs362307 site is therapeutically important, none of the available mouse models of HD have the U isoform of that SNP site (²⁶⁶⁻²⁶⁸, Table 3.1). A second, highly heterozygous SNP site, rs362273, is present in the endogenous mouse *Huntingtin* and in models of HD expressing full-length *Huntingtin*. siRNAs targeting that site are more potent than those targeting rs36207. Using the same CMV-miRNA backbone that we used to target rs362307, we designed a miRNA targeting rs362273. When we tested this miRNA against our luciferase reporters, it had a discrimination ratio of 3 and a fold repression ratio of 2.1, indicating poor discrimination between the matched and mismatched target (Figure 3.3).

Table 3.1. SNP sites and heterozygosity in cell lines and selected mouse models of HD

SNP identity for selected human SNP sites in HeLa cells and in yeast artificial chromosome (YAC [1]), bacterial artificial chromosome (BAC [2]) and CAG 140 knock-in [3] models of HD. YAC and BAC transgenic mice have full length human Huntingtin while CAG 140 mice have 140 CAGs inserted into the endogenous mouse Huntingtin locus. For the CAG 140 mice, the SNP site is listed as N/A if the site is not conserved between mouse and human Huntingtin.

Table 3.1

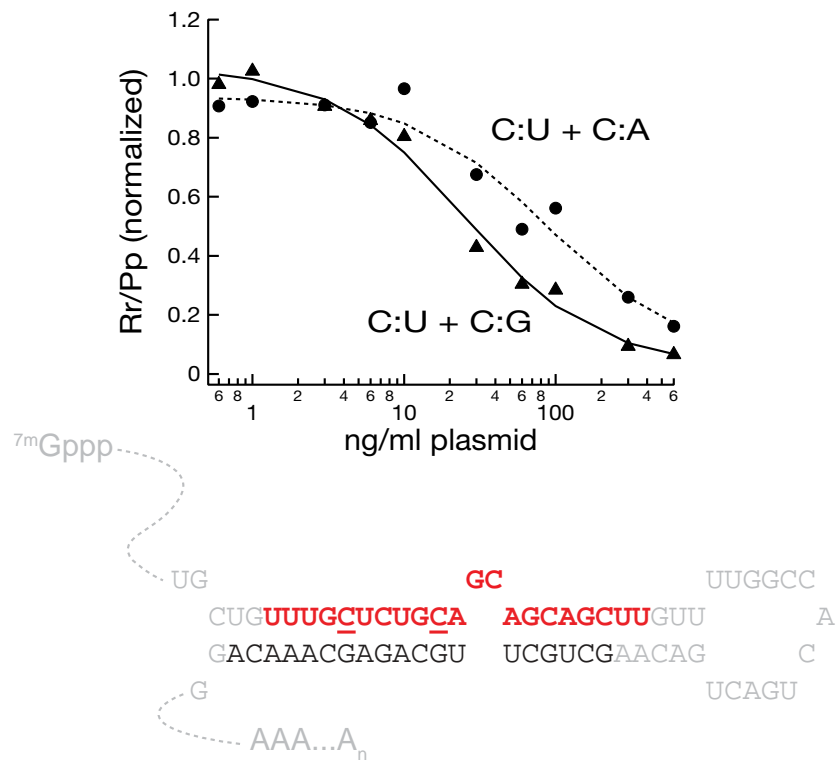
Position in human Huntingtin mRNA	Reference Number	YAC	BAC	CAG140 knock-in	HeLa cells
ORF, exon 29	rs363099	T	C	N/A (G)	C
ORF, exon 39	rs363125	C	C	N/A (A)	C
ORF, exon 50	rs362331	C	T	N/A (C)	C/T
ORF, exon 57	rs362273	G	A	G	A
ORF, exon48	rs362336	A	G	N/A (G)	A/G
3' UTR, exon 67	rs362306	A	G	N/A	G
3' UTR, exon 67	rs362268	G	C	N/A	C
3' UTR, exon 67	rs362267	T	C	N/A	C
3'UTR, exon 67	rs362307	C	C	N/A	C/T

Figure 3.3. Discrimination of an artificial miRNA at the rs362273 SNP site

Representative luciferase reporter assays for the double mismatched, CMV-promoter driven artificial miRNA targeting rs362273. The intended guide strand is shown in red and mismatches are underlined. The primary mismatch to the SNP site is at position 10 with a secondary mismatch at position 6. The IC_{50} is reported for at least three independent replicates.

Figure 3.3

IC_{50} match = 76 ± 15 ng/ml
 IC_{50} mismatch = 26 ± 10 ng/ml
 discrimination = 3
 fold repression = 2.1



U6 promoter driven miRNA hairpins produce small RNA species with multiple seed sequences

miRNAs recognize their targets through pairing of the seed sequence, nucleotides 2-7 or 8 of the guide strand. For an shRNA or miRNA, the seed sequence is determined by the location of Drosha or Dicer cleavage (Drosha for miRNAs on the 5'-arm of the hairpin, Dicer for miRNAs on the 3'-arm). Single nucleotide polymorphisms in endogenous miRNAs and miRNA precursors are associated with altered miRNA processing and function²⁶⁹⁻²⁷¹ but polymorphisms in seed regions are relatively rare^{272,273}. Endogenous miRNAs are rarely fully complementary to their targets, therefore changes affecting the seed sequence may produce mature miRNAs with a different set of mRNA targets²⁷⁴. Our SNP targeting siRNAs have at most 1 mismatch with the targeted isoform and 2 mismatches with the non-targeted isoform. Although a single nucleotide shift in cleavage site will produce a mature miRNA with a different seed sequence, the new seed sequence should also be complementary to the *Huntingtin* mRNA. Such a shift could, however, affect the ability of a miRNA to discriminate between the two *Huntingtin* isoforms. We transfected our RNAi plasmids into HeLa cells, cloned the small RNA fraction and used high throughput sequencing to characterize the processing products of different shRNA, miRNA-like hairpins and artificial miRNAs (Tables 3.2, 3.3).

Table 3.2. RNA species from HeLa cell small RNA libraries.

Table 3.2

Plasmid	Total Species	Genome Mapping	Non-coding RNAs	miRNAs	Other	Plasmid mapping
U6-mHtt-9	258,028	91,931	11,403	5,633	74,895	442
U6-mHtt-10	364,122	125,167	15,002	6,521	103,644	510
U6-2307	179,598	60,354	8,385	4,739	47,230	428
CMV-mir2273G-1	226,335	76,199	8,873	5,642	61,684	45

Table 3.3. RNA reads from HeLa cell small RNA libraries.

Table 3.3

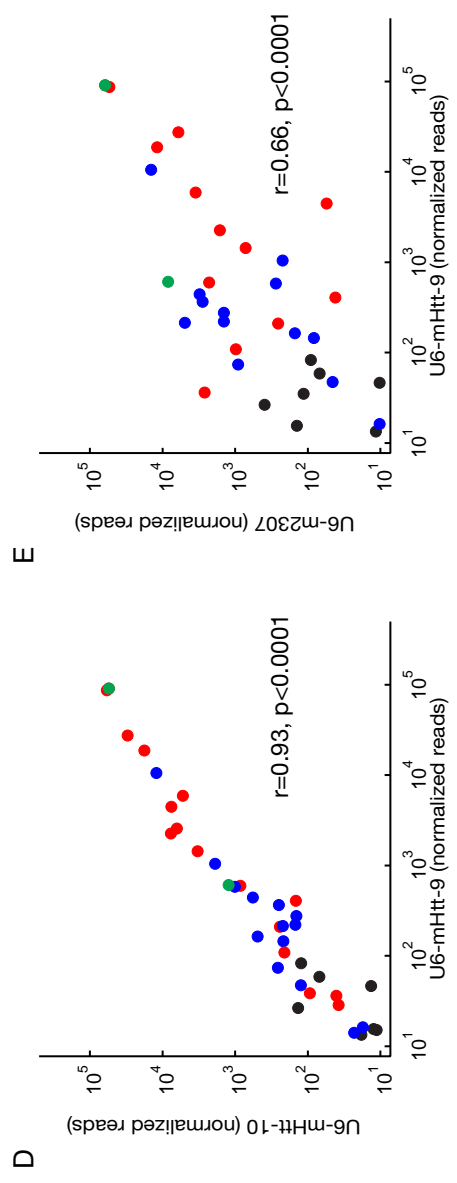
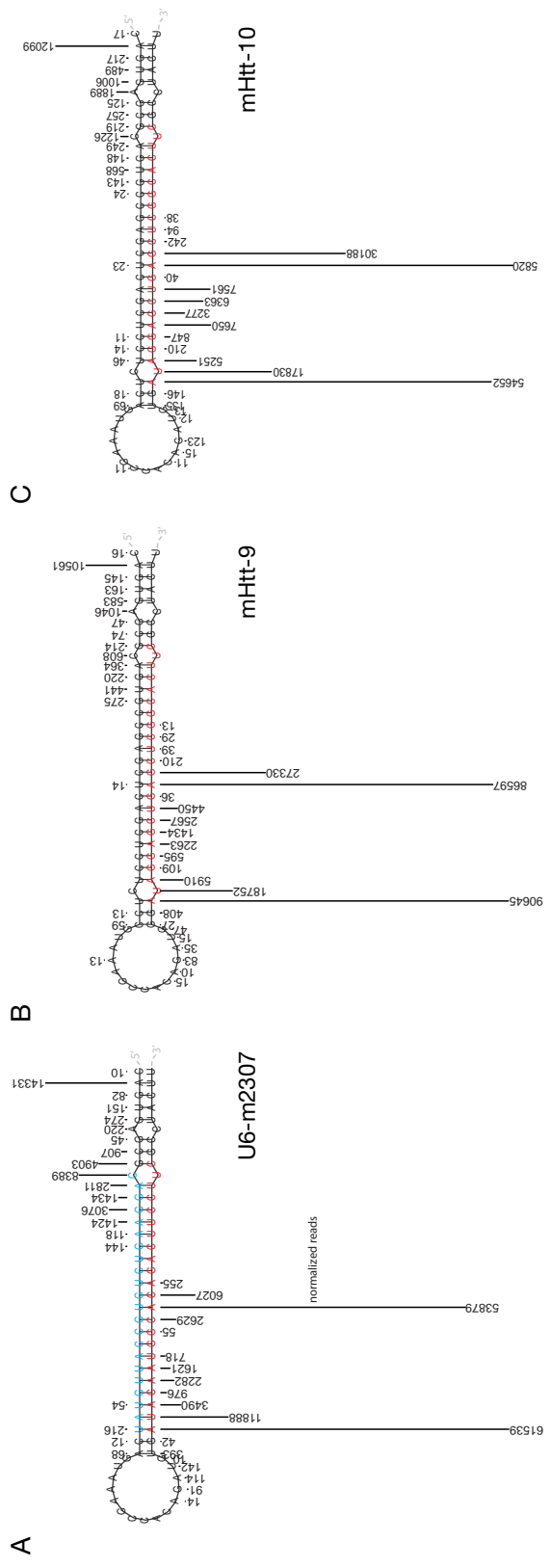
Plasmid	Total Reads	Genome Mapping	Non-coding RNAs	miRNAs	Other	Plasmid mapping
U6-mHtt-9	4,199,913	2,960,981	60,006	2,624,503	276,472	744,310
U6-mHtt-10	6,607,261	4,641,903	107,537	4,093,484	440,882	961,057
U6-2307	4,010,121	3,066,751	39,069	2,860,996	166,686	559,872
CMV-mir2273G-1	4,363,194	3,246,436	49,534	2,865,426	331,476	43,144

We found that the U6-promoter driven miRNA (U6-m2307), produces multiple species (Figure 3.4A, Table 3.2). The most abundant small RNA species produces over 61,000 reads per million, comes from the 3'-arm of the miRNA and is likely the product of the expected sequential cleavage by Drosha and Dicer. Despite its ability to discriminate between the two isoforms, the most abundant small RNA species produced by the miRNA-like plasmid does not have the same sequence as our original discriminating siRNA, but instead is 5'-shifted by a single nucleotide. This surprised us, as it suggests that there is more flexibility than we anticipated in the design of allele-specific siRNA and miRNAs. In addition to the most abundant species, we see almost 12,000 reads per million from the species originating at our intended start site (1 nucleotide 3' of the most abundant species) and a set of sequences originating 10 nucleotides downstream of these products. These products resemble those that we would expect if the unprocessed pri-miRNA is exported and cleaved once by Dicer. These additional small RNAs would likely be eliminated if the pri-miRNA transcript was extended to reduce its affinity for the nuclear export machinery. However, we expect that these small RNAs resemble the products that we would see from a simple U6-promoter driven shRNA. Although all the additional small RNAs could potentially target both *Huntingtin* isoforms through seed pairing, we see no reduction of the matched target, even at the highest plasmid concentration indicating that they are either non-functional or participate in allele-specific silencing. The presence of multiple small RNA products increases the

Figure 3.4: U6-promoter driven miRNA-like hairpins produce multiple small RNA products

(A) Distribution of reads (normalized) mapping to each start position in the 2307 hairpin. Each line is proportional to the number of reads. Positions with fewer than 10 reads per million are not displayed. (B) Distribution of reads mapping to each start position of a mouse Huntingtin targeting miRNA. (C) Hairpin as in (B) with G-C to A-U base pair change at the base of the loop. (D) Correlation analysis of sequencing reads from the two mouse Huntingtin miRNAs. Each start position is a single point. The miRNA and miRNA* are displayed in black. Reads from the loop are black, reads from the 5'-arm are blue and reads from the 3'-arm are red. The miRNA and miRNA* (most abundant species) are green. (E) Correlation analysis of sequencing reads from the 2307 miRNA and the mouse Huntingtin miRNA.

Figure 3.4



probability of seed mediated off-target effects by increasing the number of potential seed hexamer matches between small RNAs and the 3'-UTRs of transcribed mRNAs.

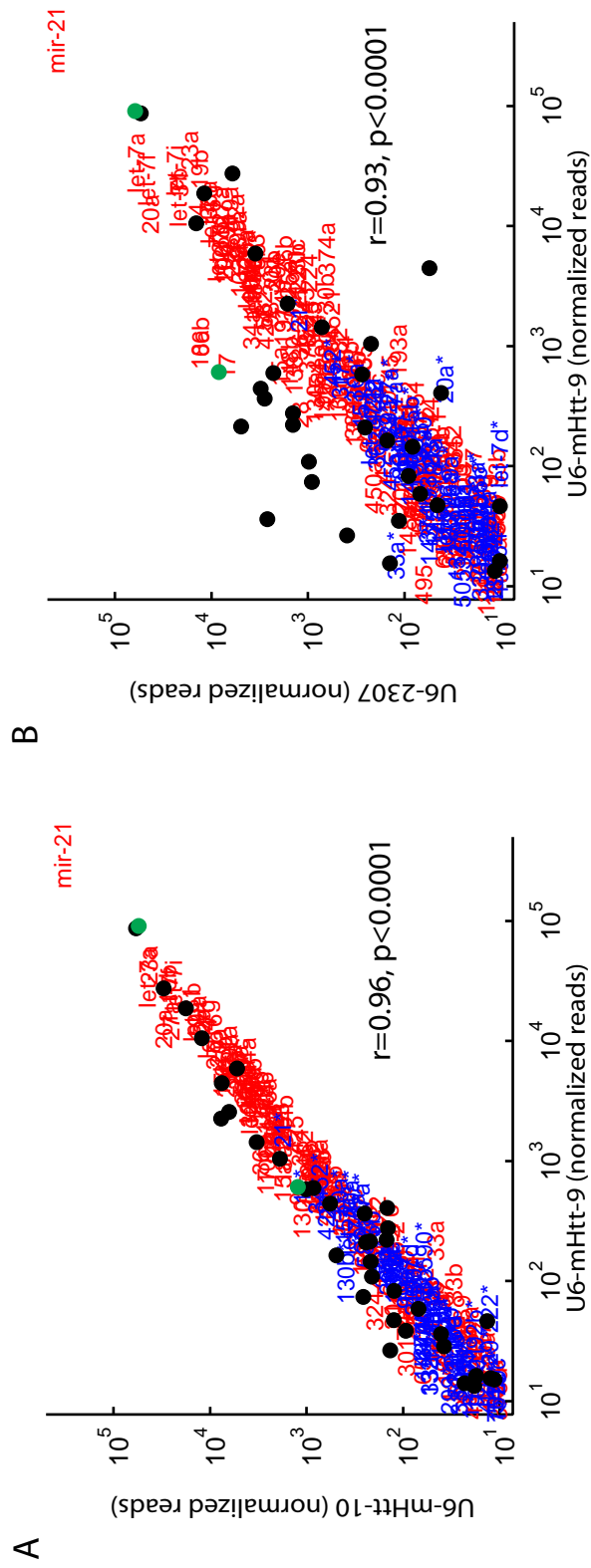
The processing of the U6-miRNA is consistent and does not depend on the inserted sequence. Inserting an unrelated sequence targeting mouse *Huntingtin* (mHtt-9, Figure 3.4B) or changing the nucleotides at the base of the loop (mHtt-10, Figure 3.4C) does not significantly alter the processing. There were no significant differences in the small RNAs mapping to the plasmid hairpin from any of the U6 miRNA constructs (Figure 3.4D,E).

U6-promoter driven miRNAs are produced at high levels relative to endogenous miRNAs. In all our samples the total number of reads mapping to the plasmid exceeded the number of reads for the most highly abundant endogenous miRNA. Only mir-21, which in all our samples generated nearly 10 times more reads than any other miRNA, was consistently more abundant than the most abundant species from our U6-promoter driven miRNAs (Figure 3.5). Endogenous miRNA profiles were not significantly different between any of the samples (Figure 3.5).

Figure 3.5. Endogenous miRNA profiles of HeLa cells transfected with U6-promoter driven artificial miRNAs

(A) Correlation analysis of sequencing reads from endogenous miRNAs from cells transfected with the two U6-promoter driven mouse Huntingtin miRNAs. The miRNA is in red, the miRNA* in blue. Reads from the transfected hairpin are overlaid in green. (B) Correlation analysis of sequencing reads mapping to endogenous miRNAs in cells transfected with the U6-2307 and mouse Huntingtin miRNAs.

Figure 3.5



CMV promoter driven artificial miRNAs produce primarily small RNAs with a single seed sequence

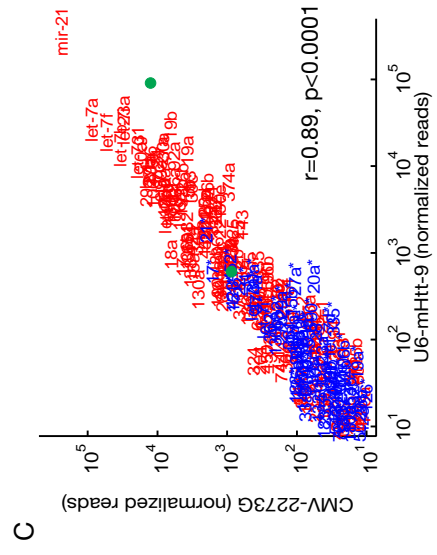
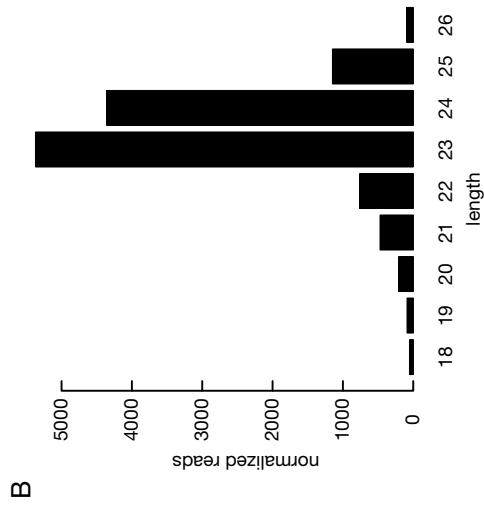
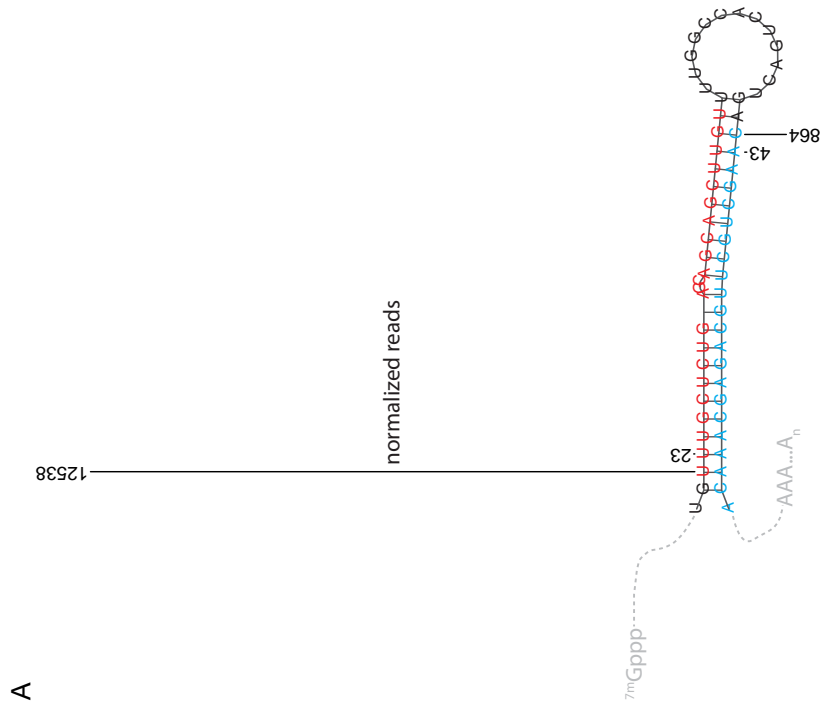
In contrast to the U6-miRNA plasmids, the CMV-miRNAs primarily produce species with a single seed sequence (Figure 3.6A, Tables 3.2, 3.3). In deep sequencing samples from HeLa cells, we detected approximately 14.5 times more of the guide/miRNA strand than the passenger/miRNA* strand, indicating that the correct strand incorporates into and is protected by Argonaute. The miRNA strand shows some length heterogeneity with a peak at 23 nucleotides (Figure 3.6B).

The artificial miRNA is expressed at high levels (Figure 3.6C). Within the sample, the number of reads per million mapping to the miRNA/guide strand (12,538) is comparable to mir-181a (12,873), mir-29a (12,856) and mir-16 (12,501). Although this indicates a high level of expression, the most abundant miRNA strand in the cells transfected with the U6-miRNA was more than 7 times higher. There were no significant differences between endogenous miRNAs in cells transfected with U6-miRNAs or with the CMV-miRNA (Figure 3.6C).

Figure 3.6. CMV promoter driven artificial miRNAs produce a single dominant small RNA species

(A) Distribution of reads (normalized) mapping to each start position in the CMV-2273G hairpin. Each line is proportional to the number of reads. Positions with fewer than 10 reads per million are not displayed. The seed sequence is highlighted. (B) Length distribution of miRNA strand reads from the CMV-2273G hairpin. (C) Correlation analysis of sequencing reads mapping to endogenous miRNAs from cells transfected with the CMV-2273G miRNA and a U6-mouse Huntingtin miRNA. The miRNA is in red, the miRNA* in blue. The miRNA and miRNA* strand from the transfected miRNA are overlaid in green.

Figure 3.6



Discrimination between matched and mismatched targets can be improved by adding additional mismatches in the 3'-region of the siRNA.

To improve discrimination at the rs362273 SNP site, we returned to our reporter assays using siRNAs to mimic the miRNA products. In our previous work, we found that adding secondary mismatches could improve discrimination. In the original rs362273 siRNA the SNP site paired with position 10 of the guide strand with a secondary mismatch at position 5. To ensure loading of the proper strand into Argonaute, our initial siRNAs contained a mismatch between position 1 of the guide strand and position 19 of the passenger strand. In the artificial miRNAs, we eliminated this mismatch and introduced a central bulge by deleting 2 nucleotides at positions 7 and 8 of the passenger strand (Figure 3.7A, Figure S3.2). We used a series of siRNAs with this structure and mismatched at 2 and 3 positions to test for discrimination between a matched and mismatched luciferase reporter (Table 3.4). The change in structure had no effect on discrimination as the p10 + p5 siRNA again had a discrimination ratio of 5 (Figure 3.7B).

Expanding the mismatch in the central region of the siRNA by adding a second mismatch at position 9 or position 11 decreased discrimination (Figure 3.7C, D) but when we added a position 16 mismatch to the p10+p5 siRNA sequence, the discrimination ratio improved to greater than 10 with less than a 35% reduction in activity from the mismatched reporter, even at the highest concentration tested (Figure 3.7E).

Figure 3.7. Screening of siRNAs to improve discrimination at rs362273

(A) Structure of the original and new siRNAs. The original contained a mismatch between position 1 of the guide strand and position 19 of the passenger strand. The new siRNAs consist of a 21 nucleotide guide strand and a 19 nucleotide passenger strand. This creates a bulge at position 12 and 13 of the guide strand.

(B)-(I) Representative data from luciferase reporter assays for siRNAs targeting the G isoform of rs362273. The SNP site is always at position 10 and is underlined. (B) position 5+10, 21mer siRNA. (C) position 10+11, 21mer siRNA. (D) position 9+10 21mer siRNA. (E) position 5+10+16 21mer siRNA. (F) position 5+10+11, 21mer siRNA. (G) position 5+9+10, 21mer siRNA. (H) position 5+10, 23mer siRNA. (I) position 5+10+16 23mer siRNA. (J)-(M). Representative data from luciferase reporter assays for siRNAs targeting the A isoform of rs362273. (J) Position 5+10, 21mer siRNA. (K) Position 5+10+16, 21mer siRNA. (L) Position 5+10, 23mer siRNA. (M) Position 5+10+16, 23mer siRNA. This data is summarized in Table 3.4.

Figure 3.7

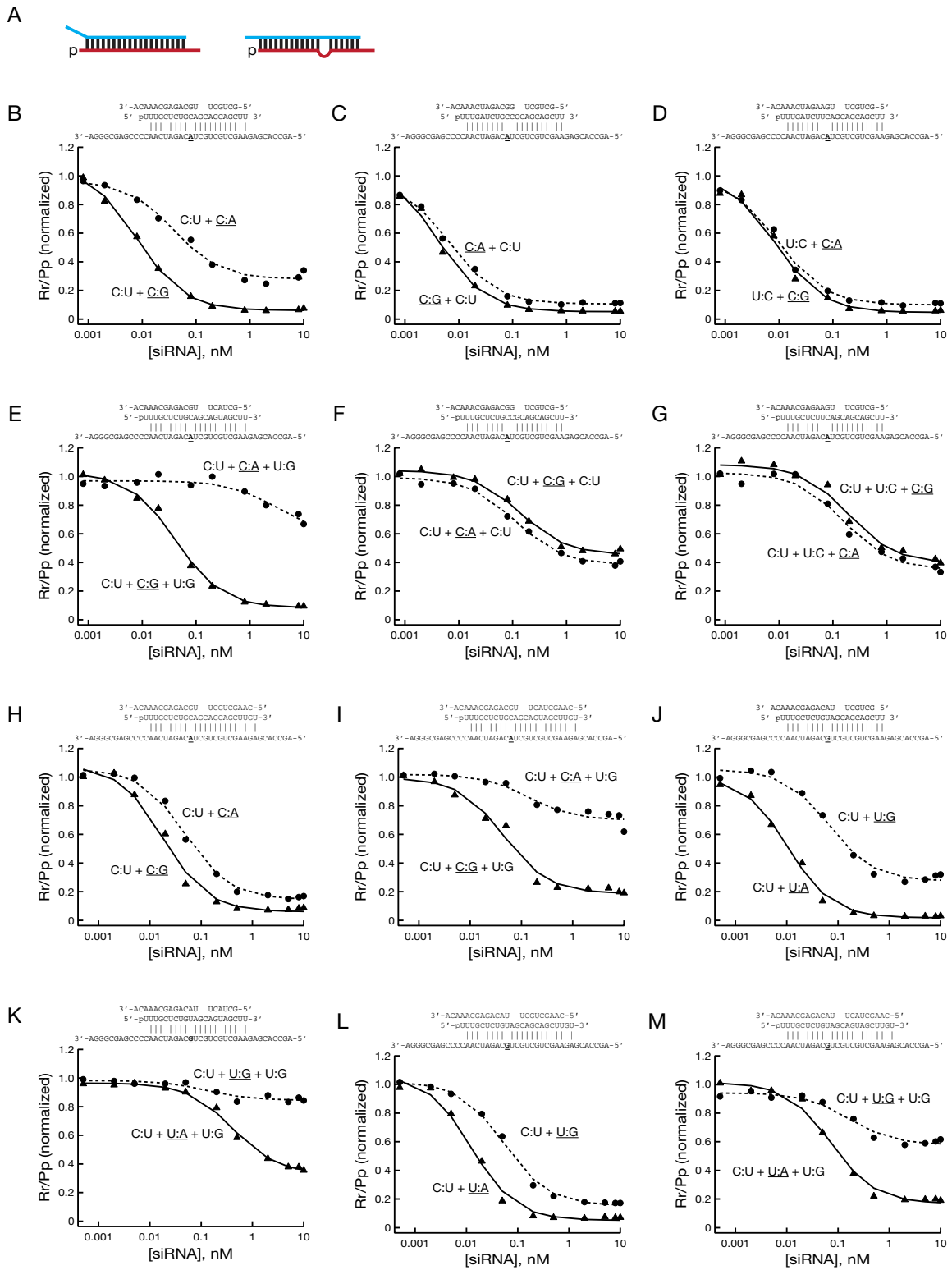


Table 3.4. Screening of siRNAs to improve discrimination at rs362273.

IC50 values and fold repression are given as the average \pm standard deviation for at least three independent experiments. The IC50 is reported as ≥ 10 for siRNAs that failed to achieve 50% inhibition at the highest concentration tested. Fold repression is calculated for the maximum concentration of 10nM.

Table 3.4

Figure	Target	plasmid	Length	Mismatch		IC50 (nM)		Discrimination		% Repression (10nM)		Fold Repression
				Position	Mismatch	Match	Mismatch	Ratio	Match	Mismatch		
3.7B	G	2273-2	21	5, <u>10</u>	0.013 ± 0.004	0.055 ± 0.019	4.3	94 ± 1	69 ± 4	5.2		
3.7C	G	2273-2	21	<u>10</u> ,11	0.006 ± 0.004	0.008 ± 0.002	1.4	94 ± 1	89 ± 2	1.9		
3.7D	G	2273-2	21	9, <u>10</u>	0.008 ± 0.002	0.010 ± 0.002	1.3	95 ± 1	87 ± 5	2.4		
3.7E	G	2273-2	21	5, <u>10</u> ,16	0.069 ± 0.036	10 ± 0	144	89 ± 2	19 ± 13	7.5		
3.7F	G	2273-2	21	5, <u>10</u> ,11	0.077 ± 0.033	0.078 ± 0.052	1.0	53 ± 7	52 ± 6	1.0		
3.7G	G	2273-2	21	5,9, <u>10</u>	0.15 ± 0.04	0.15 ± 0.02	1.0	55 ± 6	64 ± 3	0.8		
3.7H	G	2273-2	23	5, <u>10</u>	0.014 ± 0.003	0.042 ± 0.006	3.0	93 ± 1	84 ± 1	2.2		
3.7I	G	2273-2	23	5, <u>10</u> ,16	0.046 ± 0.001	6.8 ± 5.6	147	84 ± 3	46 ± 7	3.3		
3.7J	A	2273-1	21	5, <u>10</u>	0.008 ± 0.002	0.072 ± 0.008	9.1	96 ± 1	60 ± 9	10.1		
3.7K	A	2273-1	21	5, <u>10</u> ,16	0.47 ± 0.12	10 ± 0	21	65 ± 3	13 ± 5	2.5		
3.7L	A	2273-1	23	5, <u>10</u>	0.014 ± 0.006	0.076 ± 0.023	5.4	93 ± 1	83 ± 4	2.4		
3.7M	A	2273-1	23	5, <u>10</u> ,16	0.065 ± 0.013	10 ± 0	153	84 ± 4	37 ± 3	4.0		

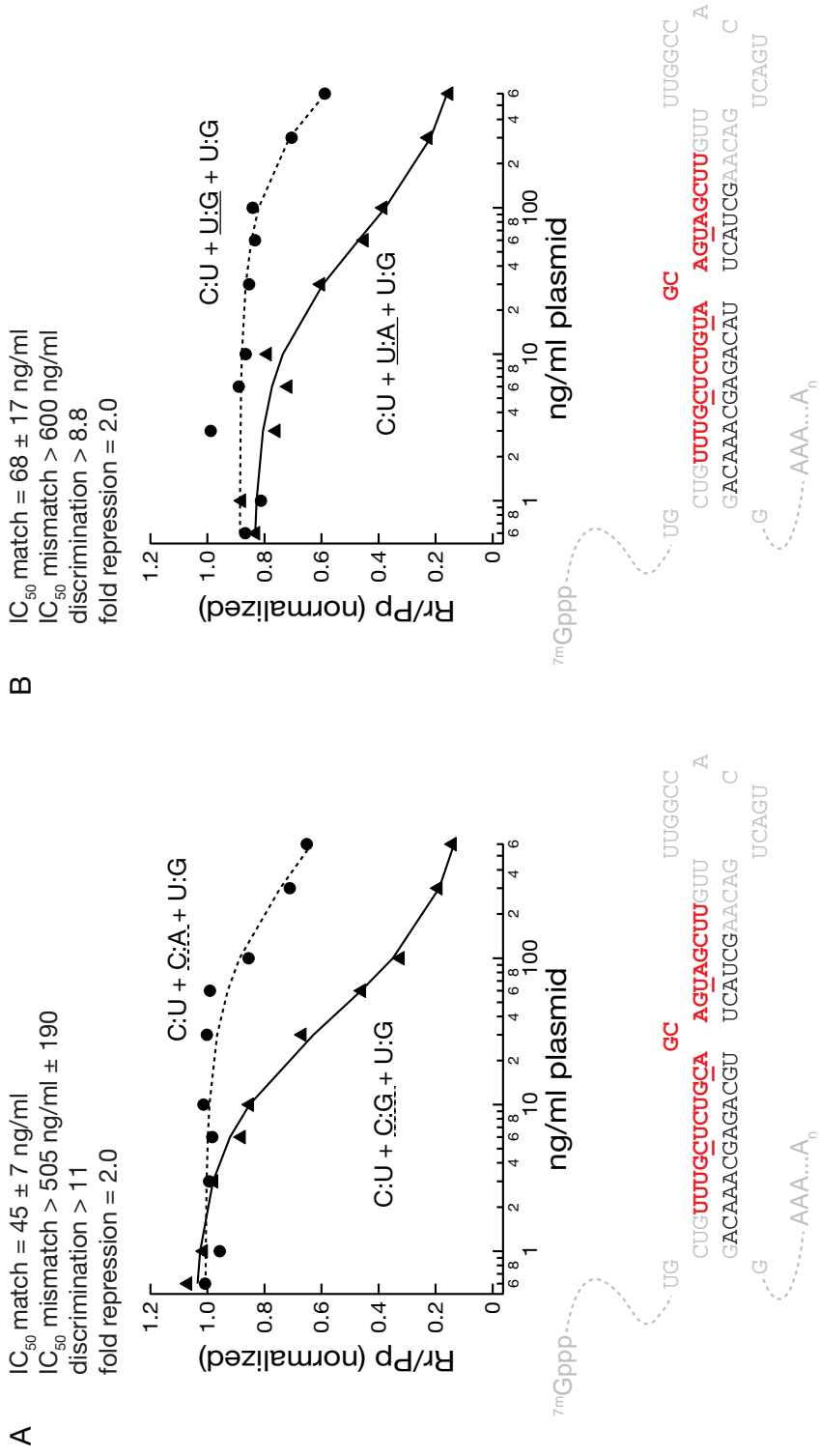
Adding a third mismatch to the centrally bulged siRNAs decreased their potency without improving discrimination (Figure 3.7F,G).

Based on our sequencing data, the most common miRNA guide was 23 nucleotides long. When we annealed this 23mer to the most common miRNA* strand, we found that discrimination decreased and silencing of the mismatched reporter increased for both the 2 mismatch and the 3 mismatch siRNA (Figure 3.7H,I) suggesting that guide strand length influences the ability of an siRNA or miRNA to discriminate between SNP isoforms. The triple mismatched 23mer retained the ability to discriminate, albeit with 40-50% silencing of the mismatched reporter (Figure 3.7I). We tested the same pattern of mismatches in an siRNA targeting the A isoform of rs362273 and saw the same general results; the additional position 16 mismatch improved discrimination in both the 21mer (Figure 3.7J,K) and 23mer siRNAs (Figure 3.7L,M). Interestingly, the 23mer siRNA was more potent than the 21mer against both the A (match) and G (mismatch) target (Figure 3.7K,M). When we placed the new triple mismatched sequence into the CMV-mir155 plasmid, it retained the ability to discriminate between the two reporters (Figure 3.8). We proceeded with our experiments using this triple mismatched design.

Figure 3.8. A triple mismatched artificial miRNA discriminates between isoforms at rs362273

Representative data from luciferase assays of artificial miRNA plasmids targeting the G (A) and the A (B) isoform of rs362273.

Figure 3.8



Self-complementary AAV9 delivery of artificial miRNAs into the mouse striatum

We incorporated the artificial miRNA targeting rs362273 into a self-complementary recombinant AAV9 virus (Figure 3.9A). We injected viruses targeting the G isoform of rs362273 (scAAV9-2273G, match), the A isoform (scAAV9-2273A, mismatch) or renilla luciferase (scAAV9-rluc, non-targeting control) directly into the striatum of 3 month old wild-type mice. After three weeks, we harvested RNA from the striatum for small RNA sequencing (Table 3.5, 3.6). We found that in these brain samples, we could only detect a small number of reads mapping to the virus (Table 3.6). In scAAV9-rluc and scAAV9-2273G samples, only the miRNA and not the miRNA* reached our threshold abundance of 10 reads per million (Table 3.7). The miRNA* was detectable in the scAAV9-2273A samples but not in the scAAV9-mirRluc or scAAV9-mir2273G samples. (Table 3.7, Figure 3.9). All three miRNAs generated comparable numbers of total reads, but the each miRNA had a distinct length distribution (Figure 3.10) which may reflect differential processing or modification of the 3'-end of the miRNA. Unlike in cell culture, the miRNAs were not detected at high abundance relative to endogenous miRNAs (Figure 3.9). We do not know if the miRNAs are present in many cells at low levels or at high levels in only a few cells. There were no significant differences in endogenous miRNAs between individual mice (Figure 3.9B,C,D) in each treatment group or between mice in different groups (Figure 3.9E,F).

Table 3.5. RNA species from mouse striatal small RNA libraries.

Table 3.5

Group	Sample ID	Total Species	Genome Mapping	Non-coding RNAs	miRNAs	Mapping to Virus
scAAV9-mirRluc	2137	108,117	25,545	5,199	5,774	14
scAAV9-mirRluc	2141	116,503	28,449	6,578	6,002	15
scAAV9-mir2273A	2137	93,160	21,268	4,354	5,216	27
scAAV9-mir2273A	2141	87,663	19,343	3,733	5,302	24
scAAV9-mir2273G	2137	92,487	21,754	4,383	5,529	20
scAAV9-mir2273G	2141	82,813	19,424	4,320	5,324	20

Table 3.6. RNA reads from mouse striatal small RNA libraries.

Table 3.6

Group	Sample ID	Total Reads	Genome Mapping	Non-coding RNAs	miRNAs	Mapping to Virus
scAAV9-mirRluc	2137	4,949,561	4,055,081	32,721	3,922,515	2,577
scAAV9-mirRluc	2141	5,352,460	4,324,547	45,773	4,125,194	5,030
scAAV9-mir2273A	2137	3,333,570	2,696,832	26,306	2,629,686	1,848
scAAV9-mir2273A	2141	4,108,820	3,391,576	22,522	3,325,411	2,491
scAAV9-mir2273G	2137	4,550,551	3,797,891	31,173	3,725,626	2,014
scAAV9-mir2273G	2141	3,737,472	3,084,269	26,151	3,005,472	2,020

Table 3.7. Small RNAs mapping to scAAV9-miRNA viruses in the mouse striatum.

The total reads for miRNA and miRNA* includes number of reads from any small RNA species perfectly matched to the virus with the same 5'-end as the expected miRNA or miRNA*. miRNA and miRNA* reads are normalized to the total number of genome mapping reads in the library minus the number of reads mapping to known non-coding RNAs. Species with less than the threshold of 10 reads per million are not reported. No other species reached the threshold in any of the samples.

Table 3.7

Injection	Sample Number	miRNA reads	miRNA* reads
scAAV9-mirRluc	2138	638	
scAAV9-mirRluc	2141	1173	
scAAV9-mir2273A	2137	656	26
scAAV9-mir2273A	2144	719	15
scAAV9-mir2273G	2139	528	
scAAV9-mir2273G	2142	649	

Figure 3.9. Self-complementary AAV9 delivery of artificial miRNAs to the mouse striatum

Mice were injected with scAAV9 viruses carrying CB-GFP-miRNAs (A). The mir2273G miRNA targets mouse Huntingtin, while the mir2273A is mismatched as in figure 3.8. The renilla luciferase miRNA serves as a non-targeting control. (B)-(C) Correlation analysis of sequencing reads mapping to endogenous mouse miRNAs from wild-type mice injected with the same virus show no significant differences between individual mice. (B) Two mice injected with scAAV9-mirRluc. (C) Two mice injected with scAAV9-mir2273A—mismatched to mouse Huntingtin (D) Two mice injected with scAAV9-mir2273G—matched to endogenous mouse Huntingtin. (E) and (F) Correlation analysis of sequencing reads mapping to endogenous mouse miRNAs from wild-type mice injected with rluc or Huntingtin SNP-targeting artificial miRNAs shows no difference between groups.

Figure 3.9

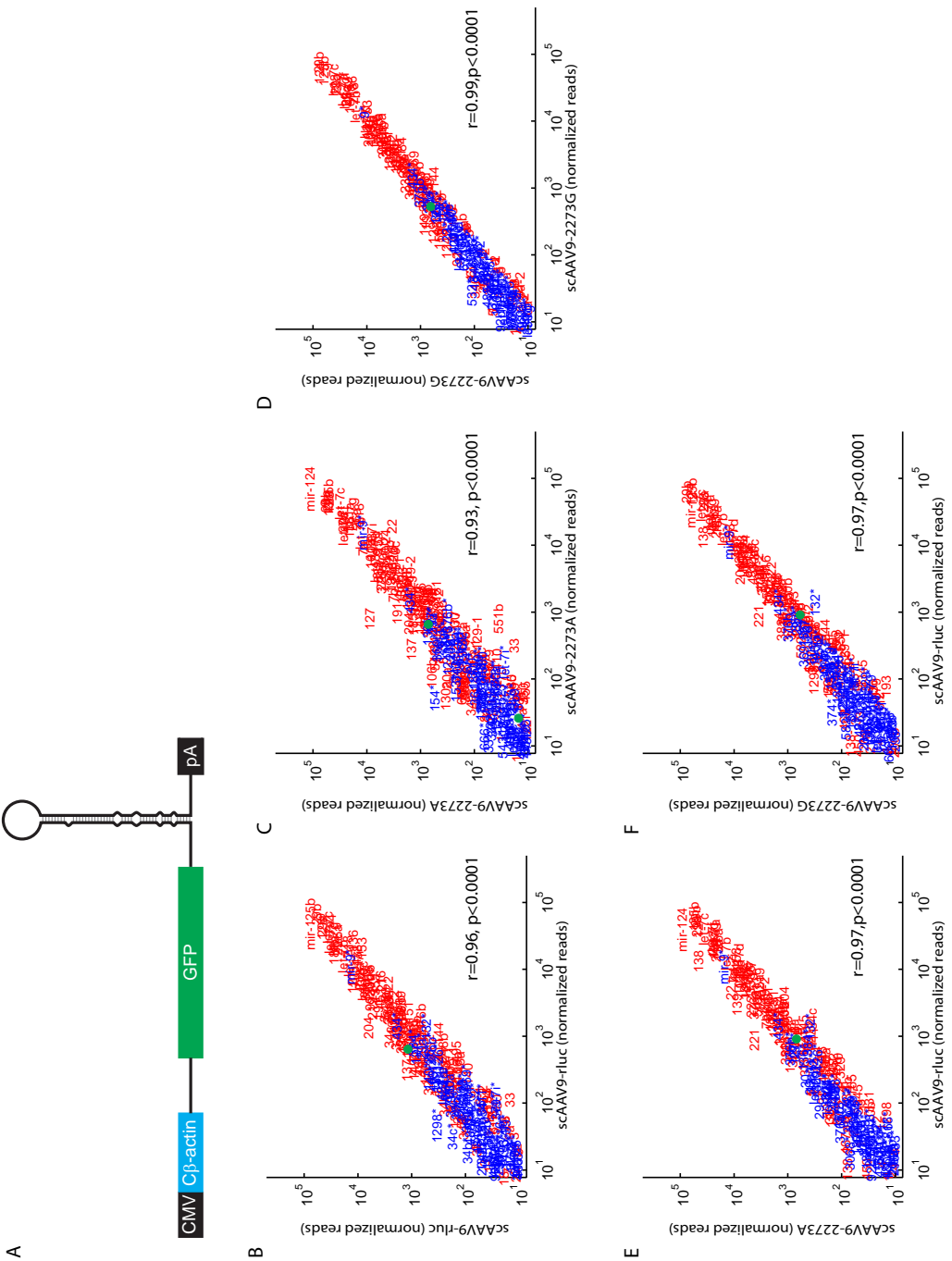
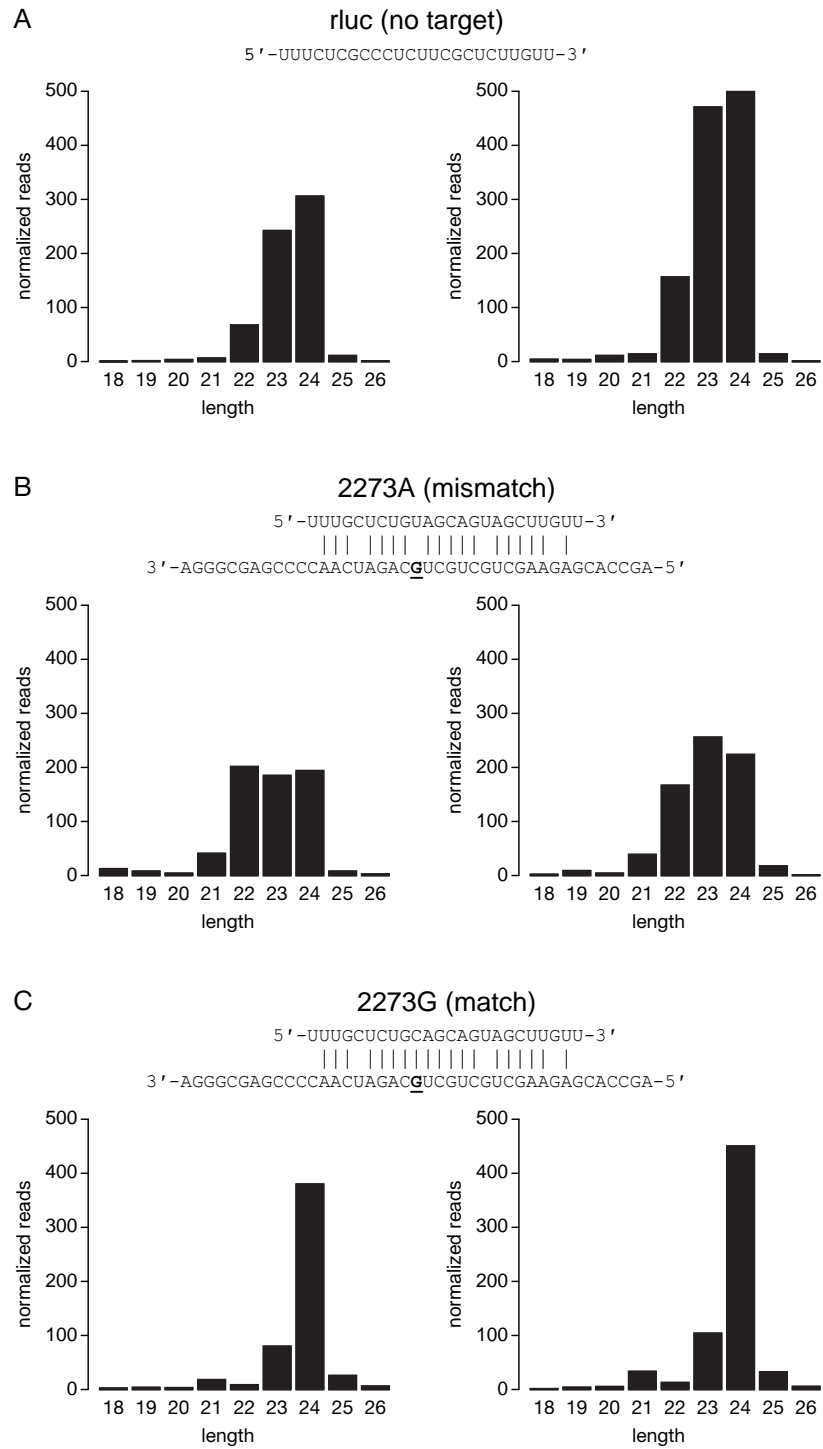


Figure 3.10. Length distributions of virally introduced artificial miRNAs

Non-targeting (scAAV9-mirRluc, A), mismatched (scAAV9-mir2273A, B) and matched (scAAV9-mir2273G, C) miRNAs produce miRNAs with distinct length distributions.

Figure 3.10



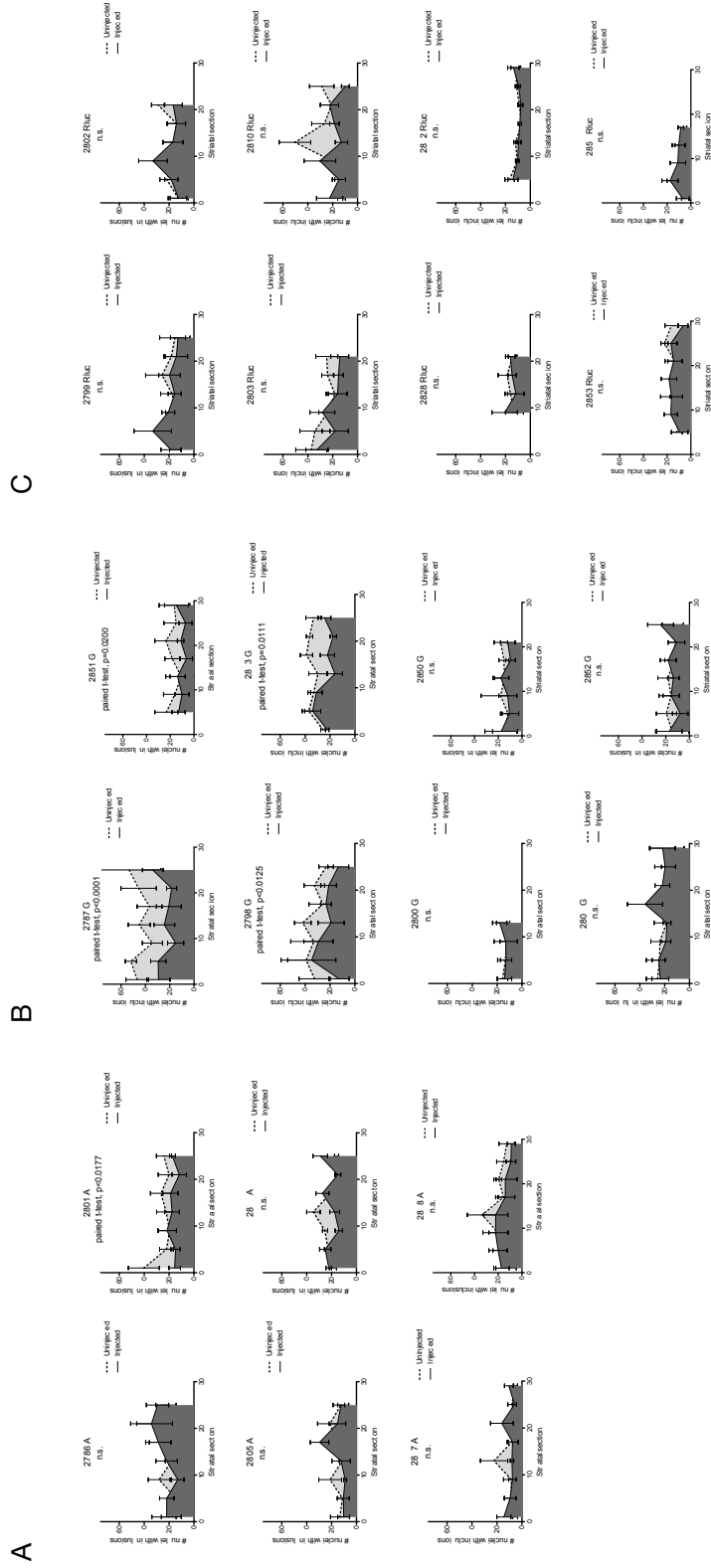
SNP targeting artificial miRNAs reduce inclusions in a mouse model of HD

We next injected the same viruses unilaterally into 3 month old homozygous *Huntingtin* CAG knock-in mice. These mice have 140 CAG repeats inserted into the mouse *Huntingtin* gene locus. They develop nuclear aggregates and inclusions starting at 4 months of age²⁶⁸. One of the mice injected with scAAV9-mir2273A died following surgery. Four months after injection, we took the mouse brains for immunohistochemistry using MW8, an antibody that recognizes aggregated mutant *Huntingtin*^{275,276}. For each mouse we counted the number of inclusions on the injected versus the non-injected side. None of the mice injected with the renilla luciferase (non targeting) control (n=8) miRNA showed any difference between sides (Figure 3.11A), whereas 1/6 of the mice injected with mir-2273A (mismatch, Figure 3.11B) and 4/8 of the mir-2273G (match, Figure 3.11C) viruses showed a significant decrease in inclusions on the injected side. In one of the scAAV9-mir2273A mice we were unable to determine the injected side therefore it was not analyzed. The decrease was not due to neuron loss as there was no difference in DARPP-32 staining between sides in any of the mice that showed a significant decrease in inclusions (Figure 3.12).

Figure 3.11. Matched but not mismatched miRNAs reduce inclusions in an HD mouse model

We injected mice unilaterally with scAAV9 viruses carrying mirRluc (non targeting control), mir2273A (mismatch), or mir2273G (match). After four months we compared the number of nuclei with Huntingtin inclusions on the injected side vs. the non injected side. There was no difference in any of the mice that had received the non-targeting control (n=8) (A). 1/6 of the mice receiving the mismatched miRNA (B) and 4/8 of the mice receiving the matched miRNA (C) had significantly fewer inclusions on the injected side.

Figure 3.11



A

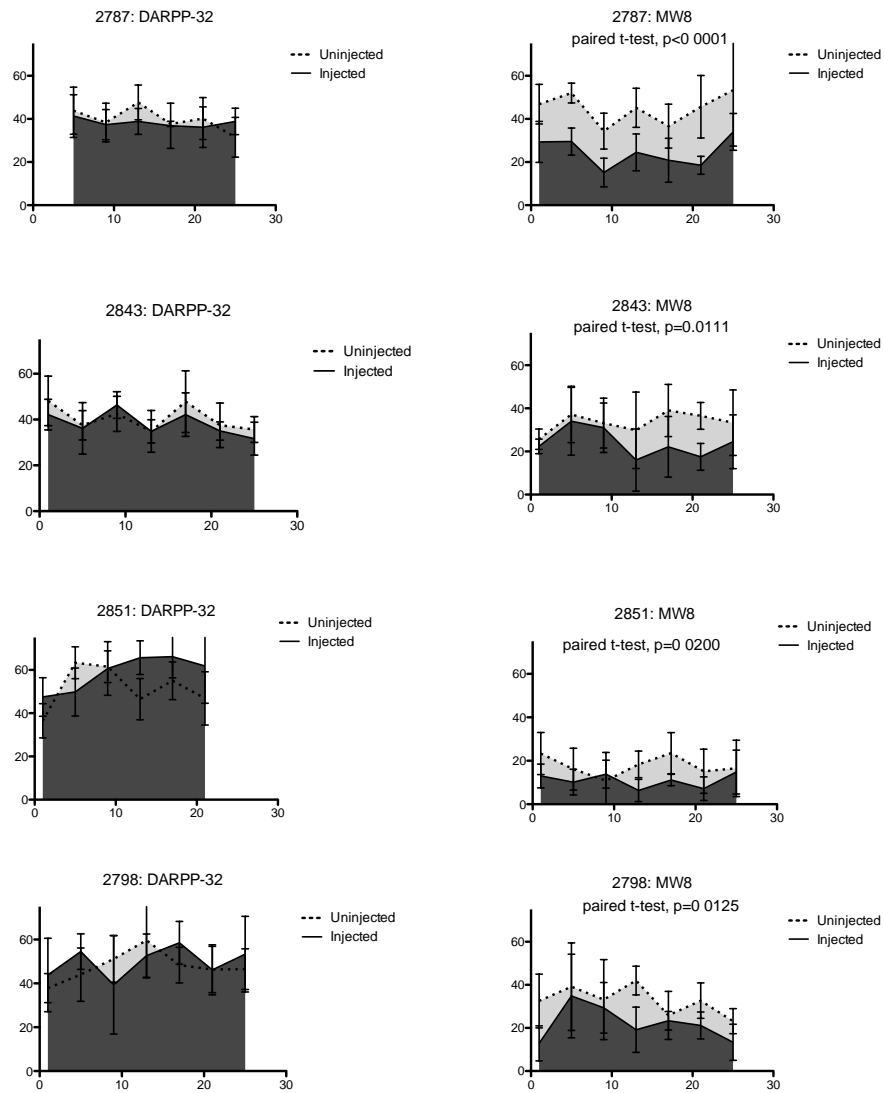
B

C

Figure 3.12. Reductions in inclusions in mice receiving scAAV9-2273G are not due to neuron loss

To ensure that the apparent reduction in inclusions in scAAV9-mir2273G treated mice was not due to neuron loss, we counted the number of DARPP32 positive neurons. There was no significant difference between sides in any of the mice.

Figure 3.12



Discussion

In previous work we have shown that targeting of single nucleotide polymorphisms in the *Huntingtin* gene is a viable therapeutic strategy for Huntington's disease²⁶¹. Unfortunately, delivery and distribution of siRNA to the brain remains challenging. In this paper, we explore an alternative approach: allele-specific RNAi gene therapy for HD. In theory, shRNA and miRNA hairpins enter the endogenous miRNA pathway and are processed and loaded into Argonaute complexes. These Argonaute complexes are functionally indistinguishable from complexes loaded with unmodified siRNA. However, endogenous miRNA processing produces multiple closely related sequences. Most of the variability is at the 3'-end where it is not known to affect miRNA function, but there is some heterogeneity in 5' processing as well. One of the challenges of targeting SNP sites is that the ideal SNP-targeting RNAi construct exists on the border between functional and non-functional; it is highly active against the matched target, yet a single nucleotide change renders it inactive. In theory, this might make SNP-targeting hairpins particularly sensitive to processing heterogeneity. Our results suggest that siRNAs which show good discrimination, particularly those that do not produce significant knockdown of a mismatched target at high concentrations, can easily be converted to artificial miRNAs. Sequence requirements for double mismatched discriminating siRNAs may be more flexible than we had initially expected as a single base shift in start position appears to produce a functional and discriminating small RNA. However,

siRNAs that show marginal discrimination or those that can produce significant knockdown of the mismatched target will need to be improved before they are incorporated into a miRNA backbone. Our reporter assays show that longer siRNAs and mature miRNAs may not discriminate as well as canonical 21 nucleotide siRNAs. Using an endogenous miRNA backbone which is processed to a shorter product could improve the ability to discriminate between matched and mismatched target.

Artificial miRNAs targeting SNP sites in human *Huntingtin* can be delivered to the striatum using scAAV9 viruses and are processed into the correct small RNA species. Matched but not mismatched miRNAs reduce inclusions in a CAG140 knock-in mouse model of HD providing proof of concept for in vivo use of virally delivered SNP targeting artificial miRNAs in the brain. This brings us one step closer to allele-specific gene therapy for HD.

Materials and Methods

Construction of shRNA and miRNA plasmids and viral vectors

For the cell culture experiments, U6-promoter driven shRNA and miRNA were generated by cloning a 71mer (shRNA) or 90mer (miRNA) into the BamHI and EcoRI sites of the pSIREN-Shuttle vector (Clontech Laboratories, Mountain View, CA). GFP-artificial miRNAs were generated by cloning into the pcDNA6.2-

GW/EmGFP-miR plasmid (Invitrogen Corporation, Carlsbad, CA). Sequences are listed in Table S3.1.

Recombinant AAV9 vectors used in this study were generated, purified, and titered by the UMass Gene Therapy Vector Core as previously described²⁷⁷. The cloning of the miRNAs at the polyA region was accomplished by inserting the pri-miRNA sequence at the NotI site 5 bp upstream of the polyA region of the CBA-GFP cassette.

Reporter Constructs and Assays

Reporter constructs were as previously described²⁶¹. HeLa cell cultures were maintained at 37°C and 5% CO₂ in DMEM (Invitrogen Corporation, Carlsbad, CA) supplemented with 10% heat inactivated FBS and 50U/ml penicillin and streptomycin (Invitrogen). For luciferase assays, cells were plated at 0.8×10^5 cells per well in 24-well plates. Twenty-four hours later, cells were washed and the medium was replaced with OptiMEM (Invitrogen). siRNAs were mixed in a total volume of 100µl/well with 0.025 µg/well of the SNP reporter (pSiCheck-2273 or pSiCheck-2307) and 1 µl of DharmaFECT DUO (Dharmacon, Lafayette, CO). Each transfection mixture was normalized to a total siRNA concentration of 10nM using siGENOME RISC-Free Control siRNA (Dharmacon). Twenty-four hours after transfection, the cells were lysed for 20 minutes in 100µl 1x passive lysis buffer (Promega Corporation, Madison, WI). Luciferase activity was read in 96-

well plates with the Dual-luciferase assay kit (Promega) using the GloMax multi-detection system (Promega).

For plasmid transfections the procedure was essentially as described above. Each transfection mixture was normalized to contain the same amount of total DNA using pIRES-eGFP (Clontech) for the U6-promoter driven constructs or pcDNA6.2-GW/EmGFP-mirLacZ control (Invitrogen) for the CMV-promoter driven constructs. The media was changed back from OptiMEM to the usual growth medium after 24 hours. Forty-eight hours after transfection, the cells were lysed and luciferase activity was read as described above. IC50 curves were generated by fitting normalized Renilla luciferase activity versus concentration in Igor Pro (WaveMetrics, Inc., Lake Oswego, OR).

Small RNA cloning

HeLa cells were plated at 1.4×10^5 cells/ml in 100mm dishes. Twenty-four hours later, cells were washed with 1x PBS and the media was changed to OptiMEM. Cells were transfected with 6 μ g of plasmid DNA using 20 μ l of DharmaFECT Duo (Dharmacon). After 24 hours the media was changed back to the usual growth medium. After 48 hours total RNA was extracted using the mirVana RNA isolation kit (Ambion, Austin, TX). Eighty micrograms of total RNA was loaded onto a 15% denaturing urea-polyacrylamide gel (National Diagnostics, Atlanta, GA) and the 18-30 nucleotide fraction was isolated. 100 pmole of 3'-adaptor (miRNA cloning linker 1, Integrated DNA Technologies, Coralville, IA) was ligated

to half the purified RNA using truncated T4 RNA Ligase 2 (New England Biolabs, Ipswich, MA) at 25°C for 8 hours in 20µl buffer containing 50mM Tris-HCl, 10mM MgCl₂, 10mM DTT, 60µg/ml BSA and 10% DMSO. Ligated product was purified on a 15% denaturing urea polyacrylamide gel (National Diagnostics) and ligated to one of four barcoded 5' RNA adapters (5'-GUU CAG AGU UCU ACA GUC CGA CGA UCC GUC-3', 5'-GUU CAG AGU UCU ACA GUC CGA CGA UCU AGC-3', 5'-GUU CAG AGU UCU ACA GUC CGA CGA UCA UCC-3', 5'-GUU CAG AGU UCU ACA GUC CGA CGA UCG CAC-3') using T4 RNA ligase (Ambion, Austin, TX) at 25°C for 8 hours. 5'-ligated product was purified on a 10% denaturing urea-polyacrylamide gel (National Diagnostics). cDNA was synthesized using the RT primer (5'-ATT GAT GGT GCC TAC AG-3'). Libraries were amplified by PCR using forward (5'-AAT GAT ACG GCG ACC ACC GAC AGG TTC AGA GTT CTA CAG TCC GA-3') and reverse (5'-CAA GCA GAA GAC GGC ATA CGA ATT GAT GGT GCC TAC AG-3') primers and sent for sequencing on the Genome analyzer II (Illumina, San Diego, CA) by the University of Massachusetts Deep Sequencing Core.

For mouse brain small RNA libraries, brains were extracted and immediately frozen on dry ice. Frozen brains were dissected and the striatum was thawed at -20°C in RNAlater-ICE (Ambion, Austin, TX). Small RNA cloning and sequencing was as described above except the starting amount of total RNA was 20µg and all the ligation reactions were scaled accordingly.

Sequence extraction, analysis and statistics

Each sequencing read was checked for the presence of a 3'-adapter by looking for a perfect match to the 6-mer corresponding to the 5' end of the 3'-adapter. Sequences without a 3'-adapter were discarded. Sequences with a 3'-adapter were sorted by barcode by matching the first 4 nucleotides of the insert to the barcodes. Sequences without perfectly matching barcodes were discarded. Sequences with both 3'-adapter and 5'-barcode were then mapped, with no mismatches, to the genome (*Homo sapiens*, USCG hg19 or *Mus musculus*, USGC mm9), the introduced shRNA or miRNA, known non-coding RNAs and pre-miRNA hairpins using Bowtie²⁷⁸. Species mapping to pre-miRNA hairpins were further annotated as miRNA or miRNA*. For each pre-miRNA, the most abundant species was annotated as the miRNA and the most abundant species on the opposite arm of the hairpin was annotated as the miRNA*. For both endogenous miRNA and sequences mapping to the introduced shRNA or miRNA, species with the same 5'-end were considered equivalent whereas we tolerated heterogeneity at the 3'-end. Therefore reads from small RNAs mapping to the same start position were summed. Small RNA reads were normalized to the number of times mapped to the genome and to the total number of genome-mapping small RNA reads minus reads mapping to non-coding RNAs. Log transformation and spearman correlation analysis was performed using GraphPad Prism version 5.04 (GraphPad Software, Inc., La Jolla, CA).

Animals and Injections

Three to four month old wild-type FVB mice or CAG140 mice were injected unilaterally with 3 μ l of scAAV9-mirRluc, scAAV9-mir2273G or scAAV9-mir2273A (viral titer 1.0×10^{13}) as previously described⁵. Following surgery, the mice were monitored for weight loss and behavioral changes. After three weeks, the wild-type mice were killed and their brains were frozen for RNA extraction and small RNA cloning. After 4 months, the CAG140 mice were perfused with 4% paraformaldehyde in PBS. The brains were removed and post-fixed in paraformaldehyde for immunohistochemistry. All animal procedures were approved by the University of Massachusetts Medical School Institutional Animal Care and Use Committee.

Immunohistochemistry and Inclusion Counting

Brains were sectioned at 40 μ m. Sections were treated with 3% hydrogen peroxide for 3 minutes and then washed with PBS. For DARPP32 labeling, sections were then treated with 0.5% TritonX for 20 minutes. All sections were incubated in normal goat serum for 3-4 hours then incubated in primary antibody overnight. The next day after incubation in biotinylated anti-rabbit IgG secondary antibody and ABC reagent using the Vectastain ABC kit (Vector Laboratories, Inc., Burlingame, CA), sections were stained with diaminobenzidine for 2 minutes. The MW8 antibody developed by Paul H. Patterson was obtained from the Developmental Studies Hybridoma Bank developed under the auspices of

the NICHD and maintained by The University of Iowa, Department of Biology, Iowa City, IA 52242. The anti-DARPP32 antibody was purchased from Abcam (EP720Y, Abcam, Cambridge, MA).

Supplemental Figures and Tables

Figure S3.1. U6 promoter driven shRNA and miRNA can cause a non-specific increase in luciferase activity.

(A) U6-shRNA targeting rs362307 (B) U6-miRNA targeting rs362307.

Figure S3.1

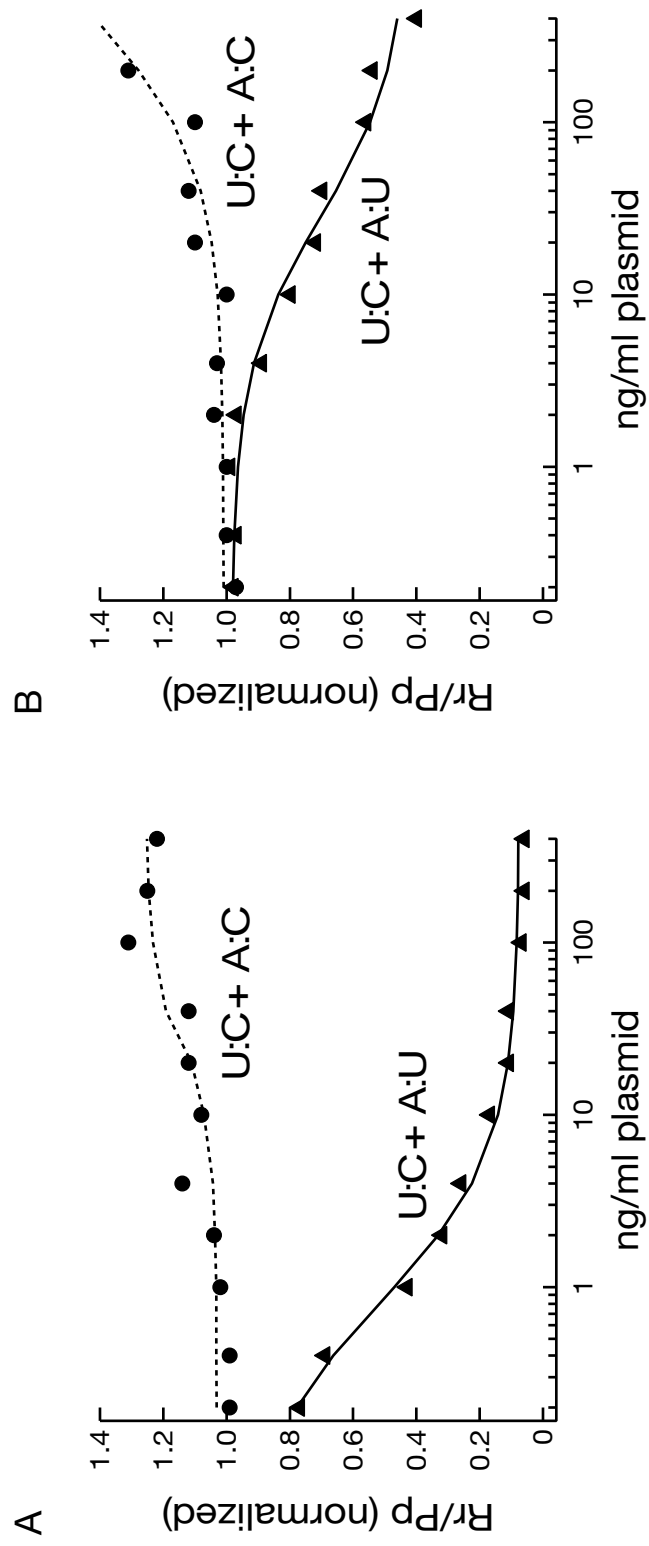


Figure S3.2. miRNAs without a central bulge are not functional against matched or mismatched targets in a luciferase reporter assay

We prepared miRNAs targeting the A isoform of the rs362273 site without the central mismatch between miRNA and miRNA* strands. To favor asymmetric loading of the guide strand into Argonaute, we introduced a mismatch to the miRNA* strand at position 1 (A) or position 2 (B) of the miRNA strand. These miRNA were not functional against either the matched or mismatched targets.

Figure S3.2

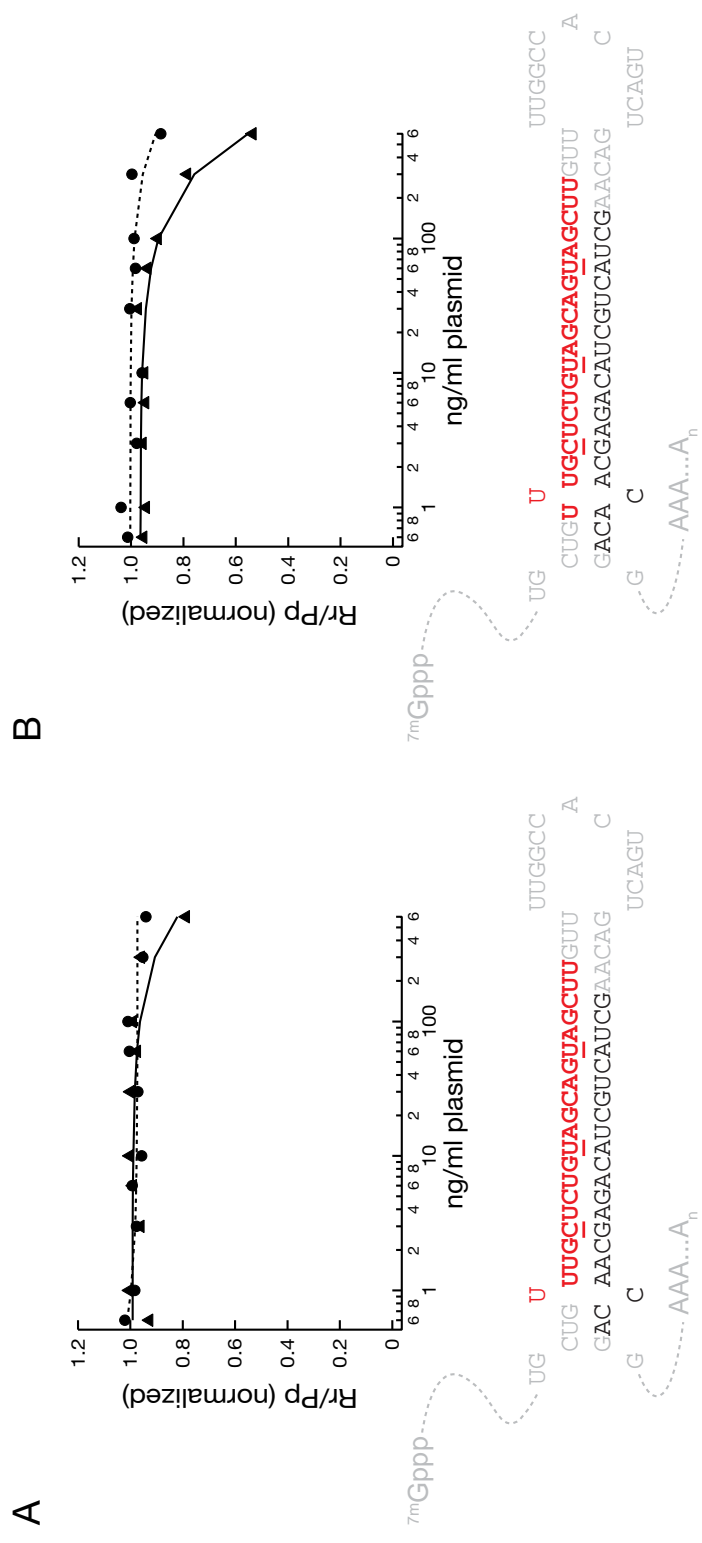


Table S3.1. shRNA and miRNA sequences

miRNA/shRNA	Sequence
mir2273A-3	CCUGGAGGCUUGCUGAAGGCUGUAUGCUGUUUGCUCUGUAGCAGUAGCUUUUGGCCACUGACUGACAAGC UACUUA CAGAGCAAA CAGGACACAAGGCCUGUUA CUAGCACUCAUGGAA CAAAUGGCC
mir2273A-5	CCUGGAGGCUUGCUGAAGGCUGUAUGCUGUUUGCUCUGUAGCAGUAGCUUUUGGCCACUGACUGACAAGC UACUGCUACAGAGCAACCAGGACACAAGGCCUGUUA CUAGCACUCAUGGAA CAAAUGGCC
mir2273A-6	CCUGGAGGCUUGCUGAAGGCUGUAUGCUGUUUGCUCUGUAGCAGUAGCUUUUGGCCACUGACUGACAAGC UACUGCUACAGAGCACACAGGACACAAGGCCUGUUA CUAGCACUCAUGGAA CAAAUGGCC
mir2273G-1	CCUGGAGGCUUGCUGAAGGCUGUAUGCUGUUUGCUCUGCAGCAGCAGCUUUUGGCCACUGACUGACAAGC UGCUTUGCAGAGCAAAACAGGACACAAGGCCUGUUA CUAGCACUCAUGGAA CAAAUGGCC
mir2273G-3	CCUGGAGGCUUGCUGAAGGCUGUAUGCUGUUUGCUCUGCAGCAGUAGCUUUUGGCCACUGACUGACAAGC UACUUGCAGAGCAAA CAGGACACAAGGCCUGUUA CUAGCACUCAUGGAA CAAAUGGCC
mir2307	CCUGGAGGCUUGCUGAAGGCUGUAUGCUGUA CAAUGGCACAGACUUC CAAUUUGGCCACUGACUGACUUGG AAGUGCCA UUGUACAGGACACAAGGCCUGUUA CUAGCACUCAUGGAA CAAAUGGCC
mirRluc	CCUGGAGGCUUGCUGAAGGCUGUAUGCUGUUUCUGCCCUUCUUCUGCUUUUGGCCACUGACUGACAAGA GCGAAGGGCGAGAAA CAGGACACAAGGCCUGUUA CUAGCACUCAUGGAA CAAAUGGCC
U6-m2307	AGUGAGCGCAGGAA GUCUGUGCCA UUGUAUCAGUAAA GCCACAGAUUGUAUCAAUUGGCACAGACUUCUUCG CCUACUUUUUUU
U6-mHtt-10	AGUGAGCGCAGU GCCGAGCUCAGCUCCUCUCA GUAAA GCCACAGAUUGUAUAGGAGCUCUGGCACUUCG CCUACUUUUUUU G
U6-mHtt-9	AGUGAGCGCAGU GCCGAGCUCAGCUCCUCUC CUGUAAA GCCACAGAUUGGUAUAGGAGCUCUGGCACUUCG CCUACUUUUUUU
U6-sh2307	GGAAGUCUGUGCCA UUGUAUCUGUAAA GCCACAGAUUGGUAUCAAUUGGCACAGACUUCUUUUUUU

Acknowledgements

This work was supported, in part, by grants from the NIH to NA, MD, and PDZ (NS038194) and from the CHDI (High Q Foundation) to NA and PDZ.

CHAPTER IV: SUMMARY AND CONCLUSIONS

Oligonucleotide Therapeutics for Huntington's disease

For patients and families, Huntington's disease is devastating. With the identification of the causative gene came the expectation that a cure would soon be found. Unfortunately, despite nearly 20 years of research into the pathogenic mechanisms of mutant *Huntingtin*, effective therapies to delay the progression of the disease remain elusive. In theory, curing Huntington's disease should be simple: turn off expression of the mutant, disease-causing *Huntingtin* gene. Several strategies have been proposed to achieve this goal. Leading strategies include oligonucleotide therapies (antisense oligonucleotides, RNAi) and small molecules or drugs designed to block translation or enhance clearance of the mutant protein. All of these strategies show promise but all come with challenges, foremost among them targeting and delivery. Although *Huntingtin* is widely expressed and pathology is not confined to the brain, neurons in the striatum and cortex are particularly vulnerable. Initial clinical trials will likely be focused on the striatum, but improvements to delivery and targeting and research into the functions of normal *Huntingtin* should drive efforts to develop more complete and safer therapies.

Progress and Challenges

Oligonucleotide therapies include virally delivered hairpins (shRNA or miRNA), siRNAs, and antisense oligonucleotides (ASOs). Antisense oligonucleotides are single stranded, chemically modified oligonucleotides. They can have various

effects on cellular mRNAs including inhibition of translation, modification of pre-mRNA splicing, and RNase H mediated degradation of complementary mRNAs. In nonhuman primates *Huntingtin* targeting ASOs are distributed broadly in the brain following delivery to the CSF ²⁷⁹ and in mice, *Huntingtin* targeting ASOs infused for two weeks into the ventricle accumulate and cause a reduction in *Huntingtin* mRNA which persists for 8 to 12 weeks ²⁷⁹.

siRNAs and virally delivered shRNAs and miRNAs are designed to harness the endogenous RNAi pathways, primarily by associating with Argonaute proteins and guiding cleavage of complementary mRNAs. siRNAs effectively reduce *Huntingtin* levels in cell culture, where they can often be delivered by transfection. In our studies, we can achieve 90-100% transfection of siRNA into HeLa cells. In the brain, siRNAs have been limited by the inability to achieve widespread distribution and efficient cellular entry. However, in Rhesus macaque, convection enhanced delivery of siRNA targeting *Huntingtin* produces silencing throughout much of the striatum ¹⁶⁷. Like ASO induced silencing, siRNA induced silencing is transient. Although the effect can be relatively long-lived, eventually the siRNAs are degraded and mRNA and protein levels recover. There is evidence from studies using ASOs that a transient reduction in *Huntingtin* produces a therapeutic effect that outlasts silencing ^{279,280} so it may not be necessary to maintain high ASO or siRNA levels at all times, but patients treated with siRNA or ASOs would still need to receive the drugs regularly and the invasive procedures to deliver these drugs locally may be cause for concern.

Implantable devices can facilitate sustained delivery, but the the presence of a foreign object in the brain long term can result in the formation of a glial scar which impedes drug distribution. In contrast, viral delivered hairpins can produce long-term silencing from a single dose although achieving broad distribution in a large brain may require delivery to multiple sites. Viral delivery has shown promise both in mice ^{2,4,6} and in non-human primates ²⁶³.

Targeting Strategies

Three targeting strategies have emerged for oligonucleotide therapies for Huntington's disease. Targeting of the CAG repeat region is the most direct approach and ASOs and peptide nucleic acids ²⁸¹ targeting the CAG repeat region can selectively reduce the levels of mutant Huntingtin in patient derived cell lines ²⁸²⁻²⁸⁵. While some of the ASOs may recruit RNase H ²⁸³, others do not support RNase H activity in vitro and may act by binding to multiple sites in the mutant mRNA and inhibiting translation ²⁸⁴. siRNAs perfectly matched to the CAG repeat region cannot discriminate between the mutant and normal *Huntingtin* mRNAs. However, introducing mismatches around the cleavage site improves discrimination ²³². Like ASOs, these mutant *Huntingtin* specific siRNAs are thought to act by inhibiting translation. Allele-specificity could be due to binding to multiple binding sites or to differential recognition of the folded structures of the mutant and wild-type *Huntingtin* mRNAs. While CAG targeted oligonucleotides can be allele-specific, off-target silencing of other CAG repeat

containing mRNAs remains a concern. Initial experiments have indicated that CAG repeat containing mRNAs are not targeted indiscriminately^{232,282}, but a complete and systematic evaluation of off-targeting silencing of CAG repeat containing mRNAs will be required before these oligonucleotides will be declared safe.

Targeting of heterozygous single nucleotide polymorphisms (SNPs), as described in this dissertation, presents an alternative to CAG targeting. Both ASOs and siRNAs have been shown to target human *Huntingtin* SNPs^{257,261,286}. ASOs can enter the nucleus and therefore can target SNPs that are present in pre-mRNA but absent in the mature mRNA. RNAi-based approaches at present can only target sequences in the mature mRNA. Consequently, ASOs have a potentially larger pool of targets than do RNAi based therapeutics. On the other hand, the toxicity and delivery profiles of the two different types of therapeutics will be different and may be suitable for different patient populations.

Ideally, an allele specific RNAi therapeutic would have high activity against the matched target and no activity against the mismatched one, but siRNAs targeting therapeutically attractive SNPs may not conform to this ideal. The SNP at position 9,633 (rs362307) is one such target. Nearly 50% of the patients we genotyped were heterozygous at that site. However, we consistently found that siRNA and miRNAs targeting this site are less effective at silencing the target than those aimed at alternative sites. In contrast, discrimination at sites targeted by potent siRNAs, such as the siRNA targeting the SNP at position 7,942

(rs362273), tends to be low. Additional mismatches can improve discrimination but at a cost, as the additional mismatches also cause loss of silencing of the matched target. While highly potent and specific SNP targeting siRNAs certainly exist¹²⁷, it seems likely that siRNAs targeting many therapeutically attractive SNPs will not fall into this category.. Partial silencing of both alleles of *Huntingtin* is beneficial in mouse models of HD^{6,110} and reduction of wild-type *Huntingtin* by 50% is tolerated in mice^{26,27}. The majority of HD patients do not develop symptoms for decades suggesting that disease progression requires an accumulation of mutant *Huntingtin* toxicity over time. A modest reduction of mutant *Huntingtin* may be sufficient to rescue vulnerable neurons.

Alternative gene therapy strategies combining knockdown of the disease causing mRNA and replacement with an RNAi resistant (“hardened”) copy are not appropriate for Huntington’s disease, as the resulting construct would be too large for packaging into current gene therapy vectors. Combination approaches such as partial silencing of mutant *Huntingtin* and simultaneous augmentation of another gene product, such as BDNF, to counteract downstream pathological processes of the disease may prove beneficial. Additional strategies combining multiple modes of delivery and targeting, for example viral delivery of anti-Huntingtin miRNAs to produce a mild reduction in Huntingtin plus occasional supplementary delivery of siRNAs or ASOs, are also likely to emerge and may ultimately provide the most benefit to patients.

Methods for designing SNP targeting siRNAs and miRNAs

We have shown that small RNA production from promoter driven hairpin constructs is sensitive to expression levels and hairpin design. shRNA or miRNA that are poorly designed but expressed at high levels may produce good silencing, but that can be accompanied by the accumulation of non-functional or suboptimal processing products. In our studies, the major off-target products are most likely the unintentional consequence of export of the pri-miRNA from the nucleus and subsequent processing by Dicer. Redesign of the U6 promoter driven miRNA by adding a longer single stranded region should prevent nuclear export of the pri-miRNA and eliminate these products. We also detected secondary products adjacent to the Dicer cleavage site which may be detectable because of high expression from the U6 promoter. Incorporation of miRNA-like elements within the hairpin might eliminate these secondary products. Alternatively, lowering expression levels by using weaker or tissue specific promoters can minimize the danger of off target effects due to overexpression

215

Single nucleotide discrimination of miRNAs seems to mirror discrimination of canonical 21 nucleotide siRNAs, with some minor discrepancies. miRNAs may exhibit slightly lower discrimination than the corresponding 21 nucleotide siRNA. In vivo, the products generated from the miRNAs are slightly longer than expected. It may be that additional matches between the 3'-end of the longer mature miRNA and the mismatched mRNA target stabilize the interaction and

promote silencing. Alternatively, the 3'-end of a longer miRNA could be shaped by tailing and trimming¹⁶⁶. We observed differences in the length distribution between SNP matched and SNP mismatched miRNAs. This could reflect differential trimming. If the miRNA can bind to both the SNP-matched and SNP-mismatched targets, but cleave only the matched target, we would expect that the mismatched miRNA might remain bound to the target and ultimately be degraded, while the matched miRNA would cleave and release its target. It is exciting to speculate that SNP discrimination could be enhanced by increased target directed destruction of the mismatched miRNA. If this occurs it would be a demonstration of target directed destruction of a miRNA by an endogenous mRNA and trimming and tailing could be used as a signature for allele-specific silencing.

Despite several attempts to systematically catalog single nucleotide discrimination at each siRNA position^{237,287}, designing discriminating siRNAs and miRNAs for disease associated SNPs remains largely a matter of trial and error. While certain positions and conformations are predicted to provide good discrimination^{237,287}, potent siRNAs are often unaffected by single nucleotide mismatches while less effective siRNAs can too easily be rendered non-functional. The most effective design strategy is one that combines systematic screening of all possible single nucleotide mismatches for potency and selectivity followed by fine-tuning of discrimination by addition of secondary mismatches and tertiary mismatches, when necessary. Eventually, if a large number of

heterozygosities are targeted in this fashion and more SNP discriminating siRNAs and miRNAs are developed, it should become possible to develop a more complete model to predict discrimination which could, in turn, be used to design better SNP discriminating sequences.

Off-target effects

RNAi therapeutics for HD could potentially affect endogenous miRNAs and mRNAs in the brain by mechanisms involving both on-target and off-target effects. In the case of miRNAs, competition for saturable components of the miRNA machinery could result in changes in endogenous miRNAs. However, it seems likely that the levels of artificial miRNA produced in our experiments, which are modest in comparison with many endogenous miRNAs, would not be sufficient to produce such a saturation effect. Changes in endogenous miRNAs might also occur via a disease specific mechanism, as there are indications that some endogenous miRNAs are disrupted in HD²²⁸⁻²³¹. We have seen that our *Huntingtin* targeting miRNAs do not have a global effect on endogenous miRNAs relative to non-targeting miRNAs, but it remains to be seen if they can shift the miRNA profile in HD mice back towards that of wild-type mice. If so, this would provide evidence that the miRNAs are effective in reducing disease pathology and an encouraging sign that endogenous miRNAs could be used as a biomarker in HD.

There is considerable concern surrounding seed-mediated off-target effects of RNAi therapeutics but the functional consequences of such off-target effects are largely unknown. The most reasonable approach to avoiding these effects is to minimize the number of 3'-UTR seed matches. While this is easier with nonallele-specific miRNAs and siRNAs¹⁹⁵, our data suggest that there is some flexibility in the design of SNP-specific siRNAs and miRNAs which could potentially be exploited to reduce potential off target effects. Unfortunately, off-target effects are particularly hard to predict from animal models¹⁸⁶ but algorithms which improve miRNA target prediction should also improve predictions of off-target effects.

The Future of Huntington's Disease Therapeutics

Restoring normal Huntingtin function

The first clinical trials of oligonucleotide therapeutics for Huntington's disease are likely to involve targeting of total *Huntingtin* by locally delivered ASOs and rAAVs carrying *Huntingtin* targeting miRNAs. However, because the long-term effects of reducing wild-type *Huntingtin* are unknown, restoring or maintaining its function is likely to remain the ultimate goal. Combination strategies involving simultaneous silencing of *Huntingtin* and replacement of other factors, (growth factors, transcription factors) will likely join allele specific silencing as a means to achieve this goal. Small molecules and oligonucleotides that aim to stabilize the CAG repeats and stall transcription could potentially achieve a specific reduction

of mutant *Huntingtin* and small molecules or drugs that enhance clearance of misfolded proteins could be used to augment the effects of *Huntingtin* silencing. Furthermore, while full length *Huntingtin* is too large for current gene therapy vectors, it is possible that studies designed to define the functional domains of the *Huntingtin* protein and how modifications to those domains influence toxicity^{288,289}, will result in the delineation of shorter functional domains or modifications, which can be engineered to replace some of the functionality of the full length wild-type protein.

Systemic Delivery

Huntingtin is widely expressed and mutant *Huntingtin* appears to have toxic effects outside the brain²⁹⁰. Innate immune activation can be detected peripherally years before the onset of clinical symptoms and increases with clinical progression²⁹¹. Treatments directed only at the striatum and cortex are not expected to ameliorate peripheral pathology therefore systemic delivery may be desirable. Systemic delivery presents an array of challenges distinct from those presented by local delivery. For neurological diseases, the most significant obstacle to systemic delivery is the blood brain barrier which provides a barrier between the blood and the brain. While some rAAV vectors can cross the blood brain barrier¹⁷⁸, their use for gene therapy is relatively recent. In order for systemically delivered vectors to reach the brain and deliver their cargo at therapeutically relevant doses, they may need to be given at high doses but

vector dose may be limited by immune responses or by toxicity in other organs. The utility of systemically delivered vectors can also be limited by the presence of neutralizing antibodies. Adding tissue specific miRNA binding sites to the expression construct can reduce expression in off-target tissues¹⁷⁹ and directed evolution can be used to generate viral capsids with therapeutically desirable properties including appropriate tropism and resistance to neutralizing antibodies^{292,293}, but these are still in the early stages of development and a significant amount of effort will be needed to demonstrate that they can be used for gene therapy. Naked or unconjugated ASOs and siRNAs do not cross the blood brain barrier, but several groups have successfully used a rabies virus glycoprotein peptide^{175,177} to target peripherally delivered siRNAs to the brain. With these advances, it seems likely that peripheral or systemic delivery will be one of the next steps in development of oligonucleotides therapies for Huntington's disease.

Gene Therapy: Developing an exit strategy

One of the main concerns for viral delivery is the lack of exit strategy. Virally delivered genes, shRNAs, and miRNAs, are generally constitutively active. While several regulated promoters are under development, they rely on the expression of additional proteins which could themselves cause toxicity. One alternative to drug regulated promoters may be a system which is responsive to pathological changes within the cell. In this scenario, a miRNA targeting *Huntingtin* could be delivered in a single procedure. The miRNA expression

construct, which would ideally contain elements that could respond to endogenous promoter and repressor elements, would turn on in response to high levels of mutant *Huntingtin* or by transcriptional changes caused by those high levels. This would result in clearance of mutant *Huntingtin*, in response to which, the miRNA would turn off. In theory, this self-regulating system would prevent potential toxicity caused by long-term *Huntingtin* silencing.

Combination Therapies

Huntington's disease patients are a diverse group. Despite the fact that the ultimate cause of the disease is the same in all patients, there is considerably variability in phenotype. Some patients experience primarily motor symptoms while others suffer more from the cognitive and emotional aspects of the disease. We have shown that the gene itself has quite a large amount of heterozygosity. Ultimately, it seems likely that no single therapy will be suitable for all patients. Local delivery may be sufficient for some, but not for others. Patients may experience different types of toxicity or they may benefit from different therapeutic combinations. As our understanding of treatment grows, we are sure to benefit from having an array of therapies from which to choose.

BIBLIOGRAPHY

1. A novel gene containing a trinucleotide repeat that is expanded and unstable on Huntington's disease chromosomes. The Huntington's Disease Collaborative Research Group. *Cell*. Mar 26 1993;72(6):971-983.
2. Machida Y, Okada T, Kurosawa M, Oyama F, Ozawa K, Nukina N. rAAV-mediated shRNA ameliorated neuropathology in Huntington disease model mouse. *Biochemical and biophysical research communications*. Apr 28 2006;343(1):190-197.
3. Wang YL, Liu W, Wada E, Murata M, Wada K, Kanazawa I. Clinico-pathological rescue of a model mouse of Huntington's disease by siRNA. *Neuroscience research*. Nov 2005;53(3):241-249.
4. Harper SQ, Staber PD, He X, et al. RNA interference improves motor and neuropathological abnormalities in a Huntington's disease mouse model. *Proceedings of the National Academy of Sciences of the United States of America*. Apr 19 2005;102(16):5820-5825.
5. DiFiglia M, Sena-Esteves M, Chase K, et al. Therapeutic silencing of mutant huntingtin with siRNA attenuates striatal and cortical neuropathology and behavioral deficits. *Proceedings of the National Academy of Sciences of the United States of America*. Oct 23 2007;104(43):17204-17209.
6. Boudreau RL, McBride JL, Martins I, et al. Nonallele-specific silencing of mutant and wild-type huntingtin demonstrates therapeutic efficacy in Huntington's disease mice. *Molecular therapy : the journal of the American Society of Gene Therapy*. Jun 2009;17(6):1053-1063.
7. Caplen NJ, Taylor JP, Statham VS, Tanaka F, Fire A, Morgan RA. Rescue of polyglutamine-mediated cytotoxicity by double-stranded RNA-mediated RNA interference. *Human molecular genetics*. Jan 15 2002;11(2):175-184.
8. Duyao M, Ambrose C, Myers R, et al. Trinucleotide repeat length instability and age of onset in Huntington's disease. *Nature genetics*. Aug 1993;4(4):387-392.
9. Stine OC, Pleasant N, Franz ML, Abbott MH, Folstein SE, Ross CA. Correlation between the onset age of Huntington's disease and length of the trinucleotide repeat in IT-15. *Human molecular genetics*. Oct 1993;2(10):1547-1549.
10. Li JL, Hayden MR, Almqvist EW, et al. A genome scan for modifiers of age at onset in Huntington disease: The HD MAPS study. *American journal of human genetics*. Sep 2003;73(3):682-687.
11. Rubinsztein DC, Leggo J, Chiano M, et al. Genotypes at the GluR6 kainate receptor locus are associated with variation in the age of onset of

- Huntington disease. *Proceedings of the National Academy of Sciences of the United States of America*. Apr 15 1997;94(8):3872-3876.
12. MacDonald ME, Vonsattel JP, Shrinidhi J, et al. Evidence for the GluR6 gene associated with younger onset age of Huntington's disease. *Neurology*. Oct 12 1999;53(6):1330-1332.
 13. Wexler NS, Young AB, Tanzi RE, et al. Homozygotes for Huntington's disease. *Nature*. Mar 12-18 1987;326(6109):194-197.
 14. Durr A, Hahn-Barma V, Brice A, Pecheux C, Dode C, Feingold J. Homozygosity in Huntington's disease. *Journal of medical genetics*. Feb 1999;36(2):172-173.
 15. Squitieri F, Gellera C, Cannella M, et al. Homozygosity for CAG mutation in Huntington disease is associated with a more severe clinical course. *Brain : a journal of neurology*. Apr 2003;126(Pt 4):946-955.
 16. Telenius H, Kremer HP, Theilmann J, et al. Molecular analysis of juvenile Huntington disease: the major influence on (CAG)_n repeat length is the sex of the affected parent. *Human molecular genetics*. Oct 1993;2(10):1535-1540.
 17. Trottier Y, Biancalana V, Mandel JL. Instability of CAG repeats in Huntington's disease: relation to parental transmission and age of onset. *Journal of medical genetics*. May 1994;31(5):377-382.
 18. Kennedy L, Evans E, Chen CM, et al. Dramatic tissue-specific mutation length increases are an early molecular event in Huntington disease pathogenesis. *Human molecular genetics*. Dec 15 2003;12(24):3359-3367.
 19. Shelbourne PF, Keller-McGandy C, Bi WL, et al. Triplet repeat mutation length gains correlate with cell-type specific vulnerability in Huntington disease brain. *Human molecular genetics*. May 15 2007;16(10):1133-1142.
 20. Andrade MA, Bork P. HEAT repeats in the Huntington's disease protein. *Nature genetics*. Oct 1995;11(2):115-116.
 21. Li W, Serpell LC, Carter WJ, Rubinsztein DC, Huntington JA. Expression and characterization of full-length human huntingtin, an elongated HEAT repeat protein. *The Journal of biological chemistry*. Jun 9 2006;281(23):15916-15922.
 22. Takano H, Gusella JF. The predominantly HEAT-like motif structure of huntingtin and its association and coincident nuclear entry with dorsal, an NF-κB/Rel/dorsal family transcription factor. *BMC neuroscience*. Oct 14 2002;3:15.
 23. Goehler H, Lalowski M, Stelzl U, et al. A protein interaction network links GIT1, an enhancer of huntingtin aggregation, to Huntington's disease. *Mol Cell*. Sep 24 2004;15(6):853-865.
 24. Strong TV, Tagle DA, Valdes JM, et al. Widespread expression of the human and rat Huntington's disease gene in brain and nonneural tissues. *Nature genetics*. Nov 1993;5(3):259-265.

25. Sharp AH, Loev SJ, Schilling G, et al. Widespread expression of Huntington's disease gene (IT15) protein product. *Neuron*. May 1995;14(5):1065-1074.
26. Duyao MP, Auerbach AB, Ryan A, et al. Inactivation of the mouse Huntington's disease gene homolog Hdh. *Science*. Jul 21 1995;269(5222):407-410.
27. Zeitlin S, Liu JP, Chapman DL, Papaioannou VE, Efstratiadis A. Increased apoptosis and early embryonic lethality in mice nullizygous for the Huntington's disease gene homologue. *Nature genetics*. Oct 1995;11(2):155-163.
28. Nasir J, Floresco SB, O'Kusky JR, et al. Targeted disruption of the Huntington's disease gene results in embryonic lethality and behavioral and morphological changes in heterozygotes. *Cell*. Jun 2 1995;81(5):811-823.
29. Dragatsis I, Levine MS, Zeitlin S. Inactivation of Hdh in the brain and testis results in progressive neurodegeneration and sterility in mice. *Nature genetics*. Nov 2000;26(3):300-306.
30. Gutekunst CA, Levey AI, Heilman CJ, et al. Identification and localization of huntingtin in brain and human lymphoblastoid cell lines with anti-fusion protein antibodies. *Proceedings of the National Academy of Sciences of the United States of America*. Sep 12 1995;92(19):8710-8714.
31. Hoffner G, Kahlem P, Djian P. Perinuclear localization of huntingtin as a consequence of its binding to microtubules through an interaction with beta-tubulin: relevance to Huntington's disease. *Journal of cell science*. Mar 1 2002;115(Pt 5):941-948.
32. DiFiglia M, Sapp E, Chase K, et al. Huntingtin is a cytoplasmic protein associated with vesicles in human and rat brain neurons. *Neuron*. May 1995;14(5):1075-1081.
33. Velier J, Kim M, Schwarz C, et al. Wild-type and mutant huntingtins function in vesicle trafficking in the secretory and endocytic pathways. *Experimental neurology*. Jul 1998;152(1):34-40.
34. Li X, Sapp E, Valencia A, et al. A function of huntingtin in guanine nucleotide exchange on Rab11. *Neuroreport*. Oct 29 2008;19(16):1643-1647.
35. Li X, Standley C, Sapp E, et al. Mutant huntingtin impairs vesicle formation from recycling endosomes by interfering with Rab11 activity. *Molecular and cellular biology*. Nov 2009;29(22):6106-6116.
36. Li X, Valencia A, Sapp E, et al. Aberrant Rab11-dependent trafficking of the neuronal glutamate transporter EAAC1 causes oxidative stress and cell death in Huntington's disease. *The Journal of neuroscience : the official journal of the Society for Neuroscience*. Mar 31 2010;30(13):4552-4561.

37. Gunawardena S, Her LS, Bruschi RG, et al. Disruption of axonal transport by loss of huntingtin or expression of pathogenic polyQ proteins in *Drosophila*. *Neuron*. Sep 25 2003;40(1):25-40.
38. Trushina E, Dyer RB, Badger JD, 2nd, et al. Mutant huntingtin impairs axonal trafficking in mammalian neurons in vivo and in vitro. *Molecular and cellular biology*. Sep 2004;24(18):8195-8209.
39. Baquet ZC, Gorski JA, Jones KR. Early striatal dendrite deficits followed by neuron loss with advanced age in the absence of anterograde cortical brain-derived neurotrophic factor. *The Journal of neuroscience : the official journal of the Society for Neuroscience*. Apr 28 2004;24(17):4250-4258.
40. Zuccato C, Ciammola A, Rigamonti D, et al. Loss of huntingtin-mediated BDNF gene transcription in Huntington's disease. *Science*. Jul 20 2001;293(5529):493-498.
41. Zuccato C, Tartari M, Crotti A, et al. Huntingtin interacts with REST/NRSF to modulate the transcription of NRSE-controlled neuronal genes. *Nature genetics*. Sep 2003;35(1):76-83.
42. Gauthier LR, Charrin BC, Borrell-Pages M, et al. Huntingtin controls neurotrophic support and survival of neurons by enhancing BDNF vesicular transport along microtubules. *Cell*. Jul 9 2004;118(1):127-138.
43. Schoenherr CJ, Anderson DJ. The neuron-restrictive silencer factor (NRSF): a coordinate repressor of multiple neuron-specific genes. *Science*. Mar 3 1995;267(5202):1360-1363.
44. Chong JA, Tapia-Ramirez J, Kim S, et al. REST: a mammalian silencer protein that restricts sodium channel gene expression to neurons. *Cell*. Mar 24 1995;80(6):949-957.
45. Rigamonti D, Bauer JH, De-Fraja C, et al. Wild-type huntingtin protects from apoptosis upstream of caspase-3. *The Journal of neuroscience : the official journal of the Society for Neuroscience*. May 15 2000;20(10):3705-3713.
46. Rigamonti D, Sipione S, Goffredo D, Zuccato C, Fossale E, Cattaneo E. Huntingtin's neuroprotective activity occurs via inhibition of procaspase-9 processing. *The Journal of biological chemistry*. May 4 2001;276(18):14545-14548.
47. Leavitt BR, van Raamsdonk JM, Shehadeh J, et al. Wild-type huntingtin protects neurons from excitotoxicity. *Journal of neurochemistry*. Feb 2006;96(4):1121-1129.
48. Zhang Y, Leavitt BR, van Raamsdonk JM, et al. Huntingtin inhibits caspase-3 activation. *The EMBO journal*. Dec 13 2006;25(24):5896-5906.
49. Van Raamsdonk JM, Pearson J, Rogers DA, et al. Loss of wild-type huntingtin influences motor dysfunction and survival in the YAC128 mouse model of Huntington disease. *Human molecular genetics*. May 15 2005;14(10):1379-1392.

50. DiFiglia M, Sapp E, Chase KO, et al. Aggregation of huntingtin in neuronal intranuclear inclusions and dystrophic neurites in brain. *Science*. Sep 26 1997;277(5334):1990-1993.
51. Trottier Y, Devys D, Imbert G, et al. Cellular localization of the Huntington's disease protein and discrimination of the normal and mutated form. *Nature genetics*. May 1995;10(1):104-110.
52. Scherzinger E, Lurz R, Turmaine M, et al. Huntingtin-encoded polyglutamine expansions form amyloid-like protein aggregates in vitro and in vivo. *Cell*. Aug 8 1997;90(3):549-558.
53. Kim YJ, Yi Y, Sapp E, et al. Caspase 3-cleaved N-terminal fragments of wild-type and mutant huntingtin are present in normal and Huntington's disease brains, associate with membranes, and undergo calpain-dependent proteolysis. *Proceedings of the National Academy of Sciences of the United States of America*. Oct 23 2001;98(22):12784-12789.
54. Lunke A, Lindenberg KS, Ben-Haiem L, et al. Proteases acting on mutant huntingtin generate cleaved products that differentially build up cytoplasmic and nuclear inclusions. *Mol Cell*. Aug 2002;10(2):259-269.
55. Gafni J, Ellerby LM. Calpain activation in Huntington's disease. *The Journal of neuroscience : the official journal of the Society for Neuroscience*. Jun 15 2002;22(12):4842-4849.
56. Wellington CL, Ellerby LM, Gutekunst CA, et al. Caspase cleavage of mutant huntingtin precedes neurodegeneration in Huntington's disease. *The Journal of neuroscience : the official journal of the Society for Neuroscience*. Sep 15 2002;22(18):7862-7872.
57. Hermel E, Gafni J, Propp SS, et al. Specific caspase interactions and amplification are involved in selective neuronal vulnerability in Huntington's disease. *Cell death and differentiation*. Apr 2004;11(4):424-438.
58. Kim YJ, Sapp E, Cuiffo BG, et al. Lysosomal proteases are involved in generation of N-terminal huntingtin fragments. *Neurobiology of disease*. May 2006;22(2):346-356.
59. Graham RK, Deng Y, Slow EJ, et al. Cleavage at the caspase-6 site is required for neuronal dysfunction and degeneration due to mutant huntingtin. *Cell*. Jun 16 2006;125(6):1179-1191.
60. Graham RK, Deng Y, Carroll J, et al. Cleavage at the 586 amino acid caspase-6 site in mutant huntingtin influences caspase-6 activation in vivo. *The Journal of neuroscience : the official journal of the Society for Neuroscience*. Nov 10 2010;30(45):15019-15029.
61. Bence NF, Sampat RM, Kopito RR. Impairment of the ubiquitin-proteasome system by protein aggregation. *Science*. May 25 2001;292(5521):1552-1555.
62. Holmberg CI, Staniszewski KE, Mensah KN, Matouschek A, Morimoto RI. Inefficient degradation of truncated polyglutamine proteins by the proteasome. *The EMBO journal*. Oct 27 2004;23(21):4307-4318.

63. Venkatraman P, Wetzel R, Tanaka M, Nukina N, Goldberg AL. Eukaryotic proteasomes cannot digest polyglutamine sequences and release them during degradation of polyglutamine-containing proteins. *Mol Cell*. Apr 9 2004;14(1):95-104.
64. Kaltenbach LS, Romero E, Becklin RR, et al. Huntingtin interacting proteins are genetic modifiers of neurodegeneration. *PLoS genetics*. May 11 2007;3(5):e82.
65. Gunawardena S, Goldstein LS. Polyglutamine diseases and transport problems: deadly traffic jams on neuronal highways. *Archives of neurology*. Jan 2005;62(1):46-51.
66. Lee WC, Yoshihara M, Littleton JT. Cytoplasmic aggregates trap polyglutamine-containing proteins and block axonal transport in a Drosophila model of Huntington's disease. *Proceedings of the National Academy of Sciences of the United States of America*. Mar 2 2004;101(9):3224-3229.
67. Beal MF, Brouillet E, Jenkins B, Henshaw R, Rosen B, Hyman BT. Age-dependent striatal excitotoxic lesions produced by the endogenous mitochondrial inhibitor malonate. *Journal of neurochemistry*. Sep 1993;61(3):1147-1150.
68. Saft C, Zange J, Andrich J, et al. Mitochondrial impairment in patients and asymptomatic mutation carriers of Huntington's disease. *Movement disorders : official journal of the Movement Disorder Society*. Jun 2005;20(6):674-679.
69. Polidori MC, Mecocci P, Browne SE, Senin U, Beal MF. Oxidative damage to mitochondrial DNA in Huntington's disease parietal cortex. *Neuroscience letters*. Sep 3 1999;272(1):53-56.
70. Bogdanov MB, Andreassen OA, Dedeoglu A, Ferrante RJ, Beal MF. Increased oxidative damage to DNA in a transgenic mouse model of Huntington's disease. *Journal of neurochemistry*. Dec 2001;79(6):1246-1249.
71. Browne SE, Bowling AC, MacGarvey U, et al. Oxidative damage and metabolic dysfunction in Huntington's disease: selective vulnerability of the basal ganglia. *Annals of neurology*. May 1997;41(5):646-653.
72. Choo YS, Johnson GV, MacDonald M, Detloff PJ, Lesort M. Mutant huntingtin directly increases susceptibility of mitochondria to the calcium-induced permeability transition and cytochrome c release. *Human molecular genetics*. Jul 15 2004;13(14):1407-1420.
73. Panov AV, Gutekunst CA, Leavitt BR, et al. Early mitochondrial calcium defects in Huntington's disease are a direct effect of polyglutamines. *Nature neuroscience*. Aug 2002;5(8):731-736.
74. Moller T. Neuroinflammation in Huntington's disease. *Journal of neural transmission*. Aug 2010;117(8):1001-1008.

75. Thomas EA. Striatal specificity of gene expression dysregulation in Huntington's disease. *Journal of neuroscience research*. Nov 1 2006;84(6):1151-1164.
76. Hanisch UK, Kettenmann H. Microglia: active sensor and versatile effector cells in the normal and pathologic brain. *Nature neuroscience*. Nov 2007;10(11):1387-1394.
77. Sapp E, Kegel KB, Aronin N, et al. Early and progressive accumulation of reactive microglia in the Huntington disease brain. *Journal of neuropathology and experimental neurology*. Feb 2001;60(2):161-172.
78. Simmons DA, Casale M, Alcon B, Pham N, Narayan N, Lynch G. Ferritin accumulation in dystrophic microglia is an early event in the development of Huntington's disease. *Glia*. Aug 1 2007;55(10):1074-1084.
79. Gerber HP, Seipel K, Georgiev O, et al. Transcriptional activation modulated by homopolymeric glutamine and proline stretches. *Science*. Feb 11 1994;263(5148):808-811.
80. Kazantsev A, Preisinger E, Dranovsky A, Goldgaber D, Housman D. Insoluble detergent-resistant aggregates form between pathological and nonpathological lengths of polyglutamine in mammalian cells. *Proceedings of the National Academy of Sciences of the United States of America*. Sep 28 1999;96(20):11404-11409.
81. Steffan JS, Kazantsev A, Spasic-Boskovic O, et al. The Huntington's disease protein interacts with p53 and CREB-binding protein and represses transcription. *Proceedings of the National Academy of Sciences of the United States of America*. Jun 6 2000;97(12):6763-6768.
82. Nucifora FC, Jr., Sasaki M, Peters MF, et al. Interference by huntingtin and atrophin-1 with cbp-mediated transcription leading to cellular toxicity. *Science*. Mar 23 2001;291(5512):2423-2428.
83. Dunah AW, Jeong H, Griffin A, et al. Sp1 and TAFII130 transcriptional activity disrupted in early Huntington's disease. *Science*. Jun 21 2002;296(5576):2238-2243.
84. Chen-Plotkin AS, Sadri-Vakili G, Yohrling GJ, et al. Decreased association of the transcription factor Sp1 with genes downregulated in Huntington's disease. *Neurobiology of disease*. May 2006;22(2):233-241.
85. Zuccato C, Belyaev N, Conforti P, et al. Widespread disruption of repressor element-1 silencing transcription factor/neuron-restrictive silencer factor occupancy at its target genes in Huntington's disease. *The Journal of neuroscience : the official journal of the Society for Neuroscience*. Jun 27 2007;27(26):6972-6983.
86. Qiu Z, Norflus F, Singh B, et al. Sp1 is up-regulated in cellular and transgenic models of Huntington disease, and its reduction is neuroprotective. *The Journal of biological chemistry*. Jun 16 2006;281(24):16672-16680.

87. Ravache M, Weber C, Merienne K, Trottier Y. Transcriptional activation of REST by Sp1 in Huntington's disease models. *PLoS one*. 2010;5(12):e14311.
88. Wang R, Luo Y, Ly PT, et al. Sp1 regulates human huntingtin gene expression. *Journal of molecular neuroscience : MN*. Jun 2012;47(2):311-321.
89. Cui L, Jeong H, Borovecki F, Parkhurst CN, Tanese N, Krainc D. Transcriptional repression of PGC-1alpha by mutant huntingtin leads to mitochondrial dysfunction and neurodegeneration. *Cell*. Oct 6 2006;127(1):59-69.
90. Li LB, Yu Z, Teng X, Bonini NM. RNA toxicity is a component of ataxin-3 degeneration in Drosophila. *Nature*. Jun 19 2008;453(7198):1107-1111.
91. Yu Z, Teng X, Bonini NM. Triplet repeat-derived siRNAs enhance RNA-mediated toxicity in a Drosophila model for myotonic dystrophy. *PLoS genetics*. Mar 2011;7(3):e1001340.
92. Banez-Coronel M, Porta S, Kagerbauer B, et al. A pathogenic mechanism in Huntington's disease involves small CAG-repeated RNAs with neurotoxic activity. *PLoS genetics*. Feb 2012;8(2):e1002481.
93. de Mezer M, Wojciechowska M, Napierala M, Sobczak K, Krzyzosiak WJ. Mutant CAG repeats of Huntingtin transcript fold into hairpins, form nuclear foci and are targets for RNA interference. *Nucleic Acids Res*. May 2011;39(9):3852-3863.
94. Steffan JS, Bodai L, Pallos J, et al. Histone deacetylase inhibitors arrest polyglutamine-dependent neurodegeneration in Drosophila. *Nature*. Oct 18 2001;413(6857):739-743.
95. Ferrante RJ, Kubitius JK, Lee J, et al. Histone deacetylase inhibition by sodium butyrate chemotherapy ameliorates the neurodegenerative phenotype in Huntington's disease mice. *The Journal of neuroscience : the official journal of the Society for Neuroscience*. Oct 15 2003;23(28):9418-9427.
96. Jia H, Pallos J, Jacques V, et al. Histone deacetylase (HDAC) inhibitors targeting HDAC3 and HDAC1 ameliorate polyglutamine-elicited phenotypes in model systems of Huntington's disease. *Neurobiology of disease*. May 2012;46(2):351-361.
97. Chen M, Ona VO, Li M, et al. Minocycline inhibits caspase-1 and caspase-3 expression and delays mortality in a transgenic mouse model of Huntington disease. *Nature medicine*. Jul 2000;6(7):797-801.
98. Smith DL, Woodman B, Mahal A, et al. Minocycline and doxycycline are not beneficial in a model of Huntington's disease. *Annals of neurology*. Aug 2003;54(2):186-196.
99. Leyva MJ, Degiacomo F, Kaltenbach LS, et al. Identification and evaluation of small molecule pan-caspase inhibitors in Huntington's disease models. *Chem Biol*. Nov 24 2010;17(11):1189-1200.

100. Tabrizi SJ, Blamire AM, Manners DN, et al. Creatine therapy for Huntington's disease: clinical and MRS findings in a 1-year pilot study. *Neurology*. Jul 8 2003;61(1):141-142.
101. Tabrizi SJ, Blamire AM, Manners DN, et al. High-dose creatine therapy for Huntington disease: a 2-year clinical and MRS study. *Neurology*. May 10 2005;64(9):1655-1656.
102. Sittler A, Lurz R, Lueder G, et al. Geldanamycin activates a heat shock response and inhibits huntingtin aggregation in a cell culture model of Huntington's disease. *Human molecular genetics*. Jun 1 2001;10(12):1307-1315.
103. Herbst M, Wanker EE. Small molecule inducers of heat-shock response reduce polyQ-mediated huntingtin aggregation. A possible therapeutic strategy. *Neuro-degenerative diseases*. 2007;4(2-3):254-260.
104. Dedeoglu A, Kubilus JK, Jeitner TM, et al. Therapeutic effects of cystamine in a murine model of Huntington's disease. *The Journal of neuroscience : the official journal of the Society for Neuroscience*. Oct 15 2002;22(20):8942-8950.
105. Ravikumar B, Vacher C, Berger Z, et al. Inhibition of mTOR induces autophagy and reduces toxicity of polyglutamine expansions in fly and mouse models of Huntington disease. *Nature genetics*. Jun 2004;36(6):585-595.
106. Bonelli RM, Hodl AK, Hofmann P, Kapfhammer HP. Neuroprotection in Huntington's disease: a 2-year study on minocycline. *International clinical psychopharmacology*. Nov 2004;19(6):337-342.
107. Huntington Study Group DI. A futility study of minocycline in Huntington's disease. *Movement disorders : official journal of the Movement Disorder Society*. Oct 15 2010;25(13):2219-2224.
108. Yamamoto A, Lucas JJ, Hen R. Reversal of neuropathology and motor dysfunction in a conditional model of Huntington's disease. *Cell*. Mar 31 2000;101(1):57-66.
109. Regulier E, Trottier Y, Perrin V, Aebischer P, Deglon N. Early and reversible neuropathology induced by tetracycline-regulated lentiviral overexpression of mutant huntingtin in rat striatum. *Human molecular genetics*. Nov 1 2003;12(21):2827-2836.
110. Drouet V, Perrin V, Hassig R, et al. Sustained effects of nonallele-specific Huntingtin silencing. *Annals of neurology*. Mar 2009;65(3):276-285.
111. Napoli C, Lemieux C, Jorgensen R. Introduction of a Chimeric Chalcone Synthase Gene into Petunia Results in Reversible Co-Suppression of Homologous Genes in trans. *The Plant cell*. Apr 1990;2(4):279-289.
112. van der Krol AR, Mur LA, Beld M, Mol JN, Stuitje AR. Flavonoid genes in petunia: addition of a limited number of gene copies may lead to a suppression of gene expression. *The Plant cell*. Apr 1990;2(4):291-299.
113. Lindbo JA, Dougherty WG. Untranslatable transcripts of the tobacco etch virus coat protein gene sequence can interfere with tobacco etch virus

- replication in transgenic plants and protoplasts. *Virology*. Aug 1992;189(2):725-733.
114. Lindbo JA, Silva-Rosales L, Proebsting WM, Dougherty WG. Induction of a Highly Specific Antiviral State in Transgenic Plants: Implications for Regulation of Gene Expression and Virus Resistance. *The Plant cell*. Dec 1993;5(12):1749-1759.
 115. Voinnet O, Baulcombe DC. Systemic signalling in gene silencing. *Nature*. Oct 9 1997;389(6651):553.
 116. Romano N, Macino G. Quelling: transient inactivation of gene expression in *Neurospora crassa* by transformation with homologous sequences. *Molecular microbiology*. Nov 1992;6(22):3343-3353.
 117. Guo S, Kemphues KJ. par-1, a gene required for establishing polarity in *C. elegans* embryos, encodes a putative Ser/Thr kinase that is asymmetrically distributed. *Cell*. May 19 1995;81(4):611-620.
 118. Fire A, Xu S, Montgomery MK, Kostas SA, Driver SE, Mello CC. Potent and specific genetic interference by double-stranded RNA in *Caenorhabditis elegans*. *Nature*. Feb 19 1998;391(6669):806-811.
 119. Kennerdell JR, Carthew RW. Use of dsRNA-mediated genetic interference to demonstrate that frizzled and frizzled 2 act in the wingless pathway. *Cell*. Dec 23 1998;95(7):1017-1026.
 120. Wianny F, Zernicka-Goetz M. Specific interference with gene function by double-stranded RNA in early mouse development. *Nature cell biology*. Feb 2000;2(2):70-75.
 121. Svoboda P, Stein P, Hayashi H, Schultz RM. Selective reduction of dormant maternal mRNAs in mouse oocytes by RNA interference. *Development*. Oct 2000;127(19):4147-4156.
 122. Elbashir SM, Harborth J, Lendeckel W, Yalcin A, Weber K, Tuschl T. Duplexes of 21-nucleotide RNAs mediate RNA interference in cultured mammalian cells. *Nature*. 2001;411(6836):494-498.
 123. Song JJ, Smith SK, Hannon GJ, Joshua-Tor L. Crystal structure of Argonaute and its implications for RISC slicer activity. *Science*. Sep 3 2004;305(5689):1434-1437.
 124. Yuan YR, Pei Y, Ma JB, et al. Crystal structure of *A. aeolicus* argonaute, a site-specific DNA-guided endoribonuclease, provides insights into RISC-mediated mRNA cleavage. *Mol Cell*. Aug 5 2005;19(3):405-419.
 125. Wang Y, Sheng G, Juranek S, Tuschl T, Patel DJ. Structure of the guide-strand-containing argonaute silencing complex. *Nature*. Nov 13 2008;456(7219):209-213.
 126. Tomari Y, Matranga C, Haley B, Martinez N, Zamore PD. A protein sensor for siRNA asymmetry. *Science*. Nov 19 2004;306(5700):1377-1380.
 127. Schwarz DS, Tomari Y, Zamore PD. The RNA-induced silencing complex is a Mg²⁺-dependent endonuclease. *Curr Biol*. May 4 2004;14(9):787-791.

128. Liu J, Carmell MA, Rivas FV, et al. Argonaute2 Is the Catalytic Engine of Mammalian RNAi. *Science*. September 3, 2004 2004;305(5689):1437-1441.
129. Rivas FV, Tolia NH, Song JJ, et al. Purified Argonaute2 and an siRNA form recombinant human RISC. *Nat Struct Mol Biol*. Apr 2005;12(4):340-349.
130. Kwak PB, Tomari Y. The N domain of Argonaute drives duplex unwinding during RISC assembly. *Nat Struct Mol Biol*. Feb 2012;19(2):145-151.
131. Lee NS, Dohjima T, Bauer G, et al. Expression of small interfering RNAs targeted against HIV-1 rev transcripts in human cells. *Nature biotechnology*. May 2002;20(5):500-505.
132. Zeng Y, Cullen BR. Sequence requirements for micro RNA processing and function in human cells. *RNA*. Jan 2003;9(1):112-123.
133. Yi R, Qin Y, Macara IG, Cullen BR. Exportin-5 mediates the nuclear export of pre-microRNAs and short hairpin RNAs. *Genes & development*. Dec 15 2003;17(24):3011-3016.
134. Kim DH, Longo M, Han Y, Lundberg P, Cantin E, Rossi JJ. Interferon induction by siRNAs and ssRNAs synthesized by phage polymerase. *Nature biotechnology*. Mar 2004;22(3):321-325.
135. Hutvagner G, McLachlan J, Pasquinelli AE, Balint E, Tuschl T, Zamore PD. A cellular function for the RNA-interference enzyme Dicer in the maturation of the let-7 small temporal RNA. *Science*. Aug 3 2001;293(5531):834-838.
136. Bernstein E, Caudy AA, Hammond SM, Hannon GJ. Role for a bidentate ribonuclease in the initiation step of RNA interference. *Nature*. Jan 18 2001;409(6818):363-366.
137. Chendrimada TP, Gregory RI, Kumaraswamy E, et al. TRBP recruits the Dicer complex to Ago2 for microRNA processing and gene silencing. *Nature*. Aug 4 2005;436(7051):740-744.
138. Khvorova A, Reynolds A, Jayasena SD. Functional siRNAs and miRNAs exhibit strand bias. *Cell*. Oct 17 2003;115(2):209-216.
139. Schwarz DS, Hutvagner G, Du T, Xu Z, Aronin N, Zamore PD. Asymmetry in the assembly of the RNAi enzyme complex. *Cell*. Oct 17 2003;115(2):199-208.
140. Strand AD, Aragaki AK, Shaw D, et al. Gene expression in Huntington's disease skeletal muscle: a potential biomarker. *Human molecular genetics*. Jul 1 2005;14(13):1863-1876.
141. Matranga C, Tomari Y, Shin C, Bartel DP, Zamore PD. Passenger-strand cleavage facilitates assembly of siRNA into Ago2-containing RNAi enzyme complexes. *Cell*. Nov 18 2005;123(4):607-620.
142. Miyoshi K, Tsukumo H, Nagami T, Siomi H, Siomi MC. Slicer function of Drosophila Argonautes and its involvement in RISC formation. *Genes & development*. Dec 1 2005;19(23):2837-2848.

143. Leuschner PJ, Ameres SL, Kueng S, Martinez J. Cleavage of the siRNA passenger strand during RISC assembly in human cells. *EMBO reports*. Mar 2006;7(3):314-320.
144. Baek D, Villen J, Shin C, Camargo FD, Gygi SP, Bartel DP. The impact of microRNAs on protein output. *Nature*. Sep 4 2008;455(7209):64-71.
145. Yoda M, Kawamata T, Paroo Z, et al. ATP-dependent human RISC assembly pathways. *Nat Struct Mol Biol*. Jan 2010;17(1):17-23.
146. Kawamata T, Seitz H, Tomari Y. Structural determinants of miRNAs for RISC loading and slicer-independent unwinding. *Nat Struct Mol Biol*. Sep 2009;16(9):953-960.
147. Cullen BR. Transcription and processing of human microRNA precursors. *Mol Cell*. Dec 22 2004;16(6):861-865.
148. Tomari Y, Du T, Zamore PD. Sorting of Drosophila small silencing RNAs. *Cell*. Jul 27 2007;130(2):299-308.
149. Forstemann K, Horwich MD, Wee L, Tomari Y, Zamore PD. Drosophila microRNAs are sorted into functionally distinct argonaute complexes after production by dicer-1. *Cell*. Jul 27 2007;130(2):287-297.
150. Meister G, Landthaler M, Patkaniowska A, Dorsett Y, Teng G, Tuschl T. Human Argonaute2 Mediates RNA Cleavage Targeted by miRNAs and siRNAs. *Molecular Cell*. 2004;15(2):185-197.
151. Azuma-Mukai A, Oguri H, Mituyama T, et al. Characterization of endogenous human Argonautes and their miRNA partners in RNA silencing. *Proceedings of the National Academy of Sciences of the United States of America*. Jun 10 2008;105(23):7964-7969.
152. Burroughs AM, Ando Y, de Hoon MJ, et al. Deep-sequencing of human Argonaute-associated small RNAs provides insight into miRNA sorting and reveals Argonaute association with RNA fragments of diverse origin. *RNA biology*. Jan-Feb 2011;8(1):158-177.
153. Hutvagner G, Zamore PD. A microRNA in a Multiple-Turnover RNAi Enzyme Complex. *Science*. September 20, 2002 2002;297(5589):2056-2060.
154. Schwarz DS, Hutvagner G, Haley B, Zamore PD. Evidence that siRNAs Function as Guides, Not Primers, in the Drosophila and Human RNAi Pathways. *Molecular Cell*. 2002;10(3):537-548.
155. Haley B, Zamore PD. Kinetic analysis of the RNAi enzyme complex. 2004;11(7):599-606.
156. Elbashir SM, Martinez J, Patkaniowska A, Lendeckel W, Tuschl T. Functional anatomy of siRNAs for mediating efficient RNAi in Drosophila melanogaster embryo lysate. *The EMBO journal*. Dec 3 2001;20(23):6877-6888.
157. Holen T, Amarzguioui M, Wiiger MT, Babaie E, Prydz H. Positional effects of short interfering RNAs targeting the human coagulation trigger Tissue Factor. *Nucleic Acids Res*. Apr 2002;30(8):1757-1766.

158. Du Q, Thonberg H, Wang J, Wahlestedt C, Liang Z. A systematic analysis of the silencing effects of an active siRNA at all single-nucleotide mismatched target sites. *Nucleic Acids Res.* 2005;33(5):1671-1677.
159. Doench JG, Sharp PA. Specificity of microRNA target selection in translational repression. *Genes & development.* Mar 1 2004;18(5):504-511.
160. Doench JG, Petersen CP, Sharp PA. siRNAs can function as miRNAs. *Genes & development.* Feb 15 2003;17(4):438-442.
161. Guo H, Ingolia NT, Weissman JS, Bartel DP. Mammalian microRNAs predominantly act to decrease target mRNA levels. *Nature.* Aug 12 2010;466(7308):835-840.
162. Lewis BP, Shih IH, Jones-Rhoades MW, Bartel DP, Burge CB. Prediction of mammalian microRNA targets. *Cell.* Dec 2003;115(7):787-798.
163. Lewis A, Redrup L. Genetic imprinting: conflict at the Callipyge locus. *Curr Biol.* Apr 2005;15(8):R291-294.
164. Bartel DP, Chen CZ. Micromanagers of gene expression: the potentially widespread influence of metazoan microRNAs. *Nature reviews. Genetics.* May 2004;5(5):396-400.
165. Broderick JA, Salomon WE, Ryder SP, Aronin N, Zamore PD. Argonaute protein identity and pairing geometry determine cooperativity in mammalian RNA silencing. *RNA.* October 1, 2011 2011;17(10):1858-1869.
166. Ameres SL, Horwich MD, Hung JH, et al. Target RNA-directed trimming and tailing of small silencing RNAs. *Science.* Jun 18 2010;328(5985):1534-1539.
167. Stiles DK, Zhang Z, Ge P, et al. Widespread suppression of huntingtin with convection-enhanced delivery of siRNA. *Experimental neurology.* Jan 2012;233(1):463-471.
168. Thakker DR, Natt F, Husken D, et al. Neurochemical and behavioral consequences of widespread gene knockdown in the adult mouse brain by using nonviral RNA interference. *Proceedings of the National Academy of Sciences of the United States of America.* Dec 7 2004;101(49):17270-17275.
169. Dorn G, Patel S, Wotherspoon G, et al. siRNA relieves chronic neuropathic pain. *Nucleic Acids Res.* 2004;32(5):e49.
170. McCormack AL, Mak SK, Henderson JM, Bumcrot D, Farrer MJ, Di Monte DA. Alpha-synuclein suppression by targeted small interfering RNA in the primate substantia nigra. *PLoS one.* 2010;5(8):e12122.
171. Soutschek J, Akinc A, Bramlage B, et al. Therapeutic silencing of an endogenous gene by systemic administration of modified siRNAs. *Nature.* Nov 11 2004;432(7014):173-178.
172. Gao S, Dagnaes-Hansen F, Nielsen EJ, et al. The effect of chemical modification and nanoparticle formulation on stability and biodistribution of

- siRNA in mice. *Molecular therapy : the journal of the American Society of Gene Therapy*. Jul 2009;17(7):1225-1233.
173. Hassani Z, Lemkine GF, Erbacher P, et al. Lipid-mediated siRNA delivery down-regulates exogenous gene expression in the mouse brain at picomolar levels. *The journal of gene medicine*. Feb 2005;7(2):198-207.
 174. Tan PH, Yang LC, Shih HC, Lan KC, Cheng JT. Gene knockdown with intrathecal siRNA of NMDA receptor NR2B subunit reduces formalin-induced nociception in the rat. *Gene therapy*. Jan 2005;12(1):59-66.
 175. Kumar P, Wu H, McBride JL, et al. Transvascular delivery of small interfering RNA to the central nervous system. *Nature*. Jul 5 2007;448(7149):39-43.
 176. Pulford B, Reim N, Bell A, et al. Liposome-siRNA-peptide complexes cross the blood-brain barrier and significantly decrease PrP on neuronal cells and PrP in infected cell cultures. *PloS one*. 2010;5(6):e11085.
 177. Alvarez-Erviti L, Seow Y, Yin H, Betts C, Lakhai S, Wood MJ. Delivery of siRNA to the mouse brain by systemic injection of targeted exosomes. *Nature biotechnology*. Apr 2011;29(4):341-345.
 178. Duque S, Joussemet B, Riviere C, et al. Intravenous administration of self-complementary AAV9 enables transgene delivery to adult motor neurons. *Molecular therapy : the journal of the American Society of Gene Therapy*. Jul 2009;17(7):1187-1196.
 179. Xie J, Xie Q, Zhang H, et al. MicroRNA-regulated, systemically delivered rAAV9: a step closer to CNS-restricted transgene expression. *Molecular therapy : the journal of the American Society of Gene Therapy*. Mar 2011;19(3):526-535.
 180. Jackson AL, Bartz SR, Schelter J, et al. Expression profiling reveals off-target gene regulation by RNAi. *Nature biotechnology*. Jun 2003;21(6):635-637.
 181. Scacheri PC, Rozenblatt-Rosen O, Caplen NJ, et al. Short interfering RNAs can induce unexpected and divergent changes in the levels of untargeted proteins in mammalian cells. *Proceedings of the National Academy of Sciences of the United States of America*. Feb 17 2004;101(7):1892-1897.
 182. Birmingham A, Anderson EM, Reynolds A, et al. 3' UTR seed matches, but not overall identity, are associated with RNAi off-targets. *Nature methods*. Mar 2006;3(3):199-204.
 183. Jackson AL, Burchard J, Schelter J, et al. Widespread siRNA "off-target" transcript silencing mediated by seed region sequence complementarity. *RNA*. Jul 2006;12(7):1179-1187.
 184. Selbach M, Schwanhauser B, Thierfelder N, Fang Z, Khanin R, Rajewsky N. Widespread changes in protein synthesis induced by microRNAs. *Nature*. Sep 4 2008;455(7209):58-63.
 185. Fedorov Y, Anderson EM, Birmingham A, et al. Off-target effects by siRNA can induce toxic phenotype. *RNA*. Jul 2006;12(7):1188-1196.

186. Burchard J, Jackson AL, Malkov V, et al. MicroRNA-like off-target transcript regulation by siRNAs is species specific. *RNA*. Feb 2009;15(2):308-315.
187. Jackson AL, Burchard J, Leake D, et al. Position-specific chemical modification of siRNAs reduces "off-target" transcript silencing. *RNA*. Jul 2006;12(7):1197-1205.
188. Vollmer J, Jepsen JS, Uhlmann E, et al. Modulation of CpG oligodeoxynucleotide-mediated immune stimulation by locked nucleic acid (LNA). *Oligonucleotides*. Spring 2004;14(1):23-31.
189. Ui-Tei K, Naito Y, Nishi K, Juni A, Saigo K. Thermodynamic stability and Watson-Crick base pairing in the seed duplex are major determinants of the efficiency of the siRNA-based off-target effect. *Nucleic Acids Res*. Dec 2008;36(22):7100-7109.
190. Ui-Tei K, Naito Y, Zenno S, et al. Functional dissection of siRNA sequence by systematic DNA substitution: modified siRNA with a DNA seed arm is a powerful tool for mammalian gene silencing with significantly reduced off-target effect. *Nucleic Acids Res*. Apr 2008;36(7):2136-2151.
191. Chen PY, Weinmann L, Gaidatzis D, et al. Strand-specific 5'-O-methylation of siRNA duplexes controls guide strand selection and targeting specificity. *RNA*. Feb 2008;14(2):263-274.
192. Bramsen JB, Laursen MB, Nielsen AF, et al. A large-scale chemical modification screen identifies design rules to generate siRNAs with high activity, high stability and low toxicity. *Nucleic Acids Res*. May 2009;37(9):2867-2881.
193. Dua P, Yoo JW, Kim S, Lee DK. Modified siRNA structure with a single nucleotide bulge overcomes conventional siRNA-mediated off-target silencing. *Molecular therapy : the journal of the American Society of Gene Therapy*. Sep 2011;19(9):1676-1687.
194. Anderson EM, Birmingham A, Baskerville S, et al. Experimental validation of the importance of seed complement frequency to siRNA specificity. *RNA*. May 2008;14(5):853-861.
195. Boudreau RL, Spengler RM, Davidson BL. Rational design of therapeutic siRNAs: minimizing off-targeting potential to improve the safety of RNAi therapy for Huntington's disease. *Molecular therapy : the journal of the American Society of Gene Therapy*. Dec 2011;19(12):2169-2177.
196. Manche L, Green SR, Schmedt C, Mathews MB. Interactions between double-stranded RNA regulators and the protein kinase DAI. *Molecular and cellular biology*. Nov 1992;12(11):5238-5248.
197. Clemens MJ, Williams BR. Inhibition of cell-free protein synthesis by pppA2'p5'A2'p5'A: a novel oligonucleotide synthesized by interferon-treated L cell extracts. *Cell*. Mar 1978;13(3):565-572.
198. Caplen NJ, Parrish S, Imani F, Fire A, Morgan RA. Specific inhibition of gene expression by small double-stranded RNAs in invertebrate and

- vertebrate systems. *Proceedings of the National Academy of Sciences of the United States of America*. Aug 14 2001;98(17):9742-9747.
199. Sledz CA, Holko M, de Veer MJ, Silverman RH, Williams BR. Activation of the interferon system by short-interfering RNAs. *Nature cell biology*. Sep 2003;5(9):834-839.
 200. Kariko K, Bhuyan P, Capodici J, Weissman D. Small interfering RNAs mediate sequence-independent gene suppression and induce immune activation by signaling through toll-like receptor 3. *Journal of immunology (Baltimore, Md. : 1950)*. Jun 1 2004;172(11):6545-6549.
 201. Kleinman ME, Yamada K, Takeda A, et al. Sequence- and target-independent angiogenesis suppression by siRNA via TLR3. *Nature*. Apr 3 2008;452(7187):591-597.
 202. Alexopoulou L, Holt AC, Medzhitov R, Flavell RA. Recognition of double-stranded RNA and activation of NF-kappaB by Toll-like receptor 3. *Nature*. Oct 18 2001;413(6857):732-738.
 203. Heil F, Hemmi H, Hochrein H, et al. Species-specific recognition of single-stranded RNA via toll-like receptor 7 and 8. *Science*. Mar 5 2004;303(5663):1526-1529.
 204. Armstrong ME, Gantier M, Li L, et al. Small interfering RNAs induce macrophage migration inhibitory factor production and proliferation in breast cancer cells via a double-stranded RNA-dependent protein kinase-dependent mechanism. *Journal of immunology (Baltimore, Md. : 1950)*. Jun 1 2008;180(11):7125-7133.
 205. Sioud M. Single-stranded small interfering RNA are more immunostimulatory than their double-stranded counterparts: a central role for 2'-hydroxyl uridines in immune responses. *European journal of immunology*. May 2006;36(5):1222-1230.
 206. Sioud M. Induction of inflammatory cytokines and interferon responses by double-stranded and single-stranded siRNAs is sequence-dependent and requires endosomal localization. *Journal of molecular biology*. May 20 2005;348(5):1079-1090.
 207. Hornung V, Guenther-Biller M, Bourquin C, et al. Sequence-specific potent induction of IFN-alpha by short interfering RNA in plasmacytoid dendritic cells through TLR7. *Nature medicine*. Mar 2005;11(3):263-270.
 208. Judge AD, Sood V, Shaw JR, Fang D, McClintock K, MacLachlan I. Sequence-dependent stimulation of the mammalian innate immune response by synthetic siRNA. *Nature biotechnology*. Apr 2005;23(4):457-462.
 209. Sioud M, Furset G, Cekaite L. Suppression of immunostimulatory siRNA-driven innate immune activation by 2'-modified RNAs. *Biochemical and biophysical research communications*. Sep 14 2007;361(1):122-126.
 210. Forsbach A, Muller C, Montino C, et al. Impact of delivery systems on siRNA immune activation and RNA interference. *Immunology letters*. Jan 30 2012;141(2):169-180.

211. Bridge AJ, Pebernard S, Ducraux A, Nicoulaz AL, Iggo R. Induction of an interferon response by RNAi vectors in mammalian cells. *Nature genetics*. Jul 2003;34(3):263-264.
212. Fish RJ, Kruihof EK. Short-term cytotoxic effects and long-term instability of RNAi delivered using lentiviral vectors. *BMC molecular biology*. Aug 3 2004;5:9.
213. Grimm D, Streetz KL, Jopling CL, et al. Fatality in mice due to oversaturation of cellular microRNA/short hairpin RNA pathways. *Nature*. May 25 2006;441(7092):537-541.
214. Grimm D, Wang L, Lee JS, et al. Argonaute proteins are key determinants of RNAi efficacy, toxicity, and persistence in the adult mouse liver. *The Journal of clinical investigation*. Sep 2010;120(9):3106-3119.
215. Giering JC, Grimm D, Storm TA, Kay MA. Expression of shRNA from a tissue-specific pol II promoter is an effective and safe RNAi therapeutic. *Molecular therapy : the journal of the American Society of Gene Therapy*. Sep 2008;16(9):1630-1636.
216. McBride JL, Boudreau RL, Harper SQ, et al. Artificial miRNAs mitigate shRNA-mediated toxicity in the brain: implications for the therapeutic development of RNAi. *Proceedings of the National Academy of Sciences of the United States of America*. Apr 15 2008;105(15):5868-5873.
217. Ulusoy A, Sahin G, Bjorklund T, Aebischer P, Kirik D. Dose optimization for long-term rAAV-mediated RNA interference in the nigrostriatal projection neurons. *Molecular therapy : the journal of the American Society of Gene Therapy*. Sep 2009;17(9):1574-1584.
218. Khodr CE, Sapru MK, Pedapati J, et al. An alpha-synuclein AAV gene silencing vector ameliorates a behavioral deficit in a rat model of Parkinson's disease, but displays toxicity in dopamine neurons. *Brain research*. Jun 13 2011;1395:94-107.
219. Bish LT, Sleeper MM, Reynolds C, et al. Cardiac gene transfer of short hairpin RNA directed against phospholamban effectively knocks down gene expression but causes cellular toxicity in canines. *Human gene therapy*. Aug 2011;22(8):969-977.
220. McManus MT, Haines BB, Dillon CP, et al. Small interfering RNA-mediated gene silencing in T lymphocytes. *Journal of immunology (Baltimore, Md. : 1950)*. Nov 15 2002;169(10):5754-5760.
221. Vickers TA, Lima WF, Nichols JG, Crooke ST. Reduced levels of Ago2 expression result in increased siRNA competition in mammalian cells. *Nucleic Acids Res*. 2007;35(19):6598-6610.
222. Castanotto D, Sakurai K, Lingeman R, et al. Combinatorial delivery of small interfering RNAs reduces RNAi efficacy by selective incorporation into RISC. *Nucleic Acids Res*. 2007;35(15):5154-5164.
223. Martin JN, Wolken N, Brown T, Dauer WT, Ehrlich ME, Gonzalez-Alegre P. Lethal toxicity caused by expression of shRNA in the mouse striatum: implications for therapeutic design. *Gene therapy*. Jul 2011;18(7):666-673.

224. Sempere LF, Freemantle S, Pitha-Rowe I, Moss E, Dmitrovsky E, Ambros V. Expression profiling of mammalian microRNAs uncovers a subset of brain-expressed microRNAs with possible roles in murine and human neuronal differentiation. *Genome biology*. 2004;5(3):R13.
225. Lim LP, Lau NC, Garrett-Engle P, et al. Microarray analysis shows that some microRNAs downregulate large numbers of target mRNAs. *Nature*. Feb 17 2005;433(7027):769-773.
226. Schaefer A, O'Carroll D, Tan CL, et al. Cerebellar neurodegeneration in the absence of microRNAs. *The Journal of experimental medicine*. Jul 9 2007;204(7):1553-1558.
227. Tao J, Wu H, Lin Q, et al. Deletion of astroglial Dicer causes non-cell-autonomous neuronal dysfunction and degeneration. *The Journal of neuroscience : the official journal of the Society for Neuroscience*. Jun 1 2011;31(22):8306-8319.
228. Johnson R, Zuccato C, Belyaev ND, Guest DJ, Cattaneo E, Buckley NJ. A microRNA-based gene dysregulation pathway in Huntington's disease. *Neurobiology of disease*. Mar 2008;29(3):438-445.
229. Packer AN, Xing Y, Harper SQ, Jones L, Davidson BL. The bifunctional microRNA miR-9/miR-9* regulates REST and CoREST and is downregulated in Huntington's disease. *The Journal of neuroscience : the official journal of the Society for Neuroscience*. Dec 31 2008;28(53):14341-14346.
230. Marti E, Pantano L, Banez-Coronel M, et al. A myriad of miRNA variants in control and Huntington's disease brain regions detected by massively parallel sequencing. *Nucleic Acids Res*. Nov 2010;38(20):7219-7235.
231. Lee ST, Chu K, Im WS, et al. Altered microRNA regulation in Huntington's disease models. *Experimental neurology*. Jan 2011;227(1):172-179.
232. Hu J, Liu J, Corey DR. Allele-selective inhibition of huntingtin expression by switching to an miRNA-like RNAi mechanism. *Chem Biol*. Nov 24 2010;17(11):1183-1188.
233. Butland SL, Devon RS, Huang Y, et al. CAG-encoded polyglutamine length polymorphism in the human genome. *BMC genomics*. 2007;8:126.
234. Rodriguez-Lebron E, Denovan-Wright EM, Nash K, Lewin AS, Mandel RJ. Intrastriatal rAAV-mediated delivery of anti-huntingtin shRNAs induces partial reversal of disease progression in R6/1 Huntington's disease transgenic mice. *Molecular therapy : the journal of the American Society of Gene Therapy*. Oct 2005;12(4):618-633.
235. Denovan-Wright EM, Rodriguez-Lebron E, Lewin AS, Mandel RJ. Unexpected off-targeting effects of anti-huntingtin ribozymes and siRNA in vivo. *Neurobiology of disease*. Mar 2008;29(3):446-455.
236. Ding H, Schwarz DS, Keene A, et al. Selective silencing by RNAi of a dominant allele that causes amyotrophic lateral sclerosis. *Aging cell*. Aug 2003;2(4):209-217.

237. Schwarz DS, Ding H, Kennington L, et al. Designing siRNA that distinguish between genes that differ by a single nucleotide. *PLoS genetics*. Sep 8 2006;2(9):e140.
238. Dykxhoorn DM, Schlehuber LD, London IM, Lieberman J. Determinants of specific RNA interference-mediated silencing of human beta-globin alleles differing by a single nucleotide polymorphism. *Proceedings of the National Academy of Sciences of the United States of America*. Apr 11 2006;103(15):5953-5958.
239. Ohnishi Y, Tamura Y, Yoshida M, Tokunaga K, Hohjoh H. Enhancement of allele discrimination by introduction of nucleotide mismatches into siRNA in allele-specific gene silencing by RNAi. *PloS one*. 2008;3(5):e2248.
240. Miller VM, Xia H, Marrs GL, et al. Allele-specific silencing of dominant disease genes. *Proceedings of the National Academy of Sciences of the United States of America*. Jun 10 2003;100(12):7195-7200.
241. Alves S, Nascimento-Ferreira I, Auregan G, et al. Allele-specific RNA silencing of mutant ataxin-3 mediates neuroprotection in a rat model of Machado-Joseph disease. *PloS one*. 2008;3(10):e3341.
242. Scholefield J, Greenberg LJ, Weinberg MS, Arbutnot PB, Abdelgany A, Wood MJ. Design of RNAi hairpins for mutation-specific silencing of ataxin-7 and correction of a SCA7 phenotype. *PloS one*. 2009;4(9):e7232.
243. Kawaguchi Y, Okamoto T, Taniwaki M, et al. CAG expansions in a novel gene for Machado-Joseph disease at chromosome 14q32.1. *Nature genetics*. Nov 1994;8(3):221-228.
244. Warby SC, Montpetit A, Hayden AR, et al. CAG expansion in the Huntington disease gene is associated with a specific and targetable predisposing haplogroup. *American journal of human genetics*. Mar 2009;84(3):351-366.
245. Liu W, Kennington LA, Rosas HD, et al. Linking SNPs to CAG repeat length in Huntington's disease patients. *Nature methods*. Nov 2008;5(11):951-953.
246. Xia H, Mao Q, Eliason SL, et al. RNAi suppresses polyglutamine-induced neurodegeneration in a model of spinocerebellar ataxia. *Nature medicine*. Aug 2004;10(8):816-820.
247. Xia X, Zhou H, Huang Y, Xu Z. Allele-specific RNAi selectively silences mutant SOD1 and achieves significant therapeutic benefit in vivo. *Neurobiology of disease*. Sep 2006;23(3):578-586.
248. Xia H, Mao Q, Paulson HL, Davidson BL. siRNA-mediated gene silencing in vitro and in vivo. *Nature biotechnology*. Oct 2002;20(10):1006-1010.
249. Ralph GS, Radcliffe PA, Day DM, et al. Silencing mutant SOD1 using RNAi protects against neurodegeneration and extends survival in an ALS model. *Nature medicine*. Apr 2005;11(4):429-433.
250. Raoul C, Abbas-Terki T, Bensadoun JC, et al. Lentiviral-mediated silencing of SOD1 through RNA interference retards disease onset and

- progression in a mouse model of ALS. *Nature medicine*. Apr 2005;11(4):423-428.
251. Dahlgren C, Zhang HY, Du Q, et al. Analysis of siRNA specificity on targets with double-nucleotide mismatches. *Nucleic Acids Res*. May 2008;36(9):e53.
 252. Miller VM, Gouvion CM, Davidson BL, Paulson HL. Targeting Alzheimer's disease genes with RNA interference: an efficient strategy for silencing mutant alleles. *Nucleic Acids Res*. 2004;32(2):661-668.
 253. Auerbach W, Hurlbert MS, Hilditch-Maguire P, et al. The HD mutation causes progressive lethal neurological disease in mice expressing reduced levels of huntingtin. *Human molecular genetics*. Oct 15 2001;10(22):2515-2523.
 254. Cattaneo E, Zuccato C, Tartari M. Normal huntingtin function: an alternative approach to Huntington's disease. *Nature reviews. Neuroscience*. Dec 2005;6(12):919-930.
 255. Riva A, Kohane IS. A SNP-centric database for the investigation of the human genome. *BMC bioinformatics*. Mar 26 2004;5:33.
 256. Riva A, Kohane IS. SNPper: retrieval and analysis of human SNPs. *Bioinformatics (Oxford, England)*. Dec 2002;18(12):1681-1685.
 257. van Bilsen PH, Jaspers L, Lombardi MS, Odekerken JC, Burright EN, Kaemmerer WF. Identification and allele-specific silencing of the mutant huntingtin allele in Huntington's disease patient-derived fibroblasts. *Human gene therapy*. Jul 2008;19(7):710-719.
 258. Barrett JC, Fry B, Maller J, Daly MJ. Haploview: analysis and visualization of LD and haplotype maps. *Bioinformatics (Oxford, England)*. Jan 15 2005;21(2):263-265.
 259. Livak KJ, Schmittgen TD. Analysis of relative gene expression data using real-time quantitative PCR and the 2(-Delta Delta C(T)) Method. *Methods*. Dec 2001;25(4):402-408.
 260. Grondin R, Kaytor MD, Ai Y, et al. Six-month partial suppression of Huntingtin is well tolerated in the adult rhesus striatum. *Brain : a journal of neurology*. Apr 2012;135(Pt 4):1197-1209.
 261. Pfister EL, Kennington L, Straubhaar J, et al. Five siRNAs targeting three SNPs may provide therapy for three-quarters of Huntington's disease patients. *Curr Biol*. May 12 2009;19(9):774-778.
 262. Lombardi MS, Jaspers L, Spronkmans C, et al. A majority of Huntington's disease patients may be treatable by individualized allele-specific RNA interference. *Experimental neurology*. Jun 2009;217(2):312-319.
 263. McBride JL, Pitzer MR, Boudreau RL, et al. Preclinical safety of RNAi-mediated HTT suppression in the rhesus macaque as a potential therapy for Huntington's disease. *Molecular therapy : the journal of the American Society of Gene Therapy*. Dec 2011;19(12):2152-2162.

264. Zeng Y, Wagner EJ, Cullen BR. Both Natural and Designed Micro RNAs Can Inhibit the Expression of Cognate mRNAs When Expressed in Human Cells. *Molecular Cell*. 2002;9(6):1327-1333.
265. Mueller C, Tang Q, Gruntman A, et al. Sustained miRNA-mediated knockdown of mutant AAT with simultaneous augmentation of wild-type AAT has minimal effect on global liver miRNA profiles. *Molecular therapy : the journal of the American Society of Gene Therapy*. Mar 2012;20(3):590-600.
266. Slow EJ, van Raamsdonk J, Rogers D, et al. Selective striatal neuronal loss in a YAC128 mouse model of Huntington disease. *Human molecular genetics*. Jul 1 2003;12(13):1555-1567.
267. Gray M, Shirasaki DI, Cepeda C, et al. Full-length human mutant huntingtin with a stable polyglutamine repeat can elicit progressive and selective neuropathogenesis in BACHD mice. *The Journal of neuroscience : the official journal of the Society for Neuroscience*. Jun 11 2008;28(24):6182-6195.
268. Menalled LB, Sison JD, Dragatsis I, Zeitlin S, Chesselet MF. Time course of early motor and neuropathological anomalies in a knock-in mouse model of Huntington's disease with 140 CAG repeats. *The Journal of comparative neurology*. Oct 6 2003;465(1):11-26.
269. Gottwein E, Cai X, Cullen BR. A novel assay for viral microRNA function identifies a single nucleotide polymorphism that affects Drosha processing. *Journal of virology*. Jun 2006;80(11):5321-5326.
270. Duan R, Pak C, Jin P. Single nucleotide polymorphism associated with mature miR-125a alters the processing of pri-miRNA. *Human molecular genetics*. May 1 2007;16(9):1124-1131.
271. Sun G, Yan J, Noltner K, et al. SNPs in human miRNA genes affect biogenesis and function. *RNA*. Sep 2009;15(9):1640-1651.
272. Saunders MA, Liang H, Li WH. Human polymorphism at microRNAs and microRNA target sites. *Proceedings of the National Academy of Sciences of the United States of America*. Feb 27 2007;104(9):3300-3305.
273. Iwai N, Naraba H. Polymorphisms in human pre-miRNAs. *Biochemical and biophysical research communications*. Jun 17 2005;331(4):1439-1444.
274. Kawahara Y, Zinshteyn B, Sethupathy P, Iizasa H, Hatzigeorgiou AG, Nishikura K. Redirection of silencing targets by adenosine-to-inosine editing of miRNAs. *Science*. Feb 23 2007;315(5815):1137-1140.
275. Ko J, Ou S, Patterson PH. New anti-huntingtin monoclonal antibodies: implications for huntingtin conformation and its binding proteins. *Brain research bulletin*. Oct-Nov 1 2001;56(3-4):319-329.
276. Khoshnan A, Ko J, Patterson PH. Effects of intracellular expression of anti-huntingtin antibodies of various specificities on mutant huntingtin aggregation and toxicity. *Proceedings of the National Academy of Sciences of the United States of America*. Jan 22 2002;99(2):1002-1007.

277. Gao GP, Alvira MR, Wang L, Calcedo R, Johnston J, Wilson JM. Novel adeno-associated viruses from rhesus monkeys as vectors for human gene therapy. *Proceedings of the National Academy of Sciences of the United States of America*. Sep 3 2002;99(18):11854-11859.
278. Langmead B, Trapnell C, Pop M, Salzberg SL. Ultrafast and memory-efficient alignment of short DNA sequences to the human genome. *Genome biology*. 2009;10(3):R25.
279. Kordasiewicz HB, Stanek LM, Wancewicz EV, et al. Sustained Therapeutic Reversal of Huntington's Disease by Transient Repression of Huntingtin Synthesis. *Neuron*. Jun 21 2012;74(6):1031-1044.
280. Lu XH, Yang XW. "Huntingtin Holiday": Progress toward an Antisense Therapy for Huntington's Disease. *Neuron*. Jun 21 2012;74(6):964-966.
281. Nielsen PE, Egholm M, Berg RH, Buchardt O. Sequence-selective recognition of DNA by strand displacement with a thymine-substituted polyamide. *Science*. Dec 6 1991;254(5037):1497-1500.
282. Hu J, Matsui M, Corey DR. Allele-selective inhibition of mutant huntingtin by peptide nucleic acid-peptide conjugates, locked nucleic acid, and small interfering RNA. *Annals of the New York Academy of Sciences*. Sep 2009;1175:24-31.
283. Hu J, Matsui M, Gagnon KT, et al. Allele-specific silencing of mutant huntingtin and ataxin-3 genes by targeting expanded CAG repeats in mRNAs. *Nature biotechnology*. May 2009;27(5):478-484.
284. Gagnon KT, Pendergraff HM, Deleavey GF, et al. Allele-selective inhibition of mutant huntingtin expression with antisense oligonucleotides targeting the expanded CAG repeat. *Biochemistry*. Nov 30 2010;49(47):10166-10178.
285. Evers MM, Pepers BA, van Deutekom JC, et al. Targeting several CAG expansion diseases by a single antisense oligonucleotide. *PloS one*. 2011;6(9):e24308.
286. Carroll JB, Warby SC, Southwell AL, et al. Potent and selective antisense oligonucleotides targeting single-nucleotide polymorphisms in the Huntington disease gene / allele-specific silencing of mutant huntingtin. *Molecular therapy : the journal of the American Society of Gene Therapy*. Dec 2011;19(12):2178-2185.
287. Huang H, Qiao R, Zhao D, et al. Profiling of mismatch discrimination in RNAi enabled rational design of allele-specific siRNAs. *Nucleic Acids Res*. Dec 2009;37(22):7560-7569.
288. Thompson LM, Aiken CT, Kaltenbach LS, et al. IKK phosphorylates Huntingtin and targets it for degradation by the proteasome and lysosome. *The Journal of cell biology*. Dec 28 2009;187(7):1083-1099.
289. Gu X, Greiner ER, Mishra R, et al. Serines 13 and 16 are critical determinants of full-length human mutant huntingtin induced disease pathogenesis in HD mice. *Neuron*. Dec 24 2009;64(6):828-840.

290. van der Burg JM, Bjorkqvist M, Brundin P. Beyond the brain: widespread pathology in Huntington's disease. *Lancet neurology*. Aug 2009;8(8):765-774.
291. Bjorkqvist M, Wild EJ, Thiele J, et al. A novel pathogenic pathway of immune activation detectable before clinical onset in Huntington's disease. *The Journal of experimental medicine*. Aug 4 2008;205(8):1869-1877.
292. Perabo L, Buning H, Kofler DM, et al. In vitro selection of viral vectors with modified tropism: the adeno-associated virus display. *Molecular therapy : the journal of the American Society of Gene Therapy*. Jul 2003;8(1):151-157.
293. Perabo L, Endell J, King S, et al. Combinatorial engineering of a gene therapy vector: directed evolution of adeno-associated virus. *The journal of gene medicine*. Feb 2006;8(2):155-162.

**APPENDIX I: THERAPEUTIC SILENCING OF MUTANT *HUNTINGTIN* WITH
SIRNA ATTENUATES STRIATAL AND CORTICAL NEUROPATHOLOGY AND
BEHAVIORAL DEFICITS**

DiFiglia M., Sena-Esteves M., Chase K., Sapp E., Pfister E., Sass M., Yoder J., Reeves P., Pandey R.K., Rajeev K.G., Manoharan M., Sah D.W., Zamore P.D., Aronin N. (2007). Therapeutic silencing of mutant *huntingtin* with siRNA attenuates striatal and cortical neuropathology and behavioral deficits. *Proceedings of the National Academy of Sciences USA* 104, 17204-17209.

Therapeutic silencing of mutant huntingtin with siRNA attenuates striatal and cortical neuropathology and behavioral deficits

M. DiFiglia*, M. Sena-Esteves*, K. Chase †, E. Sapp*, E. Pfister †, M. Sass †, J. Yoder*, P. Reeves*, R. K. Pandey ‡, K. G. Rajeev ‡, M. Manoharan ‡, D. W. Y. Sah ‡, P. D. Zamore §, and N. Aronin †¶

*Department of Neurology, Massachusetts General Hospital, Charlestown, MA 02114; Departments of †Medicine and ‡Biochemistry and Molecular Pharmacology, University of Massachusetts Medical School, Worcester, MA 01655; and †Alnylam Pharmaceuticals, Cambridge, MA 02142

Communicated by Craig Mello, University of Massachusetts Medical School, Worcester, MA, August 31, 2007 (received for review May 4, 2007)

Huntington's disease (HD) is a neurodegenerative disorder caused by expansion of a CAG repeat in the huntingtin (Htt) gene. HD is autosomal dominant and, in theory, amenable to therapeutic RNA silencing. We introduced cholesterol-conjugated small interfering RNA duplexes (cc-siRNA) targeting human Htt mRNA (siRNA-Htt) into mouse striata that also received adeno-associated virus containing either expanded (100 CAG) or wild-type (18 CAG) Htt cDNA encoding huntingtin (Htt) 1–400. Adeno-associated virus delivery to striatum and overlying cortex of the mutant Htt gene, but not the wild type, produced neuropathology and motor deficits. Treatment with cc-siRNA-Htt in mice with mutant Htt prolonged survival of striatal neurons, reduced neuropil aggregates, diminished inclusion size, and lowered the frequency of clasping and footslips on balance beam. cc-siRNA-Htt was designed to target human wild-type and mutant Htt and decreased levels of both in the striatum. Our findings indicate that a single administration into the adult striatum of an siRNA targeting Htt can silence mutant Htt, attenuate neuronal pathology, and delay the abnormal behavioral phenotype observed in a rapid-onset, viral transgenic mouse model of HD.

gene delivery | gene silencing | Huntington's disease | neurodegenerative disease | RNAi

Huntington's disease (HD) is an autosomal dominant disease caused by a CAG repeat expansion in the Htt gene (1). Mutant Htt causes neuronal death, dementia, and movement dysfunction; there is no effective treatment. In an inducible transgenic mouse model of HD, turning off transgene expression reversed neuropathology and motor deficits (2). Lowering mutant Htt gene expression in brain may treat HD. In mice, viral vector delivery of short hairpin RNAs (shRNAs) against mutant Htt gene exon 1 or genes that cause other neurodegenerative disorders reduced neuropathology and motor deficits (3–10). Brain delivery of adeno-associated virus (AAV)-shRNA against mutant Htt improved signs of disease in HD transgenic models (7, 11). In the inaugural study on RNAi targeting Htt in vivo, shRNA against Htt in AAV2, delivered to the N171–82Q transgenic model of HD, improved ambulation at 4 months and rotarod performance at 10 and 18 weeks after injection (7). Five and one-half months after shRNA administration, quantitative RT-PCR revealed a 50% reduction in striatal Htt mRNA. Statistical changes in quantification of Htt protein reduction and inclusions were not reported. AAV5 delivery of shRNA against Htt in the R6/1 murine model of HD showed a 25% decrease in Htt protein and an 80% reduction in Htt mRNA 10 weeks after shRNA injection (10). The shRNA delayed onset of clasping by 2 weeks (20–22 weeks), and treated mice had fewer clasps. No difference in rotarod performance was detected. Inclusion size and number decreased in the striatum, but not in the cortex, compared with the corresponding contralateral brain regions. The authors provided an important caveat that one of the shRNAs had off-target effects; the cause of the off-target effects

was not established. shRNA in AAV2 or AAV5 was used to target EGFP to knock down EGFP-Htt in another transgenic model of HD (11). shRNA reversed pathology after the onset of pathologic changes; however, behaviors were not studied. Administration of large amounts of siRNA against Htt in a Lipofectamine 2000 suspension into the lateral ventricle of newborn R6/2 transgenic mice (exon 1 of Htt) reduced whole-brain levels of mutant Htt in two mice and Htt mRNA up to 7 days posttreatment, delayed the onset of clasping, rotarod, and open-field phenotypes, and improved survival (12). Statistical quantification of neuropathology was not reported. Thus, prior studies examining RNAi against Htt provided the groundwork for therapeutic gene silencing in HD. Most of the studies used viral delivery of shRNA, and the study using siRNA required liposome delivery to newborns, with the potential liposome neuronal toxicity.

Caveats attend the use of shRNAs, which can be toxic when integrated into the host genome (13, 14), in part because shRNA production is unregulated. Long siRNAs (>29 nt) and shRNAs are prone to activate off-target gene expression (15). For patient safety, shRNA will need to be able to be switched off, currently a hurdle in viral delivery systems.

An alternative strategy for HD therapy is the use of small-interfering RNAs (siRNAs), ≈21-nt RNA duplexes. siRNA has been administered into cerebroventricles, vasculature, intrathecal space, and parenchyma (16–20). siRNAs were found effective and safe when introduced into mice and non-human primates (19, 21, 22). Several limitations impede progress in using siRNAs as a treatment for HD: entry and effectiveness in adult neurons without the use of potentially toxic transfection reagents; a clear demonstration that gene silencing reduces protein expression; and an improvement in behavioral deficits and neuropathology, especially neuron survival. Because bioactive molecules conjugated to cholesterol have improved cellular uptake in vitro (23), LDL receptors have been detected in brain (24), and cholesterol conjugation enhances siRNA uptake in

Author contributions: M.D., M.S.-E., D.W.Y.S., P.D.Z., and N.A. designed research; M.D., M.S.-E., K.C., E.S., E.P., M.S., J.Y., P.R., and N.A. performed research; M.D., M.S.-E., R.K.P., K.G.R., M.M., D.W.Y.S., and N.A. contributed new reagents/analytic tools; M.D., K.C., E.S., E.P., P.D.Z., and N.A. analyzed data; and M.D., M.S.-E., D.W.Y.S., P.D.Z., and N.A. wrote the paper.

Conflict of interest statement: P.D.Z. is a cofounder and scientific advisory board member of Alnylam Pharmaceuticals. D.W.Y.S., M.M., K.G.R., and R.K.P. are employees of Alnylam Pharmaceuticals.

Freely available online through the PNAS open access option.

Abbreviations: AAV, adeno-associated virus; AAV Htt18Q, AAV containing Htt cDNA producing Htt with 18 polyglutamines; HD, Huntington's disease; Luc, luciferase; shRNA, short hairpin RNA; siRNA, small interfering RNA.

¶To whom correspondence should be addressed at: University of Massachusetts Medical School, 55 Lake Avenue North, Worcester, MA 01655. E-mail: neil.aronin@umassmed.edu.

This article contains supporting information online at www.pnas.org/cgi/content/full/0708285104/DC1.

© 2007 by The National Academy of Sciences of the USA

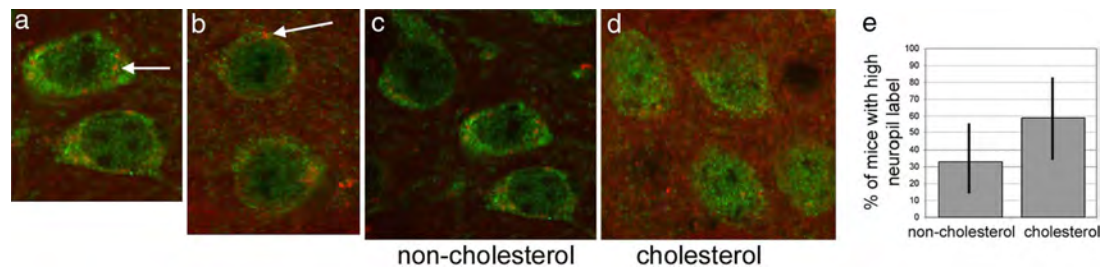


Fig. 1. Cholesterol-conjugated and unconjugated siRNA-*Htt* enters neurons. (a and b) Laser confocal images of DARPP32-labeled striatal neurons (green) treated with Cy3-siRNA-*Htt*. The striatum was injected with 10 μ M unconjugated (a) or cc (b) Cy3-siRNA-*Htt*. Cy3 fluorescence appears in the neuronal cytoplasm as distinct bodies (red-orange color at arrows). Images were from striata 5 days (a) and 1 day (b) after injection. (c and d) Cy3 fluorescence in the striatal neuropil surrounding the DARPP32-labeled neurons. (e) Percent of mice with high Cy3 fluorescence in neuropil after injection of cc-siRNA-*Htt* ($n = 17$) or unconjugated siRNA-*Htt* ($n = 18$); not significant in Fisher's exact test. Bars indicate the confidence intervals.

cells outside of the central nervous system (16), we speculated that cholesterol-conjugated (cc) siRNA might enter neurons *in vivo*.

An *in vivo*, rapid-onset model of HD would be optimal to test gene silencing in brain. The current rapid mouse model of HD shows mutant *Htt*-induced pathology after 2 months. Transgenic mice expressing exon 1 of mutant *Htt* [R6/2 (25)] develop nuclear inclusions throughout the brain at 2 months of age and exhibit a rapidly progressing, severe phenotype. Other transgenic or knock-in mice expressing mutant *Htt* exhibit late-onset, mild phenotypes, often after 6 months of age (26, 27), and lack prominent neuronal loss. Neither model is ideal to test transient effects of a single injection of siRNA against *Htt* introduced directly to the striatum. We therefore developed an acute, *in vivo*, HD mouse model tailored to addressing the efficacy of siRNA. Here, we used AAV to deliver a 1,395-nt cDNA fragment of human mutant *Htt* into mouse striatum to evaluate the effectiveness of an siRNA targeting human *Htt*.

Results

Unconjugated and cc-siRNAs Enter Medium Spiny Striatal Neurons. To confirm that the siRNA introduced into the striatum entered neurons, we examined striata of mice injected with Cy3-labeled siRNA-*Htt*. Cholesterol conjugation improves siRNA delivery in hepatocytes (16), so we compared delivery of cc-siRNA and unconjugated siRNA in neurons. Brain tissue was processed 1–5 days after injection and examined for immunoreactive localization of DARPP32, which is selectively expressed by medium size striatal spiny neurons. At the level of the striatal injection, Cy3 immunofluorescent bodies were present in the cytoplasm of the majority of DARPP32-positive striatal neurons at all concentrations tested, regardless of cholesterol conjugation (Fig. 1 a and b). Quantitative analysis showed that 86% and 88% of DARPP32-positive neurons exposed to Cy3 cc-siRNA (10 μ M) and unconjugated Cy3 siRNA (10 μ M) contained Cy3-labeled bodies (range 76–100% in both). These findings indicate that siRNA had entered the majority of striatal neurons. We typically observed a higher level of Cy3 fluorescence in the neuropil surrounding DARPP32-labeled cell bodies after injection of Cy3 cc-siRNA than unconjugated Cy3 siRNA (Fig. 1 c and d), although the difference did not achieve statistical significance (Fig. 1 e; median; 59% versus 33%, $P \leq 0.18$, respectively). These results suggested, but do not prove, that neuronal processes take up the cc-siRNA more readily than the unconjugated siRNA. We therefore used cc-siRNA in our subsequent studies.

Single Intra-striatal Injection of siRNA-*Htt* Protects Striatal Neurons from Mutant *Htt* Neuropathology. *Htt* knock-in mice manifest neuropathology and motor deficits late and then sporadically at

10 months of age. Transgenic models vary in the extent of gene expression, brain regions involved, neuropathology, and behaviors (28). We therefore developed a rapid-onset murine model of HD, in which timed neuropathology and motor impairments were predictable, robust, and experimentally testable. AAV vectors are known to be effective for the delivery of exogenous genes into the rodent brain (29). Normal mice received a unilateral striatal injection of AAV *Htt*18Q or AAV *Htt*100Q (*Htt* cDNA coding for amino acids 1–400 of *Htt*, with either 18 or 100 CAG repeats, respectively). Two independent preparations of AAV *Htt*100Q virus were used (group 1 and group 2). Immunoperoxidase labeling with anti-*Htt* revealed intense *Htt* immunoreactivity in neurons within the dorsal half of the striatum, deep layers of the cortex, and septal area ipsilateral to the injection 2 weeks after injection (Fig. 2 a). In AAV *Htt*100Q-infected mice, degenerating and shrunken *Htt*-labeled neurons appeared in cortex layers 5 and 6 and in the dorsal striatum. In the striatum of some mice, neurons were markedly depleted from a core region around the site of AAV *Htt*100Q injection (Fig. 2 a), resulting in a region of diminished *Htt* immunoreactivity. No such loss of neurons was evident in mice injected with AAV *Htt*18Q. Measurements of somal cross-sectional area showed that neurons expressing AAV *Htt*100Q were significantly smaller compared with neurons expressing AAV *Htt*18Q (Fig. 2 b and c Left; mean \pm SD; AAV *Htt*18Q versus AAV *Htt*100Q, 149 ± 10.4 versus 113 ± 10.1 ; $P \leq 0.003$) or neurons with wild-type *Htt* in the noninjected striata (not shown). However, the size of striatal neurons expressing AAV *Htt*100Q was not different in mice cotreated with cc-siRNA-*Htt* (113 ± 10.1) compared with mice cotreated with control cc-siRNA against luciferase (siRNA-*Luc*; 119 ± 6 ; Fig. 2 c Right).

Stereology in Nissl-stained sections showed that the number of neurons in AAV *Htt*100Q-injected regions of striatum was reduced compared with noninjected striata; neuronal number in the injected striata of group 2 mice was lower compared with mice in group 1 (Fig. 2 d). AAV *Htt*100Q-infected striata of group 1 mice cotreated with cc-siRNA-*Htt* had significantly more neurons compared with those given cc-siRNA-*Luc* (Fig. 2 d, mean \pm SD; cc-siRNA-*Htt* versus cc-siRNA-*Luc*, 5.3 ± 0.6 versus 3.5 ± 0.9 , $P \leq 0.01$). Neuronal survival was not improved by cotreatment with cc-siRNA-*Htt* compared with cc-siRNA-*Luc* in group 2 mice, most likely because of the more significant neuronal loss caused by AAV *Htt*100Q in group 2 [Fig. 2 d, mean \pm SD; cc-siRNA-*Luc* versus cc-siRNA-*Htt*, 2.87 ± 1.1 versus 2.13 ± 0.7 , not significant (29)].

Striatal and cortical neurons infected with AAV *Htt*100Q had strong diffuse nuclear labeling or intranuclear aggregates when immunolabeled with anti-*Htt* antisera (Fig. 2 b Inset and Fig. 3 a and b). Nuclear inclusions were detected in striatal (Fig. 3 c) and

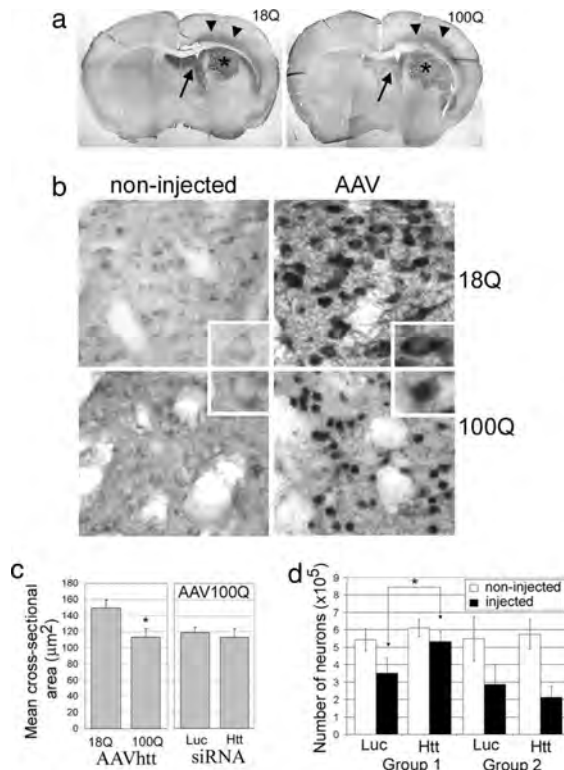


Fig. 2. Cholesterol-conjugated siRNA-Htt reversed neuropathology in the AAV HD mouse model. (a) Brain sections from normal mice that received a unilateral striatal injection of AAV Htt 18Q (Left) or AAV Htt 100Q (Right). Sections were immunoperoxidase-labeled by using anti-Htt antisera. Exogenous human wild-type and mutant Htt expression is visible in dorsal striatum (asterisks), septal nuclei (arrows), and deep layers of the cortex (arrowheads). (b) Htt-labeled striatal cells infected with AAV Htt 100Q are smaller than cells expressing Htt18Q or neurons in the noninjected striatum. Insets show examples of Htt-labeled cells at higher magnification. (c) Mean \pm SD for the cross-sectional area of immunoreactive striatal neurons in mice infected with AAV Htt 18Q or AAV Htt 100Q (Left) and mice infected with AAV Htt 100Q and cotreated with siRNA-Luc (Luc) or siRNA-Htt (Htt) (Right). Neuronal size is reduced in striatal cells expressing mutant Htt100Q compared with striatal cells expressing Htt18Q (Left; *, $P \leq 0.003$; $n = 8$ mice per group; 50 cells per mouse; Student's *t* test) but is not changed by cotreatment with cc-siRNA-Htt (Right; $n = 4$ per group). (d) Number of neurons determined by stereology in Nissl-stained sections in noninjected and AAV Htt 100Q-injected striatum. Bar graphs show mean \pm SD for number of neurons. Group 1 (Left): *, $P \leq 0.01$, Student's *t* test. Group 2 (Right): not significant.

cortical neurons with EM48 antibody, which detects only aggregated Htt. cc-siRNA-Htt treatment significantly reduced the median size of nuclear inclusions in striatal neurons in AAV Htt100Q-infected mice and in cortical neurons in group 1 AAV Htt100Q-infected mice (Fig. 3 d, medians; group 1: cortex, cc-siRNA-Luc versus cc-siRNA-Htt, 6.89 versus 5.86, $P \leq 0.01$; striatum, cc-siRNA-Luc versus cc-siRNA-Htt, 9.08 versus 7.78, $P \leq 0.01$; group 2: cortex, cc-siRNA-Luc versus cc-siRNA-Htt, 6.22 versus 6.29, not significant; striatum, cc-siRNA-Luc versus cc-siRNA-Htt, 8.7 versus 6.18, $P \leq 0.004$). The reduction in inclusion size by cc-siRNA-Htt suggests that buildup of inclusions is related to levels of accumulation of mutant Htt. Striata injected with AAV Htt18Q showed robust cytoplasmic staining in neurons with anti-Htt antisera but lacked inclusions with EM48

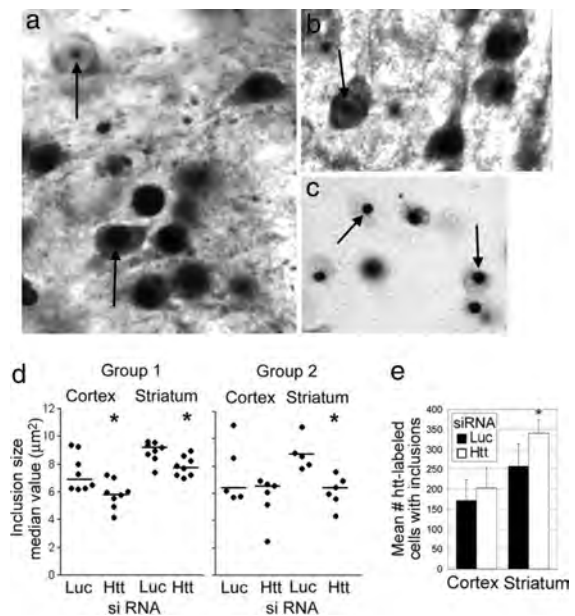


Fig. 3. Inclusion pathology was reduced in AAV Htt 100Q mice treated with cc-siRNA-Htt. Immunoperoxidase labeling was done with anti-Htt antisera. (a and b) Neurons with AAV Htt 100Q inclusions in striatum and cortex. (c) Nuclear inclusions in striatal neurons labeled with EM48 antisera. (d) Scatter plot showing size distribution of inclusions in the two groups of mice treated with AAV Htt 100Q. Densitometry was performed with EM48-stained sections. Horizontal bars indicate the medians. cc-siRNA-Htt (Htt) treatment reduces median inclusion size compared with cc-siRNA-Luc (Luc). Group 1: $n = 8, 8, 8, 8$; cortex, $P \leq 0.01$; striatum, $P \leq 0.01$. Group 2: $n = 5, 6, 5, 6$. Cortex, not significant; striatum, $P \leq 0.004$. One hundred cells per mouse were evaluated. Mann-Whitney *U* test; *, $P \leq 0.01$ for cortex and striatum. (e) Density of Htt-labeled neurons with inclusions per 2,500 μm^2 . cc-siRNA-Htt treatment increased the number of Htt-labeled neurons with inclusions. Findings are significant for striatum (*, $P \leq 0.002$; Student's *t* test; cc-siRNA-Luc, $n = 9$; cc-siRNA-Htt, $n = 8$).

or anti-Htt antisera (Fig. 2 b and b Inset). The density of anti-Htt-labeled striatal neurons with inclusions was significantly higher in cc-siRNA-Htt-treated mice than in cc-siRNA-Luc-treated mice (Fig. 3 e, mean \pm SD; group 1: striatum, cc-siRNA-Luc versus cc-siRNA-Htt, 258 ± 55.1 versus 340 ± 32.2 , $P \leq 0.002$). These data support results from stereology, which showed that administration of cc-siRNA-Htt increased survival of striatal neurons expressing mutant Htt (Fig. 2 d, group 1).

In HD brain, mutant N-Htt fragments accumulate in degenerating neuronal processes called dystrophic neurites (30). In HD transgenic mice, analogous neuronal processes are evident as neuropil aggregates (30, 31). Neuropil aggregates were detected in striata infected with AAV Htt100Q (Fig. 4 a) but not in striata infected with AAV Htt18Q (data not shown). There was a higher density of neuropil aggregates in group 1 mice compared with group 2 mice, a finding possibly due to the presence of more neurons in group 1 compared with group 2 (Fig. 2 c and d). Neuropil aggregates in striatum were significantly lower in all AAV Htt100Q mice treated with cc-siRNA-Htt compared with those treated with cc-siRNA-Luc (Fig. 4, mean \pm SD; group 1: cc-siRNA-Luc versus cc-siRNA-Htt, 5.73 ± 2.45 versus 1.85 ± 1.42 , $P \leq 0.002$; group 2: cc-siRNA-Luc versus cc-siRNA-Htt, 2.69 ± 1.60 versus 1.03 ± 0.51 , $P \leq 0.036$). Reducing expression of mutant Htt reduced formation of neuropil aggregates.

In summary, introduction of N-terminal mutant Htt fragment

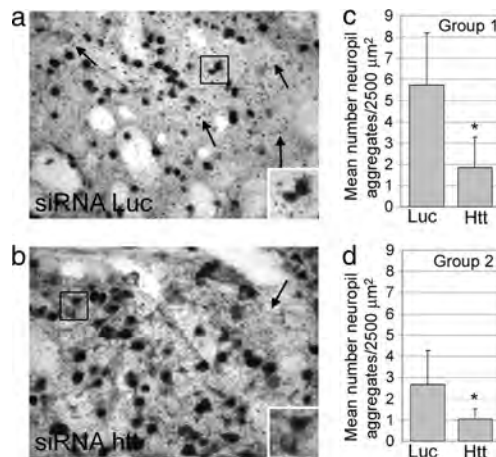


Fig. 4. Mutant Htt neuropil aggregates were reduced by cc-siRNA-Htt. (a and b) Htt labeling in neuropil aggregates (arrows) in the striatum from mice treated with AAV Htt100Q and cc-siRNA-Luc (a) or cc-siRNA-Htt (b). The aggregates are small structures (a), which are faintly visible in (b). The boxes in (a) and (b) denote the brain region in the insets. (c and d) Bar graphs showing number of neuropil aggregates in group 1 and group 2 AAV Htt100Q mice treated with cc-siRNA-Luc (Luc) or cc-siRNA-Htt (Htt). Group 1: $n = 8$ per treatment; *, $P \leq 0.002$. Group 2: cc-siRNA-Luc, $n = 5$; cc-siRNA-Htt, $n = 6$; *, $P \leq 0.036$. Student's t test; one $\times 40$ field per mouse.

into the mouse striatum by AAV Htt delivery recapitulated neuropathological features of HD, and cotreatment with siRNA targeting Htt ameliorated neuropathology.

Single Intrastratial Injection of siRNA-Htt Ameliorated Mutant Htt-Induced Motor Dysfunction. When suspended by the tail, neurologically impaired mice retract their limbs, a response called claspings. We found that more AAV Htt100Q mice clasped 14 days after injection compared with AAV Htt18Q mice (Fig. 5 a; 62.5% versus 15%, respectively, $P \leq 0.02$). The frequency of claspings in AAV Htt100Q mice was significantly reduced by cotreatment with cc-siRNA-Htt compared with cc-siRNA-Luc

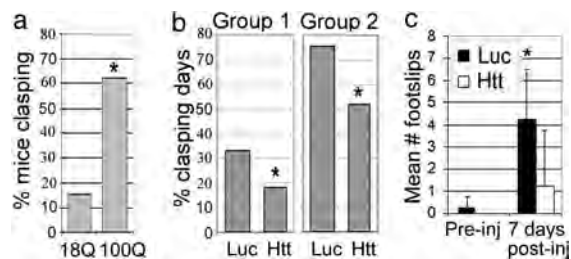


Fig. 5. AAV Htt100Q mice show reduced motor deficits in the presence of cc-siRNA-Htt. (a) Percent of mice clasping 14 days after injection with AAV Htt18Q and AAV Htt100Q. Mice with AAV Htt100Q had significantly more clasping days than mice injected with AAV Htt18Q. AAV Htt18Q, 15% clasping, $n = 13$; AAV Htt100Q, 62.5% clasping, $n = 16$ ($P = 0.02$). (b) AAV Htt100Q mice cotreated with cc-siRNA-Htt had fewer clasping days than mice coinjected with cc-siRNA-Luc (group 1: cc-siRNA-Luc, 33%, $n = 9$, versus cc-siRNA-Htt, 18%, $n = 8$; *, $P = 0.01$; group 2: cc-siRNA-Luc, 75%, $n = 5$, versus cc-siRNA-Htt, 52%, $n = 6$; *, $P \leq 0.02$; Fisher's exact test). (c) Shown are mean \pm SD footslips that occurred during beam walking for mice injected with AAV Htt100Q. Mean footslips were reduced in the presence of cc-siRNA-Htt compared with cc-siRNA-Luc. *, $P \leq 0.01$; Student's t test; $n = 4$ per group.

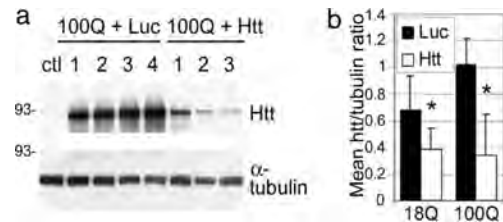


Fig. 6. Silencing human Htt mRNA reduced amount of exogenous wild-type and mutant Htt in the striatum. (a) Lysates were prepared from dorsal striatum 2.7 days after coinjection of AAV Htt18Q or AAV Htt100Q with either cc-siRNA-Luc or cc-siRNA-Htt. The Western blot was probed first with anti-Htt antibody (Upper) and then reprobed with anti-tubulin antibody (Lower). Shown is expression of Htt100Q in mice treated with cc-siRNA-Luc or cc-siRNA-Htt. (b) Bar graphs show mean Htt/tubulin ratios from densitometry of Western blot films for mice infected with AAV Htt18Q ($n = 4$) or AAV Htt100Q ($n = 3$) and treated with cc-siRNA-Luc or cc-siRNA-Htt. *, $P = 0.03$ for AAV Htt18Q; *, $P = 0.01$ for AAV Htt100Q.

(Fig. 5 b; cc-siRNA-Luc versus cc-siRNA-Htt; group 1: 33% versus 18%, $P \leq 0.01$; group 2: 75.6% versus 51.9%, $P \leq 0.02$). The percent of clasping days in the two groups of AAV Htt100Q mice positively correlated with the extent of neuronal death observed in the striatum. Mice injected with AAV Htt100Q and coinjected with cc-siRNA-Luc showed an increased number of footslips on the beam 7 days after injection. In contrast, AAV Htt100Q mice coinjected with cc-siRNA-Htt did not show a significant increase in footslips during beam walking, relative to the number observed before injection (Fig. 5 c; 7 days after injection; cc-siRNA-Luc, 4.25 ± 2.22 , versus cc-siRNA-Htt, 1.25 ± 2.5 , $P \leq 0.01$). cc-siRNA-Htt protected mice from motor deficits caused by AAV Htt100Q.

Single Intrastratial Injection of siRNA-Htt Decreases Human Htt Gene Expression in Mouse Brain. To examine whether RNAi accounted for improvement in neuropathology and motor deficits, we measured human Htt in the brain at the location of the AAV Htt delivery 2.7 days after injection. Brain lysates from mice injected with AAV Htt18Q or AAV Htt100Q, and cc-siRNA-Htt or cc-siRNA-Luc, were analyzed by Western blotting. Densitometry showed that coinjection of cc-siRNA-Htt reduced levels of Htt-18Q and Htt-100Q protein by 56% and 66%, respectively, compared with levels observed with the cc-siRNA-Luc (Fig. 6; mean \pm SD; AAV Htt18Q, cc-siRNA-Luc versus cc-siRNA-Htt, 0.68 ± 0.25 versus 0.38 ± 0.16 , $P = 0.03$; AAV Htt100Q, cc-siRNA-Luc versus cc-siRNA-Htt, 1.02 ± 0.19 versus 0.34 ± 0.31 , $P \leq 0.01$). We conclude that the observed improvements in neuropathology and behavior reflect silencing of the AAV Htt100Q gene by the cc-siRNA-Htt.

Single Intrastratial Injection of siRNA Does Not Stimulate a Specific Immunogenic Response. siRNAs exceeding 23 bp and shRNAs have been associated with an immunogenic response (32). We examined reactive microglia (CD11B immunoreactivity) and reactive astrocytes (30) (GFAP immunoreactivity) in mice injected with PBS or cc-siRNA-Luc. siRNA concentrations were the same as those used for coinjection with AAV. Astrocytic and microglial labeling did not differ between PBS and cc-siRNA treatments [supporting information (SI) Figs. 7]. cc-siRNAs did not change animal weight or temperature (SI Table 1).

Discussion

RNAi offers a promising therapy for autosomal dominantly inherited neurodegenerative disease. In theory, RNAi can target the underlying cause of HD, by silencing expression of the

mutant protein. AAV-shRNA delivered to brain improved signs of disease in transgenic models of HD (7, 11). Here, we describe a new virus-mediated transgenic model of HD in the adult mouse that mimics features of HD within 2 weeks and use this model to test the effects of gene silencing with siRNA targeting Htt mRNA. Our findings demonstrated that cc-siRNA- Htt entered adult striatal neurons and effected a reduction in mutant Htt protein that ameliorated both the neuropathology and the motor deficits caused by the virally delivered mutant Htt protein.

A single administration of cc-siRNA- Htt was sufficient to attenuate multiple neuropathological features and aberrant motor behaviors in the rapid-onset model of HD: the transgene silencing subdued expression of mutant Htt in the striatum for at least 3 days and sustained a benefit in motor behavior for 1 week. The improvement in motor behaviors correlated with improvement in neuropathology, indicating that gene silencing of mutant Htt ameliorated striatal neuronal dysfunction. Our results demonstrate that siRNA treatment with a clinically relevant formulation provides therapeutically meaningful benefit in an adult mouse model of HD. Together, these findings indicate that the RNAi effect is durable and that siRNA therapeutics might be deliverable in pulses rather than in continuous flow. The effect of a single siRNA injection appears to be widespread. Although our siRNA treatment was directed to the striatum, the size of inclusions in some mice was reduced in cortical neurons. siRNA administration correlated with an increase in the number of neurons with inclusions. This *in vivo* finding supports cellular HD models in which nuclear inclusion formation is dissociated with cell survival (33, 34) and could offer a survival advantage (35).

siRNA modified by cholesterol conjugation was used because of prior demonstration that cholesterol conjugation might improve siRNA access to tissues (16). It is not clear whether cholesterol conjugation increased Cy3-siRNA uptake into somata of DARPP32-labeled medium size spiny neurons in striatum. However, at low concentrations, a trend toward more Cy3-cc-siRNA than unconjugated siRNA uptake was apparent in regions surrounding cell bodies and in white matter, raising the possibility that neuronal processes, rather than cell bodies, preferentially take up cc-siRNA. It is possible that coinjection of siRNA with AAV- Htt improved the siRNA's neuronal delivery. Pilot studies have indicated that cc-siRNA enters primary striatal neurons in the absence of AAV and that two injections of siRNA- Htt can silence endogenous Htt (SI Figs. 8 and 9). Further study will be needed to assess optimal delivery of unconjugated and modified siRNAs in reducing levels of mutant Htt in the brain.

Safety and flexibility of small RNAs, either in shRNA or siRNA, are paramount for therapeutic gene silencing. The siRNA duplex used here, which targeted a sequence of Htt 5' to the CAG repeat of Htt mRNA, was well tolerated in the brain. Based on the extent of reactive microglia and astrocytes, siRNA administration into the striatum did not elicit an inflammatory response greater than vehicle injection alone. The cc-siRNA did not change animal weight or temperature (SI Table 1).

Viral delivery of a disease gene presents an alternative approach to traditional transgenic models for understanding pathophysiology and testing potential therapeutics. Lentivirus has been used to generate a rat model of HD (36). Delivery of truncated mutant Htt in lentivirus produced neuropathological features of HD but not behavioral phenotypes. In our model, AAV- Htt spread through dorsal striatum and deep cortical layers, areas affected early in HD. Cortical neurons are thought to contribute to striatal neuron vulnerability, because of loss of brain-derived neurotrophic factor from cortical neurons projecting to striatum (37). This AAV- Htt transgenic model has compelling features that provide a useful system for testing therapeutic candidates for HD; the model shows the neuro-

pathological changes found in HD, including neuronal loss and motor deficits, both of which occur with a rapid time course and are amenable to quantification. The model distinguishes between CAG repeat number in wild-type and mutant Htt gene expression, despite overexpression of both genes.

Treatment of HD and other autosomal dominant neurodegenerative diseases will require intervention for years, if not decades. siRNA has a distinct advantage in providing a predictable and finite term of action; therefore, siRNA treatment can be adjusted or stopped should side effects arise. shRNA delivered by either genomic or epigenetic incorporation would not be conducive to regulation and could be prone to activation of IFN-dependent pathways (32). However, in concept, viral delivery of shRNA offers long-term intraneuronal siRNA expression. The next challenge in testing siRNA therapeutics in brain disease will be the safe delivery of small RNAs to maximize target specificity, with the capacity to distinguish between mutant and wild-type alleles.

Methods

Plasmid DNA and AAV Preparation. We cloned N-terminal Htt cDNA with 18 CAG or 100 CAG repeats into plasmid pAAV-CBA-W, which encodes a chimeric promoter bearing the CMV enhancer element and the chicken β -actin promoter. The Htt cDNA codes 365 aa apart from the polyglutamine repeats. The vector was packaged into AAV1/8 mosaic vector. Viral titers up to 1.05×10^{13} (for 18Q) and 1.8×10^{13} (for 100Q) were obtained.

Animals, Stereotaxic Injections, and Behavioral Assessment. The animal protocol abided was approved by the University of Massachusetts Medical School (A-978). The right striata of mice were coinjected with 3 μ l of virus delivering AAV Htt18Q or AAV Htt100Q and a cc-siRNA- Htt or cc-siRNA- Luc (0.5 μ l of 1 mM) by using a micropump syringe. Animals were monitored twice daily for weight, temperature, clamping, and beam walking. Mice were killed at 2 weeks for immunohistochemical studies. A group of mice was injected intrastrially with 2 μ l of Cy3-labeled cc-siRNA- Htt or unconjugated siRNA- Htt at 10 μ M. Animals were killed 1, 3, and 5 days after injection. A group of mice was injected with AAV Htt18Q ($n = 4$) or AAV Htt100Q ($n = 4$) and coinjected with cc-siRNA- Luc or siRNA- Htt. Mice were killed 3 days after injection, and the brains were harvested for biochemical analysis. Data were analyzed by using Student's *t* test or Fisher's exact test.

Immunohistochemistry. Antisera included anti-Htt (against Htt 1–17 aa) and EM48 polyclonal antibody [gift of Steven Hersch (Massachusetts General Hospital); 1:5,000] to detect Htt aggregates; anti-DARPP32 antibody (Chemicon; 1:1,000) and anti-GFAP polyclonal antisera (Chemicon; AB5804; 1:1,000) for astrocytes; and rat monoclonal antibody (Chemicon; AB1387z; 1:500) for CD11B for microglia. For further details, see ref. 23.

Quantitative Microscopic Analysis. To measure the density of Htt-labeled neurons, four adjacent microscopic fields in layer 6 of cortex and five fields in striatum bordering the corpus callosum were selected by using a $\times 20$ objective lens. Total cells with inclusions (per 2,500 μ m²) were determined for mice in each group: cc-siRNA- Luc ($n = 9$) or cc-siRNA- Htt ($n = 9$). Stereological methods were performed for neuronal number (26, 38). No significant differences in striatal volumes were obtained between injected and noninjected striata. Mean volume was used to calculate total neuronal number.

For inclusion size, three microscopic fields in cortex and striatum were evaluated at $\times 40$ objective in EM48-immunolabeled sections. Images were captured by using a SPOT camera (Diagnostic Instruments), and the cross-sectional area of inclusion size was determined by using SigmaScan Pro software

(Jandel Scientific). About 100 cells were measured per mouse per region (range from 50–140 cells), and median inclusion size was determined and compared by Mann–Whitney U. Neuropil aggregates in striatum were counted in $\times 40$ fields of 40- μm sections labeled with anti-Htt antisera. The results were grouped by treatment (cc-siRNA- Luc and cc-siRNA- Htt), and the mean number of aggregates per area was determined. To examine neuronal cross-sectional area, sections labeled with anti-Htt antibody were observed at $\times 40$ on the injected and noninjected side of the striatum and analyzed as above. The cross-sectional area of 50 Htt-labeled neurons per striata was determined by using SigmaScan Pro. Mean neuronal size was determined for each animal and grouped according to CAG repeat length and treatment condition.

Biochemical Analysis. The dorsal striatum from injected and noninjected sides of the brain was dissected on ice and incubated in lysis buffer [50 mM Tris (pH 7.4), 1% Nonidet P-40, 250 mM NaCl, 5 mM EDTA plus protease inhibitor mixture (Roche) and pepstatin A, 1 $\mu\text{g}/\text{ml}$]. Five-microgram protein samples were analyzed by Western blot with anti-Htt antisera and tubulin as described in ref. 39. Densitometry was performed by using SigmaScan Pro to obtain the signal intensity of Htt-18Q, Htt-100Q, and tubulin.

Preparation of siRNAs. The guide strand contained three phosphorothioate backbone modification—two at the 3' end and one at 5' end of the sequence to enhance nuclease stability and a 5' unpaired end to promote its assembly into the RNA-induced silencing complex (40). The passenger strand contained 3' cholesterol and three phosphorothioate linkages (13, 41). The guide strand was complementary to a region of Htt mRNA 5' to the CAG repeats. cc-siRNA- Htt comprised guide 5'-UpsUC AUC AGC UUU UCC AGG GpsUpsC-3' and passenger 5'-CpsCC UGG AAA AGC UGA UGA CGpsGps-chol-3'. Control cc-siRNA- Luc comprised guide 5'-UCG AAG uAC UcA GCGuA AGTps T-3' and passenger 5'-cuu AcG cuG AGu Acu ucG ATpsTps-Chol-3'. (The lowercase letters represent nucleotides with 2'-O-methyl modifications, ps denotes phosphorothioate, and Chol denotes cholesterol.) To generate Cy3-labeled siRNAs, Quasar-570 (Cy3) was conjugated to the 5' end of the passenger strand.

We thank Michael Hayden (University of British Columbia, Vancouver, BC, Canada) for the gift of YAC 128 transgenic mice. This work was supported by National Institutes of Health Grant NS38194 (to N.A., P.D.Z., and M.D.), the High Q Foundation (N.A. and P.D.Z.), a National Institutes of Health Endocrine Training Grant (to the University of Massachusetts Medical School), and the Diabetes Endocrine Research Center at the University of Massachusetts Medical School.

- Huntington's Disease Collaborative Research Group (1993) *Cell* 72:971–983.
- Yamamoto A, Lucas JJ, Hen R (2000) *Cell* 101:57–66.
- Singer O, Marr RA, Rockenstein E, Crews L, Coufal NG, Gage FH, Verma IM, Masliah E (2005) *Nat Neurosci* 8:1343–1349.
- Raoul C, Abbas-Terki T, Bensadoun JC, Guillot S, Haase G, Szulc J, Henderson CE, Aebischer P (2005) *Nat Med* 11:423–428.
- Xia H, Mao Q, Eliason SL, Harper SQ, Martins IH, Orr HT, Paulson HL, Yang L, Kotin RM, Davidson BL (2004) *Nat Med* 10:816–820.
- Ding H, Schwarz DS, Keene A, Affar el B, Fenton L, Xia X, Shi Y, Zamore PD, Xu Z (2003) *Aging Cell* 2:209–217.
- Harper SQ, Staber PD, He X, Eliason SL, Martins IH, Mao Q, Yang L, Kotin RM, Paulson HL, Davidson BL (2005) *Proc Natl Acad Sci USA* 102:5820–5825.
- Miller VM, Xia H, Marrs GL, Gouvion CM, Lee G, Davidson BL, Paulson HL (2003) *Proc Natl Acad Sci USA* 100:7195–7200.
- Ralph GS, Radcliffe PA, Day DM, Carthy JM, Leroux MA, Lee DC, Wong LF, Bilsland LG, Greensmith L, Kingsman SM, et al. (2005) *Nat Med* 11:429–433.
- Rodriguez-Lebron E, Denovan-Wright EM, Nash K, Lewin AS, Mandel RJ (2005) *Mol Ther* 12:618–633.
- Machida Y, Okada T, Kurosawa M, Oyama F, Ozawa K, Nukina N (2006) *Biochem Biophys Res Commun* 343:190–197.
- Wang YL, Liu W, Wada E, Murata M, Wada K, Kanazawa I (2005) *Neurosci Res* 53:241–249.
- Snoe O, Jr, Rossi JJ (2006) *Nat Methods* 3:689–695.
- Grimm D, Street KL, Jopling CL, Storm TA, Pandey K, Davis CR, Marion P, Salazar F, Kay MA (2006) *Nature* 441:537–541.
- Aleman LM, Doench J, Sharp PA (2007) *RNA* 13:385–395.
- Soutschek J, Akinc A, Bramlage B, Charisse K, Constien R, Donoghue M, Elbashir S, Geick A, Hadwiger P, Harborth J, et al. (2004) *Nature* 432:173–178.
- Song E, Zhu P, Lee SK, Chowdhury D, Kussman S, Dykxhoorn DM, Feng Y, Palliser D, Weiner DB, Shankar P, et al. (2005) *Nat Biotechnol* 23:709–717.
- Lewis DL, Wolff JA (2005) *Methods Enzymol* 392:336–350.
- Dorn G, Patel S, Wotherspoon G, Hemmings-Mieszczak M, Barclay J, Natt FJ, Martin P, Bevan S, Fox A, Ganju P, et al. (2004) *Nucleic Acids Res* 32:e49.
- Thakker DR, Natt F, Husken D, Maier R, Muller M, van der Putten H, Hoyer D, Cryan JF (2004) *Proc Natl Acad Sci USA* 101:17270–17275.
- Heidel JD, Hu S, Liu XF, Triche TJ, Davis ME (2004) *Nat Biotechnol* 22:1579–1582.
- Li BJ, Tang Q, Cheng D, Qin C, Xie FY, Wei Q, Xu J, Liu Y, Zheng BJ, Woodle MC, et al. (2005) *Nat Med* 11:944–951.
- Cheng K, Ye Z, Guntaka RV, Mahato RI (2006) *J Pharmacol Exp Ther* 317:797–805.
- Hofmann SL, Russell DW, Goldstein JL, Brown MS (1987) *Proc Natl Acad Sci USA* 84:6312–6316.
- Davies SW, Turmaine M, Cozens BA, DiFiglia M, Sharp AH, Ross CA, Scherzinger E, Wanker EE, Mangiarini L, Bates GP (1997) *Cell* 90:537–548.
- Laforet GA, Sapp E, Chase K, McIntyre C, Boyce FM, Campbell M, Cadigan BA, Warzecki L, Tagle DA, Reddy PH, et al. (2001) *J Neurosci* 21:9112–9123.
- Lin CH, Tallaksen-Greene S, Chien WM, Cearley JA, Jackson WS, Crouse AB, Ren S, Li XJ, Albin RL, Detloff PJ (2001) *Hum Mol Genet* 10:137–144.
- Menalled LB (2005) *NeuroRx* 2:465–470.
- McCown TJ (2005) *Curr Gene Ther* 5:333–338.
- DiFiglia M, Sapp E, Chase KO, Davies SW, Bates GP, Vonsattel JP, Aronin N (1997) *Science* 277:1990–1993.
- Gutekunst CA, Li SH, Yi H, Mulroy JS, Kuemmerle S, Jones R, Rye D, Ferrante RJ, Hersch SM, Li XJ (1999) *J Neurosci* 19:2522–2534.
- Reynolds A, Anderson EM, Vermeulen A, Fedorov Y, Robinson K, Leake D, Karpilow J, Marshall WS, Khvorova A (2006) *RNA* 12:988–993.
- Saudou F, Finkbeiner S, Devys D, Greenberg ME (1998) *Cell* 95:55–66.
- Kim M, Lee HS, LaForet G, McIntyre C, Martin EJ, Chang P, Kim TW, Williams M, Reddy PH, Tagle D, et al. (1999) *J Neurosci* 19:964–973.
- Arrasate M, Mitra S, Schweitzer ES, Segal MR, Finkbeiner S (2004) *Nature* 431:805–810.
- de Almeida LP, Ross CA, Zala D, Aebischer P, Deglon N (2002) *J Neurosci* 22:3473–3483.
- Zuccato C, Liber D, Ramos C, Tarditi A, Rigamonti D, Tartari M, Valenza M, Cattaneo E (2005) *Pharmacol Res* 52:133–139.
- Hyman BT, Gomez-Isla T, Irizarry MC (1998) *J Neuropathol Exp Neurol* 57:305–310.
- DiFiglia M, Sapp E, Chase K, Schwarz C, Meloni A, Young C, Martin E, Vonsattel JP, Carraway R, Reeves SA, et al. (1995) *Neuron* 14:1075–1081.
- Schwarz DS, Hutvagner G, Du T, Xu Z, Aronin N, Zamore PD (2003) *Cell* 115:199–208.
- Krutzfeldt J, Rajewsky N, Braich R, Rajeev KG, Tuschl T, Manoharan M, Stoffel M (2005) *Nature* 438:685–689.